Eclética Química

Volume 48 • number 2 • year 2023

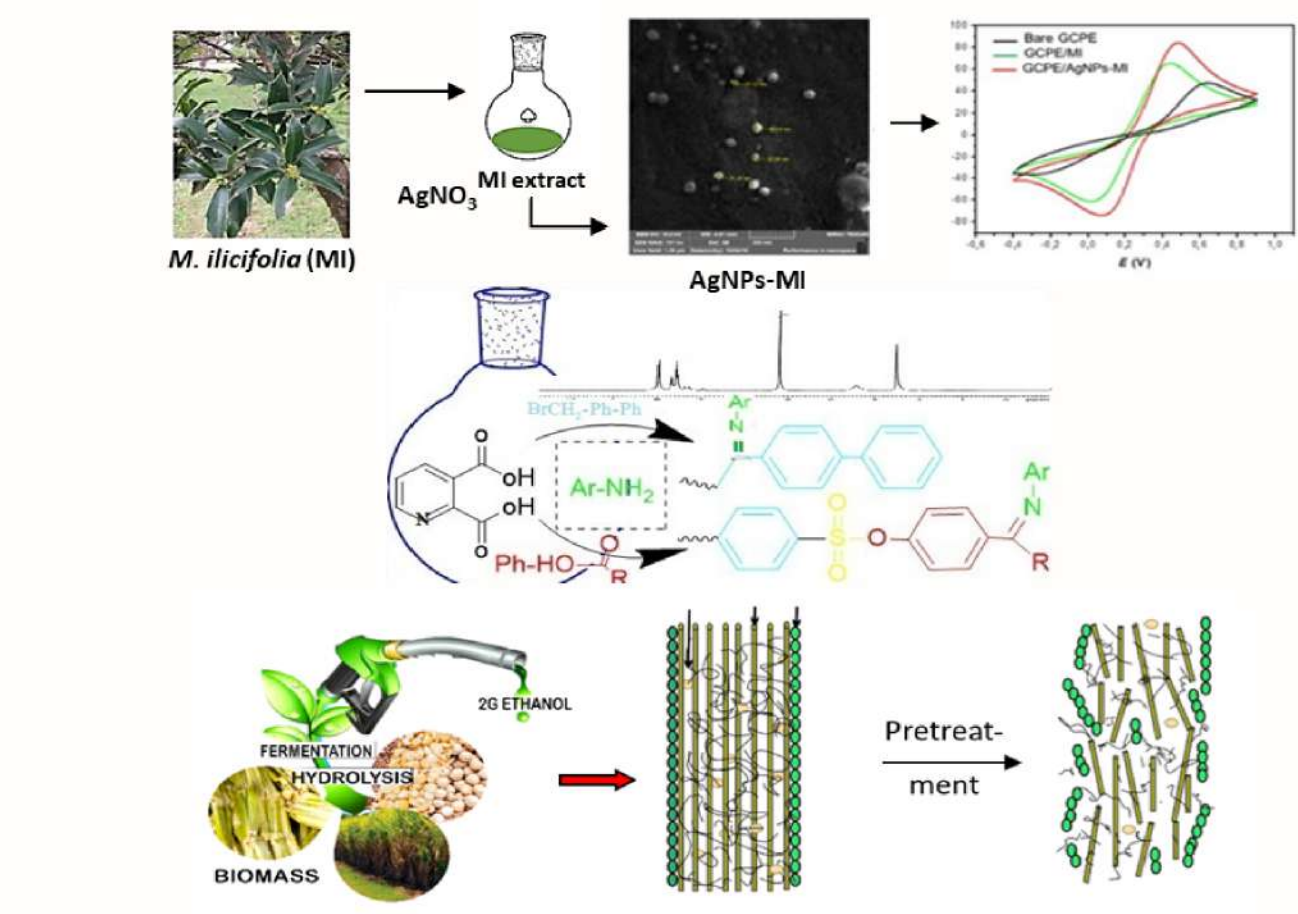

Chemistry & Social Media

Social media-based learning in Chemistry learning: A review

Alternative energy

Second-generation ethanol: concept, production and challenges

Green synthesis

Detection of dopamine using glassy carbon electrodes modified with AgNPs synthetized with *Monteverdia ilicifolia extract*

Quinolinic acid

Synthesis of some new substituted imines from aldehydes and ketones derived from quinolinic acid

Antioxidant activity

Synthesis, structural and spectroscopic properties of Co(II), Ni(II) and Cu(II) complexes with 2-((2-chlorobenzylidene)amino) acetohydrazide hydrate and their Antimicrobial and antioxidant activities

unesp
UNIVERSIDADE ESTADUAL PAULISTA
"JÚLIO DE MESQUITA FILHO"

Instituto de Química
UNESP
Araraquara

ISSN 1678-4618

Editorial Team

Editor-in-Chief

Editors

Editorial Advisory Board

EDITORIAL PRODUCTION

Ctrl K Produção Editorial – Araraquara, Brazil
digite@ctrlk.com.br

Eclética Química

Editorial

revista.iq.unesp.br

| Vol. 48 | n. 2 | 2023 |

Editorial

The Editor proudly announces the new issue of **Eclética Química** in which readers will find reviews and original articles covering different areas of Chemistry and Education in Chemistry. This issue is opened with the exam of empirical articles about social media increasing the motivation to study chemistry for high school and undergraduate students. For that, the method of Systematic Literature Review was used to identify, analyze, and interpret findings on the research topics. In these topics, the effect of using social media in chemistry learning was discussed. Obviously, learners can interact and connect with each other in new manners by means of social media. Afterwards, a review on the second-generation (2G) ethanol, which indicates to be the progress of science all over the world, using biological agents, the driving force for the large-scale production of important materials in the economy, such as biofuel. The discussion of concepts, production methodologies and challenges for the energy sector considering 2G ethanol are the focus of this review. It is noticed that the 2G ethanol production methodologies have been implemented as a potential low-cost alternative energy generation in accordance with the principles of Green Chemistry. In the sequence, the description of the green synthesis of silver nanoparticles (AgNPs) using the aqueous extract of *Monteverdia ilicifolia* (MI) leaves as stabilizing and reducing agent, i.e., a new application for a well-known medicinal plant used in Brazil, is presented. The authors have characterized the AgNPs-MI obtained using an extensive number of techniques, demonstrating the effectiveness of MI to cover the AgNPs and stabilizing the suspension. Once deposited on glassy carbon electrode, the AgNPs were effective as electrochemical sensor to determine dopamine, improving electrochemical properties and enhancing their electroanalytical performance. Follow the description of several steps necessary to prepare some substituted imines from quinolinic acid. These substituted imines can make several reactions such as electrophilic, nucleophilic, dienophile, and aza-diene reaction. Imine compounds exhibit a wide range of useful biological activity, such as inflammatory, antimalarial, analgesic, antioxidant, antimicrobial, anthelmintic, antitubercular and anticancer. They can be also used as starting material in many fields, including organometal compounds. Complete this issue the description of the preparation of Co(II), Ni(II) and Cu(II) complexes with the ligands derived from 2-chlorobenzaldehyde, glycine and hydrazine hydrate and the characterization of these compounds by means of different techniques. Antimicrobial and antioxidant activities were calculated and the antibacterial activity against two Gram-positive and two Gram-negative bacteria was evaluated, and the antifungal activity was assessed against two fungal strains. The results showed that the most metal complexes have much higher antibacterial and antifungal activity compared to the parent ligand.

The Editor and his team are grateful to all the authors for their valuable contributions, and the reviewers for their outstanding collaboration, and kindly invite you to submit your manuscript to **Eclética Química**.

Assis Vicente Benedetti
Editor-in-Chief of Eclética Química

Digital Databases

DOAJ DIRECTORY OF OPEN ACCESS JOURNALS

SCIFINDER A CAS SOLUTION

FSTA

REDIB

latindex

Scopus

Google Scholar

redalyc LA HEMEROTECA CIENTÍFICA EN LÍNEA

evisa.

EBSCO Discovery Service

biblat Bibliografía Latinoamericana en revistas de investigación científica y social

IAEA International Nuclear Information System INIS

Supporters

Instituto de Química

unesp UNIVERSIDADE ESTADUAL PAULISTA "JÚLIO DE MESQUITA FILHO"

ABEC BRASIL Associação Brasileira de Editores Científicos

CNPq

*Click on the images to follow the links.
EBSCO and FSTA has no link available. The address is for subscribers only.

Eclética Química

Author Guidelines
revista.iq.unesp.br

| Vol. 48 | n. 2 | 2023 |

INSTRUCTIONS FOR AUTHORS

BEFORE YOU SUBMIT

1. Check Eclet. Quim.'s focus and scope

Eclética Química is a peer-reviewed quarterly publication supported by Institute of Chemistry of São Paulo State University (UNESP). It publishes original researches as articles, reviews and short reviews in **all areas of Chemistry**.

2. Types of papers

a. Original articles
b. Reviews
c. Short reviews
d. Communications
e. Technical notes
f. Articles in education in chemistry and chemistry-related areas

Manuscripts submitted for publication as full articles and communications must contain original and unpublished results and should not have been submitted elsewhere either partially or whole. Manuscript originating from scientific initiation, course completion monographs, Dissertations or PhD Thesis already deposited in Universities' repositories is accepted without considering it a violation of the journal's rules. Eclética Química also accepts preprints.

a. Original articles

The manuscript must be organized in sections as follows:

1. Introduction
2. Experimental
3. Results and Discussion
4. Conclusions

References

Sections titles must be written in bold and sequentially numbered; only the first letter should be in uppercase letter. Subsections, numbered as exemplified, should be written in normal and italic letters; only the first letter should be in uppercase letter.

Example:

1. Introduction
1.1 History

2. Experimental
2.1 Surface characterization
2.1.1 Morphological analysis

b. Reviews

Review articles should be original and present state-of-the-art overviews in a coherent and concise form covering the most relevant aspects of the topic that is being revised and indicate the likely future directions of the field. Therefore,

before beginning the preparation of a Review manuscript, send a letter (one page maximum) to the Editor with the subject of interest and the main topics that would be covered in the Review manuscript. The Editor will communicate his decision in two weeks. Receiving this type of manuscript does not imply acceptance to be published in **Eclet. Quim.** It will be peer-reviewed.

c. Short reviews

Short reviews should present an overview of the state-of-the-art in a specific topic within the scope of the journal and limited to 5,000 words. Consider a table or image as corresponding to 100 words. Before beginning the preparation of a Short Review manuscript, send a letter (one page maximum) to the Editor with the subject of interest and the main topics that would be covered in the Short Review manuscript.

d. Communications

Communications should cover relevant scientific results and are limited to 1,500 words or three pages of the journal, not including the title, authors' names, figures, tables and references. However, Communications suggesting fragmentation of complete contributions are strongly discouraged by Editors.

e. Technical notes

Descriptions of methods, techniques, equipment or accessories developed in the authors' laboratory, as long as they present chemical content of interest. They should follow the usual form of presentation, according to the peculiarities of each work. They should have a maximum of 25 pages, including figures, tables, diagrams, etc.

f. Articles in education in chemistry and chemistry-correlated areas

Research manuscript related to undergraduate teaching in Chemistry and innovative experiences in undergraduate and graduate education. They should have a maximum of 25 pages, including figures, tables, diagrams, and other elements.

3. Special issues

Special issues with complete articles dedicated to Symposia and Congresses and to special themes or in honor of scientists with relevant contributions in Chemistry and correlate areas can be published by **Eclet. Quim.** under the condition that a previous agreement with Editors is established. All the guides of the journal must be followed by the authors.

4. Approval

Ensure all authors have seen and approved the final version of the article prior to submission. All authors must also approve the journal you are submitting to.

ETHICAL GUIDELINES

Before starting the submission process, please be sure that **all ethical aspects mentioned below were followed**. Violation of these ethical aspects may preclude authors from submitting or publishing articles in **Eclet. Quim.**

a. Coauthorship: The corresponding author is responsible for listing as coauthors only researchers who have really taken part in the work, for informing them about the entire manuscript content and for obtaining their permission to submit and publish it.
Two Corresponding authors for an article may be accepted provided both have equivalent contribution to the article, being one of them permanent in the Institution.

b. Nonauthors: Explicit permission of a nonauthor who has collaborated with personal communication or discussion to the manuscript being submitted to **Eclet. Quim.** must be obtained before being cited.

c. Unbiased research: Authors are responsible for carefully searching for all the scientific work relevant to their reasoning irrespective of whether they agree or not with the presented information.

d. Citation: Authors are responsible for correctly citing and crediting all data taken from other sources. This requirement is not necessary only when the information is a result of the research presented in the manuscript being submitted to **Eclet. Quim.**

e. Direct quotations: The word-for-word reproduction of data or sentences as long as placed between quotation marks and correctly cited is not considered ethical deviation when indispensable for the discussion of a specific set of data or a hypothesis.

f. Do not cite: Master's Degree dissertations and PhD theses are not accepted; instead, you must cite the publications resulted from them.

g. Plagiarism: Plagiarism, self-plagiarism, and the suggestion of novelty when the material was already published are unaccepted by **Eclet. Quim.** Before reviewing a manuscript, the **Turnitin antiplagiarism software** will be used to detect any ethical deviation.

h. Simultaneous submissions: of the same manuscript to more than one journal is considered an ethical deviation and is conflicted to the declaration has been done below by the authors.

i. Studies with humans or other animals: Before submitting manuscripts involving human beings, materials from human or animals, the authors need to confirm that the procedures established, respectively, by the institutional committee on human experimentation and Helsinki's declaration, and the recommendations of the animal care institutional committee were followed. Editors may request complementary information on ethical aspects.

COPYRIGHT NOTICE

The corresponding author transfers the copyright of the submitted manuscript and all its versions to **Eclet. Quim.**, after having the consent of all authors, which ceases if the manuscript is rejected or withdrawn during the review process.

When a published manuscript in **Eclet. Quim.** is also published in another journal, it will be immediately withdrawn from **Eclet. Quim.** and the authors informed of the Editor decision.

PUBLICATION CHARGES

Eclética Química is supported by the Institute of Chemistry/UNESP and publication is free of charge for authors.

MANUSCRIPT PREPARATION

COVER LETTER

We provide a template to help you prepare your cover letter. To download it, click **here**.

The cover letter MUST include:

1. Identification of authors

a. The authors' full names (they must be written in full and complete, separated by comma)

~~João M. José~~	Incorrect
~~J. M. José~~	Incorrect
João Maria José	Correct!

b. E-mail addresses and affiliations (**neither more nor less than two instances**) of all authors;
c. ORCID ID links;
d. A plus sign (+) indicating the corresponding author and your contact phone number.

Example:

Author Full Name[1+], Author Full Name[2]

1. University, Faculty or Institute, City, Country.
2. Company, Division or Sector or Laboratory, City, Country.

+ Author 1: address@mail.com, ORCID: https://orcid.org/xxxx-xxxx-xxxx-xxxx, Phone: +xx xxxxxxxx
Author 2: address@mail.com, ORCID: https://orcid.org/xxxx-xxxx-xxxx-xxxx, Phone: +xx xxxxxxxx

2. Authors' contribution

We request authors to include author contributions according to CRediT taxonomy standardized contribution descriptions. CRediT (Contributor Roles Taxonomy) is a high-level taxonomy, including 14 roles, that can be used to represent the roles typically played by contributors to scientific scholarly output. The roles describe each contributor's specific contribution to the scholarly output.

a. Please, visit this link (https://casrai.org/credit/) to find out which role(s) the authors fit into;
b. Do not modify the role names; do not write "all authors" in any role. Do not combine two or more roles in one line.
c. If there are any roles that no author has engaged in (such as funding in papers that were not funded), write "Not applicable" in front of the name of the role;
d. Write the authors' names according to the **American Chemistry Society (ACS) citation style**.

Example:

Conceptualization: Foster, J. C.; O'Reilly, R. K.
Data curation: Varlas, S.; Couturaud, B.; Coe, J.; O'Reilly, R. K.
Formal Analysis: Foster, J. C.; Varlas, S.
Funding acquisition: Not applicable.
Investigation: Foster, J. C.; O'Reilly, R. K.
Methodology: Coe, J.; O'Reilly, R. K.

Project administration: O'Reilly, R. K.
Resources: Coe, J.
Software: Not applicable.
Supervision: O'Reilly, R. K.
Validation: Varlas, S.; Couturaud, B.
Visualization: Foster, J. C.
Writing – original draft: Foster, J. C.; Varlas, S.; Couturaud, B.; Coe, J.; O'Reilly, R. K.
Writing – review & editing: Foster, J. C.; Varlas, S.; Couturaud, B.; Coe, J.; O'Reilly, R. K.

3. Indication of reviewers

We kindly ask the authors to suggest **five** suitable reviewers, providing full name, affiliation, and email.

4. Other information

a. The authors must write one paragraph remarking the novelty and relevance of the work;
b. The corresponding author must declare, on behalf of the other authors, that the manuscript being submitted is original and its content has not been published previously and is not under consideration for publication elsewhere;
c. The authors must inform if there is any conflict of interest.

5. Acknowledgements and funding

Acknowledgements and funding information will be requested after the article is accepted for publication.

6. Data availability statement

A data availability statement informs the reader where the data associate with your published work is available, and under what conditions they can be accessed. Therefore, authors must inform if:

Data will be available upon request;
All dataset were generated or analyzed in the current study; or
Data sharing is not applicable.

MANUSCRIPT

We provide a template to help you prepare your manuscript. To download it, click **here**.

1. General rules

Only manuscripts written in English are accepted. British or American usage is acceptable, but they should not be mixed. Non-native English speakers are encouraged to have their manuscripts professionally revised before submission.

Manuscripts must be sent in editable files as *.doc, *.docx or *.odt. The text must be typed using font style Times New Roman and size 12. Space between lines should be 1.5 mm and paper size A4, top and bottom margins 2.5 cm, left and right margins 2.0 cm.

All contributions must include an **abstract** (170 words maximum), t**hree to five keywords** and a **graphical abstract** (8 cm wide × 8 cm high).

Appendix should be included at the end of the main text of the manuscript.

Supplementary information: all type of articles accepts supplementary information (SI) that aims at complementing the main text with material that, for any reason, cannot be included in the article.

TITLE

The title should be concise, explanatory and represent the content of the work. The title must have only the first letter of the sentence in uppercase. The following are not allowed: acronyms, abbreviations, geographical location of the research, en or em dashes (which must be replaced by a colon). Titles do not have full point.

ABSTRACT

Abstract is the summary of the article. The abstract must be written as a running text not as structured topics, but its content should present background, objectives, methods, results, and conclusion. It cannot contain citations. The text should be written in a single paragraph with a **maximum of 170 words**.

KEYWORDS

Keywords are intended to make it easier for readers to find the content of your text. As fundamental tools for database indexing, they act as a gateway to the text. The correct selection of keywords significantly increases the chances that a document will be found by researchers on the topic, and consequently helps to promote the visibility of an article within a myriad of publications.

FIGURES, TABLES AND EQUATIONS

Figures, tables and equations must be written with initial capital letter followed by their respective number and period, in bold, without adding zero "**Table 1**", preceding an explanatory title. Tables, Figures and Equations should appear after the first citation and should be numbered according to the ascending order of appearance in the text (1, 2, 3...).

Figures, tables, schemes and photographs already published by the same or different authors in other publications may be reproduced in manuscripts of **Eclet. Quim.** only with permission from the editor house that holds the copyright.

Nomenclature, abbreviations, and symbols should follow IUPAC recommendations.

DATA AVAILABILITY STATEMENT

The data availability statement informs the reader where the data associate with your work is available, and under what conditions they can be accessed. They also include links (where applicable) to the data set.

a. The data are available in a data repository (cite repository and the DOI of the deposited data);
b. The data will be available upon request;
c. All data sets were generated or analyzed in the current study;
d. Data sharing is not applicable (in cases where no data sets have been generated or analyzed during the current study, it should be declared).

GRAPHICAL ABSTRACT

The graphical abstract must summarize the manuscript in an interesting way to catch the attention of the readers. As already stated, it must be designed with 8 cm wide × 8 cm high, and a 900-dpi resolution is mandatory for this journal. It must be submitted as *.jpg, *.jpeg, *.tif or *.ppt files as supplementary file.

We provide a template to help you prepare your GA. To download it, click **here**.

SUPPLEMENTARY INFORMATION

When appropriate, important data to complement and a better comprehension of the article can be submitted as Supplementary File, which will be published online and will be made available as links in the original article. This might include additional figures, tables, text, equations, videos or other materials that are necessary to fully document the research contained in the paper or to facilitate the readers' ability to understand the work.

Supplementary material should be presented in appropriate .docx file for text, tables, figures and graphics. All supplementary figures, tables and videos should be referred in the manuscript body as "Table S1, S2…", "Fig. S1, S2…" and "Video S1, S2 …".

At the end of the main text the authors must inform: This article has supplementary information.

Supplementary information will be located following the article with a different DOI number from that of the article, but easily related to it.

CITATION STYLE GUIDE

From 2021 on, the journal will follow the **ACS citation style**.

Indication of the sources is made by authorship and date. So, the reference list is organized alphabetically by author.

Each citation consists of two parts: the in-text citation, which provides brief identifying information within the text, and the reference list, a list of sources that provides full bibliographic information.

We encourage the citation of primary research over review articles, where appropriate, in order to give credit to those who first reported a finding. Find out more about our commitments to the principles of San Francisco Declaration on Research Assessment (DORA).

What information you must cite?

a. Exact wording taken from any source, including freely available websites;
b. Paraphrases of passages;
c. Summaries of another person's work;
d. Indebtedness to another person for an idea;
e. Use of another researchers' work;
f. Use of your own previous work.

You do not need to cite **common knowledge**.

Example:
Water is a tasteless and odorless liquid at room temperature (common knowledge, no citation needed)

In-text citations

You can choose the cite your references within or at the end of the phrase, as showed below.

Within the cited information:

One author: Finnegan (2004) states that the primary structure of this enzyme has also been determined.
Two authors: Finnegan and Roman (2004) state that the structure of this enzyme has also been determined.
Three or more authors: Finnegan *et al.* (2004) state that the structure of this enzyme has also been determined.
PREPRINT Reference: Finnegan et al. (2004, PREPRINT) state that the structure of this enzyme has also been determined.

At the end of the cited information:

One author: The primary structure of this enzyme has also been determined (Finnegan, 2004).
Two authors: The primary structure of this enzyme has also been determined (Finnegan and Roman, 2004).
Three or more authors: The primary structure of this enzyme has also been determined (Finnegan *et al.*, 2004).
PREPRINT Reference: The primary structure of this enzyme has also been determined (Finnegan *et al.*, 2004, PREPRINT).

If you need to cite more than one reference in the same brackets, separate them with semicolon and write them in alphabetic order:

The primary structure of this enzyme was determined (Abel *et al.*, 2011; Borges, 2004; Castro *et al.*, 2021).

Bibliographic references

Article from scientific journals
Foster, J. C.; Varlas, S.; Couturaud, B.; Coe, J.; O'Reilly, R. K. Getting into Shape: Reflections on a New Generation of Cylindrical Nanostructures' Self-Assembly Using Polymer Building Block. *J. Am. Chem. Soc*. **2019**, *141* (7), 2742−2753. https://doi/10.1021/jacs.8b08648

Book
Hammond, C. *The Basics of Crystallography and Diffraction*, 4th ed.; International Union of Crystallography Texts on Crystallography, Vol. 21; Oxford University Press, 2015.

Book chapter
Hammond, C. Crystal Symmetry. In *The Basics of Crystallography and Diffraction*, 4th ed.; International Union of Crystallography Texts on Crystallography, Vol. 21; Oxford University Press, 2015; pp 99−134.

Book with editors
Mom the Chemistry Professor: Personal Accounts and Advice from Chemistry Professors Who Are Mothers, 2nd ed.; Woznack, K., Charlebois, A., Cole, R. S., Marzabadi, C. H., Webster, G., Eds.; Springer, 2018.

Website
ACS Publications Home Page. https://pubs.acs.org/ (accessed 2019-02-21).

Document from a website
American Chemical Society, Committee on Chemical Safety, Task Force for Safety Education Guidelines. *Guidelines for Chemical Laboratory Safety in Academic Institutions*. American Chemical Society, 2016. https://www.acs.org/content/dam/acsorg/about/governance/committees/chemicalsafety/publications/acs-safety-guidelines-academic.pdf (accessed 2019-02-21).

Conference proceedings
Nilsson, A.; Petersson, F.; Persson, H. W.; Jönsson, H. Manipulation of Suspended Particles in a Laminar Flow. In Micro Total Analysis Systems 2002, Proceedings of the μTAS 2002 Symposium, Nara, Japan, November 3−7, 2002; The Netherlands, 2002; pp 751−753. https://doi.org/10.1007/978-94-010-0504-3_50

Governmental and legislation information
Department of Commerce, United States Patent and Trademark Office. Section 706.02 Rejection of Prior Art [R-07.2015]. *Manual of Patent Examining Procedure (MPEP)*, 9th ed., rev. 08.2017, last revised January 2018. https://www.uspto.gov/web/offices/pac/mpep/s706.html#d0e58220 (accessed 2019-03-20).

PREPRINT
Fugivara, C. S.; Guilherme, L. H.; Benedetti, A. V. Microstructure of a passive film galvanostatically grown on stainless steel. ChemRxiv. [PREPRINT] September 20, 2021. https://doi.org/10.26434/chemrxiv.xxxxxx.v1 (accessed 2021-12-19).

Patent
Lois-Caballe, C.; Baltimore, D.; Qin, X.-F. Method for Expression of Small RNA Molecules within a Cell. US 7 732 193 B2, 2010.

Streaming data
American Chemical Society. Game of Thrones Science: Sword Making and Valyrian Steel. *Reactions*. YouTube, April 15, 2015. https://www.youtube.com/watch?v=cHRcGoje4j4 (accessed 2019-02-28).

For more information, you can access the ACS Style Quick Guide and the Williams College LibGuides.

SUBMITTING YOUR MANUSCRIPT

The corresponding author should submit the manuscript online by clicking **here**. If you are a user, register by clicking **here**.

At the **User home** page, click in **New submission**.

In Step 1, select a section for your manuscript, verify one more time if you followed all these rules in **Submission checklist**, add Comments for the Editor if you want to, and click Save and continue.

In Step 2, you will **upload your manuscript**. Remember it will pass through a double-blind review process. So, do not provide any information on the authorship.

In Step 3, enter **submission's metadata**: authors' full names, valid e-mail addresses and ORCID ID links (with "http" not "https"). Add title, abstract, contributors and supporting agencies, and the list of references.

In Step 4, upload the **cover letter**, the **graphical abstract** and other **supplementary material** you want to include in your manuscript.

In Step 5, you will be able to check all submitted documents in the **File summary**. If you are certain that you have followed all the rules until here, click in **Finish submission**.

REVIEW PROCESS

The time elapsed between the submission and the first response of the reviewers is around three months. The average time elapsed between submission and publication is around seven months.

Resubmission (manuscripts "rejected in the present form" or subjected to "revision") must contain a letter with the responses to the comments/criticism and suggestions of reviewers/editors should accompany the revised manuscript.

All modifications made to the original manuscript must be highlighted.

If you want to check our Editorial process, click **here**.

EDITOR'S REQUIREMENTS

Authors who have a manuscript accepted in **Eclet. Quim.** may be invited to act as reviewers.

Only the authors are responsible for the correctness of all information, data and content of the manuscript submitted to **Eclet. Quim.** Thus, the Editors and the Editorial Board cannot accept responsibility for the correctness of the material published in **Eclet. Quim.**

Proofs

After accepting the manuscript, **Eclet. Quim.** technical assistants will contact you regarding your manuscript page proofs to correct printing errors only, i.e., other corrections or content improvement are not permitted. The proofs shall be returned in three working days (72 h) via email.

Appeal

Authors may only appeal once about the decision regarding a manuscript. To appeal against the Editorial decision on your manuscript, the corresponding author can send a rebuttal letter to the editor, including a detailed response to any comments made by the reviewers/editor. The editor will consider the rebuttal letter, and if dimmed appropriate, the manuscript will be sent to a new reviewer. The Editor decision is final.

Contact

If you have any question, please contact our team:

Prof. Assis Vicente Benedetti
Editor-in-Chief
assis.v.benedetti@unesp.br

Letícia Amanda Miguel
Technical support
ecletica@ctrlk.com.br

SUMMARY

REVIEW Article

ORIGINAL ARTICLES

Eclética Química

Review article

revista.iq.unesp.br

| Vol. 48 | n. 2 | 2023 |

Social media-based learning in Chemistry learning: A review

Hayuni Retno Widarti[1+], Titin Sriwahyuni[1], Deni Ainur Rokhim[1,2], Afis Baghiz Syafrudin[1]

1. State University of Malang, Department of Chemical Education, East Java, Indonesia.
2. Chemistry and PKWU, SMAN 3 Sidoarjo, East Java, Indonesia.

+Corresponding author: Hayuni Retno Widarti, **Phone:** +62 81232458494, **Email address:** hayuni.retno.fmipa@um.ac.id

ARTICLE INFO

Article history:
Received: November 01, 2022
Accepted: January 02, 2023
Published: April 01, 2023

Section Editors: Assis Vicente Benedetti

Keywords:
1. chemistry learning
2. literature review
3. social media
4. social media-based learning
5. student motivation

ABSTRACT: Social media-based learning can involve students in open, competitive, and running learning according to the speed of each understanding. This study aims to examine empirical articles about social media increasing the motivation to study chemistry for high school and undergraduate students using the Systematic Literature Review method, namely, to identify, analyze, and interpret findings on research topics published from 2018 to 2022. Five articles were identified through the publish or perish search engine using Scopus databases. The articles studied reviewed the effect of using social media in learning. The results of the study focused on the use of social media in chemistry learning which can increase student motivation for both high school and undergraduate students.

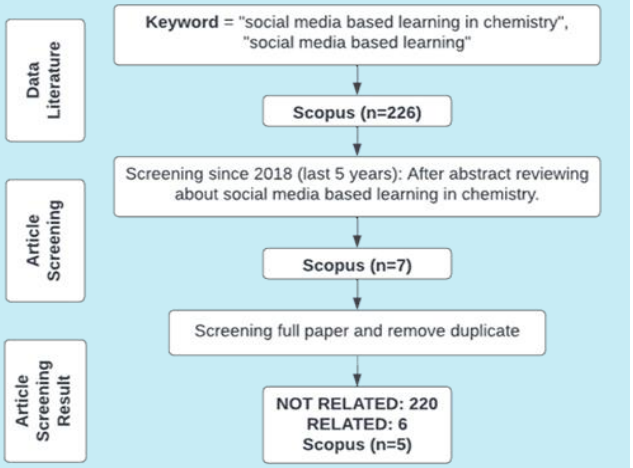

CONTENTS

Eclética Química, vol. 48, n. 2, 2023, 17-21
ISSN: 1678-4618
DOI: 10.26850/1678-4618eqj.v48.2.2023.p17-21

1. Introduction

Today, the Internet has become a lifestyle for most people in the world, with the current world population of over 7.7 billion and Internet users being 4.4 billion. The field of education has gained many new approaches to improve learning, one of which is social media-based learning. Social media-based learning can involve students in intense, open, competitive learning, and can do problem-solving with enthusiasm where students can discover new things in a relaxed and informal atmosphere but at the same time stay focused and motivated (Zdravkova, 2016). This is highly expected in a learning process where students can be more motivated and enthusiastic in participating in learning. Social media-based learning can also change students from passive learners to active learners so that learning can be student-centered (Ziegler, 2007). The above benefits can of course be achieved with the help of social interactions fostered by students, students' technological knowledge, and the role of the teacher to manage and control class activities (Rinda *et al.*, 2018).

The active role of students in the learning process has direct involvement with the learning model applied by educators. This is often found because students often experience an atmosphere and enthusiasm for learning that does not absorb and accept the material presented by the teacher. High school chemistry teaching materials have many concepts that are quite difficult for students to grasp, making many students less confident in understanding the material because it is abstract, simplified from the actual situation, sequential, and tiered (Lutfi and Hidayah, 2021).

Learning science, especially chemistry in schools using social media-based learning models, is an effective method to improve explanation and understanding of basic chemistry topics (Fosu *et al.*, 2019). The use of appropriate learning methods and strategies by educators will determine a good and effective chemistry learning process (Sari *et al.*, 2017). Previous research has shown that the use of social media in learning has a positive effect on student-learning and can increase self-efficacy so that many researchers continue to develop social media-based learning media by using various features in it (Hayes *et al.*, 2020).

Based on research conducted by Danjou (2020), social media-based learning can allow each student to progress at their own space because the material can be accessed anytime, anywhere, and can be watched/viewed many times. Research conducted by Smith (2014) on chemistry learning showed that involving students in creating chemistry video content keeps them enthusiastic and helps to develop their creativity and communication skills.

A literature review conducted by Beemt *et al.* (2020) with the topic of increasing students' understanding of the use of social media in the learning process states that the role of social media in learning is to motivate students and to increase transparency in communication (internal and external), assessment and evaluation. However, this can be achieved if the teacher as educator also has good technology skills.

Various kinds of content designs and social media features are designed in chemistry learning, such as DingTalk and WeChat, which are proven to make learning activities interesting and can be used to attract students' attention in the classroom (Xiao *et al.*, 2020). In another study that mentions the use of technology-based learning tools, the content presented aims to help students interact in the management experience by learning skills and knowledge to improve literacy (Hight *et al.*, 2021). Literacy in reading is very important so that students can explore a lot of reading sources that support the subject matter provided by the teacher (Putri *et al.*, 2022).

This research has been conducted so that it may become the latest research trend regarding social media-based learning that can be applied to chemistry material for both high school and undergraduate students. Therefore, the research objectives and appropriate learning methods will provide an overview of the interest in this social media-based research. The learning outcomes that social media-based learning researchers will emphasize are the focus of the current review. Thus, the main research question that the study seeks to answer is: Can social media increase motivation to study chemistry for high school and undergraduate students?

2. Experimental

The method of writing a journal review in searching for literature data using a Systematic Literature Review, which is a method that has stages of identifying, evaluating, and interpreting findings and is used to answer predetermined research questions (Shay and Lafata, 2015). In this review, the Scopus database was used to obtain social media-based learning research articles, using the publish or perish software.

In this study, the data used with the keyword "social media-based learning in chemistry" with a journal publication time span of 2018–2022 (last 5 years). After the application was run, the researcher read the title and abstract of the article to select articles that met the following inclusion criteria: 1) Articles about social media-based learning in chemistry learning; 2)

Eclética Química, vol. 48, n. 2, 2023, 17-21
ISSN: 1678-4618
DOI: 10.26850/1678-4618eqj.v48.2.2023.p17-21

Publication of reputable, accredited, and full-text articles. This study has exclusion criteria, namely articles not related to social media-based learning in chemistry learning as well as articles published before 2018.

The search results found 226 articles related to the related topics studied. Then, reselection was carried out based on inclusion criteria so that 7 articles were obtained. Furthermore, the data were sorted by assessing and considering the suitability of the research topic, abstract, and research content in order to obtain 5 articles that met all the requirements.

The article search process described above can be seen in Fig. 1.

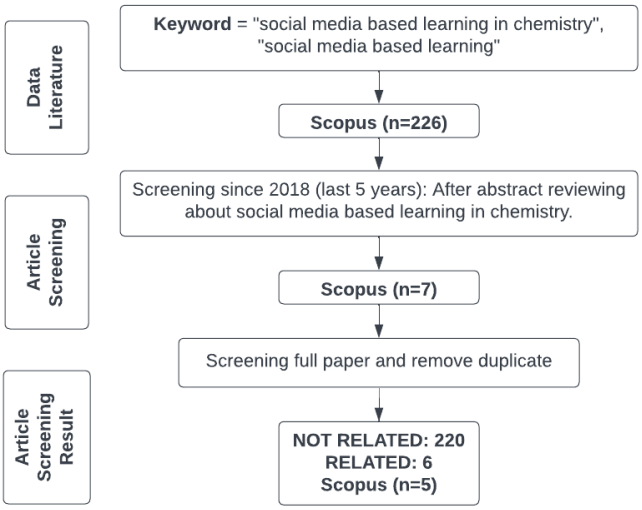

Figure 1. Search flowchart.

3. Results and discussion

The analyzed results of the review research focused on the influence of social media use in learning in senior high schools and undergraduate colleges.

Literature study information in terms of abstracts, background, research questions, objectives, methods, and research results are presented in Table 1. Of the 5 articles reviewed, 1 article was published in 2018, 1 article was published in 2019, 2 articles were published in 2020, and 1 article was published in 2021. The following chemistry learning materials that can be applied to social media-based learning can also be seen in Table 1.

Based on Table 1, the results of research in social media-based chemistry learning can be said to be effective and able to increase the motivation to study chemistry. The participation of students in making videos can in fact increase the enthusiasm for learning so that it can have a positive effect on student learning outcomes, which is in line with the research results of Hight *et al.* (2021). However, this literature review found a gap between the possible learning experiences of students on social media and the learning outcomes or learning focus they assessed.

Two important aspects that have not been discussed in this research are: how social media content is designed and implemented; and that diversity and innovation in compiling social media content that is easy for students to understand is very important and should play a very important role in making learning effective and more interactive.

Table 1. Social media-based learning.

Author	Use of social media	Results
Hurst (2018)	Learning chemistry using the Snapchat platform, especially the Story feature to share things related to chemistry in everyday life.	Snapchat can be used to engage students in chemistry by contextualizing the subject matter in the real world together by giving students insight into the research and living environment, especially in chemistry. Based on the data obtained from the research, it is known that 83% of the 59 respondents said they felt more engaged with chemistry because of Snapchat.
Fosu *et al.* (2019)	Students are asked to publish their study results using the Twitter application	From the survey, it appears that students have a positive perception of the use of social media for studying chemistry. About 83 (61.48%) students strongly agreed that social media can be a good platform to support the learning of chemistry. Based on their posts, it is evident that students found the social media platform to be a convenient medium for learning, and even wished that the platform was frequently used for teaching. Students reported that using Twitter helped in their understanding of the material.
Danjou (2020)	Chemistry learning is carried out asynchronously and synchronously. Synchronous sessions were carried out with the teacher sharing learning videos via Facebook so that students can access them anytime and anywhere.	Learning becomes more efficient because teachers do many alternative technologies in learning. Based on data, 95% of respondents think that the use of videos visible on Facebook is more suitable for exercise solutions explanation without requiring more effort than for live explanation. From the activities that have been carried out, students feel enthusiastic about learning chemistry.

Continue…

Eclética Química, vol. 48, n. 2, 2023, 17-21
ISSN: 1678-4618
DOI: 10.26850/1678-4618eqj.v48.2.2023.p17-21

Hayes et al. (2020)	Innovative video creation and posted on the TikTok app with the aim of introducing the audience that chemistry is fun.	The video that was made was successfully watched 8,500 times and managed to attract visitors by 82.7% of the initial number.
Hight et al. (2021)	Making creative chemistry learning videos using TikTok.	From the research conducted, it is proven that the involvement of students in making learning videos can increase students' understanding of the material that will be made later.

4. Conclusions

The results of research in social media-based chemistry learning can be said to be effective and able to increase the motivation to study chemistry. The effectiveness of a social media platform in increasing the motivation to study chemistry for high school and undergraduate students has its own advantages and disadvantages, so the decision regarding the use of learning media lies in the mastery skills of the teacher to apply media, especially social media in learning. There are many types of platforms that can be applied in learning chemistry such as Twitter, Instagram, Facebook, YouTube, Discord, and many more. The characteristics of the right platform are that the platform can support learning outcomes both in the short and long term.

Social media has the potential to connect a broad knowledge into small parts that can be separated. How students perceive and what can be utilized from this different social media-based learning experience needs further exploration.

Authors' contribution

Conceptualization: Widarti, H. R.; Rokhim, D. A.
Data curation: Sriwahyuni, T.; Syafrudin, A. B.
Formal Analysis: Sriwahyuni, T.
Funding acquisition: Not applicable.
Investigation: Not applicable.
Methodology: Sriwahyuni, T.
Project administration: Widarti, H. R
Resources: Rokhim, D. A.
Software: Not applicable.
Supervision: Not applicable.
Validation: Not applicable.
Visualization: Sriwahyuni, T.
Writing – original draft: Widarti, H. R.; Sriwahyuni, T.; Rokhim, D. A.; Syafrudin, A. B.
Writing – review & editing: Widarti, H. R.; Sriwahyuni, T.; Rokhim, D. A.; Syafrudin, A. B.

Data availability statement

All data sets were generated or analyzed in the current study

Funding

Not applicable.

Acknowledgments

Not applicable.

References

Beemt, A.; Thurlings, M.; Willems, M. Towards an understanding of social media use in the classroom: a literature review. *Technol. Pedagogy Educ*. **2020**, *29* (1), 35–55. https://doi.org/10.1080/1475939X.2019.1695657

Danjou, P.-E. Distance Teaching of Organic Chemistry Tutorials During the COVID-19 Pandemic: Focus on the Use of Videos and Social Media. *J. Chem. Educ.* **2020**, *97* (9), 3168–3171 https://doi.org/10.1021/acs.jchemed.0c00485

Fosu, M. A.; Gupta, T.; Michael, S. Social Media in Chemistry: Using a Learning Management System and Twitter to Improve Student Perceptions and Performance in Chemistry. In *Technology Integration in Chemistry Education and Research (TICER)*; Gupta, T., Belford, R. E., Eds.; ACS Symposium Series, **2019**; Vol. 18, pp 185–208. https://doi.org/10.1021/bk-2019-1318.ch013

Hayes, C.; Stott, K.; Lamb, K. J.; Hurst, G. A. "Making Every Second Count": Utilizing TikTok and Systems Thinking to Facilitate Scientific Public Engagement and Contextualization of Chemistry at Home. *J. Chem. Educ.* **2020**, *97* (10), 3858–3866. https://doi.org/10.1021/acs.jchemed.0c00511

Hight, M. O.; Nguyen, N. Q.; Su, T. A. Chemical Anthropomorphism: Acting Out General Chemistry Concepts in Social Media Videos Facilitates Student-Centered Learning and Public Engagement. *J. Chem. Educ.* **2021**, *98* (4), 1283–1289. https://doi.org/10.1021/acs.jchemed.0c01139

Hurst, G. A. Utilizing Snapchat to facilitate engagement with and contextualization of undergraduate chemistry. *J. Chem. Educ*. **2018**, *95* (10), 1875–1880. https://doi.org/10.1021/acs.jchemed.8b00014

Eclética Química, vol. 48, n. 2, 2023, 17-21
ISSN: 1678-4618
DOI: 10.26850/1678-4618eqj.v48.2.2023.p17-21

Lutfi, A.; Hidayah, R. Gamification for Learning Media: Learning Chemistry with Games Based on Smartphone. *J. Phys.: Conf. Ser.* **2021**, *1899* (1), 012167. https://doi.org/10.1088/1742-6596/1899/1/012167

Putri, I. Y. V. S.; Rahayu, S.; Dasna, I. W. *Game-Based Learning Application in Chemistry Learning: A Systematic Literature Review*. *Jurnal Pendidikan MIPA*. **2022**, *23* (1), 1–12.

Rinda, R. K.; Novawan, A.; Miqawati, A. H. Students' Perspectives on Social Media-Based Learning of Writing Through Instagram. *JEAPCo*, **2018**, *5* (1), 23–33.

Sari, S.; Anjani, R.; Farida, I.; Ramdhani, M. A. Using Android-Based Educational Game for Learning Colloid Material. *J. Phys.: Conf. Ser*. **2017**, *895*, 012012. https://doi.org/10.1088/1742-6596/895/1/012012

Shay, L. A.; Lafata, J. E. Where Is the Evidence? A Systematic Review of Shared Decision Making and Patient Outcomes. *Med. Decis. Making*. **2015**, *35* (1), 114–131. https://doi.org/10.1177/0272989X14551638

Smith, D. K. ITube, YouTube, WeTube: Social Media Videos in Chemistry Education and Outreach. *J. Chem. Educ.* **2014**, *91* (10), 1594–1599. https://doi.org/10.1021/ed400715s

Xiao, C.; Cai, H.; Su, Y.; Shen, L. Online Teaching Practices and Strategies for Inorganic Chemistry Using a Combined Platform Based on DingTalk, Learning@ZJU, and WeChat. *J. Chem. Educ.* **2020**, *97* (9), 2940–2944. https://doi.org/10.1021/acs.jchemed.0c00642

Zdravkova, K. Reinforcing Social Media Based Learning, Knowledge Acquisition and Learning Evaluation. *Procedia Soc. Behav. Sci*. **2016**, *228*, 16–23. https://doi.org/10.1016/j.sbspro.2016.07.003

Ziegler, S. G. The (mis)education of Generation M. *Learn. Media. Technol.* **2007**, *32* (1), 69–81. https://doi.org/10.1080/17439880601141302

Eclética Química, vol. 48, n. 2, 2023, 17-21
ISSN: 1678-4618
DOI: 10.26850/1678-4618eqj.v48.2.2023.p17-21

Eclética Química

Review article

revista.iq.unesp.br

| Vol. 48 | n. 2 | 2023 |

Second-generation ethanol: concept, production and challenges

Pedro Vinícius Costa Medeiros[1], Paulo Henrique Medeiros Theophilo[2], Gisele Simone Lopes[2+], Lívia Paulia Dias Ribeiro[1]

1. University for International Integration of the Afro-Brazilian Lusophony, Advanced Center for Analytical Technologies, Redenção, Brazil.
2. Federal University of Ceará, Laboratory for Applied Chemical Studies, Fortaleza, Brazil.

+Corresponding author: Gisele Simone Lopes, **Phone:** +55 85 988346399, **Email address:** gslopes@ufc.br

ARTICLE INFO

Article history:
Received: March 07, 2022
Accepted: March 03, 2023
Published: April 01, 2023

Section Editors: Marcos Carlos de Mattos

Keywords:
1. 2G ethanol
2. biomass
3. alternative energy

ABSTRACT: The use of biological agents for the large-scale production of biofuels has stood out as successful processes for the advancement of science in the world. The growing exploitation of biomass in the agricultural sector and the emergence of new energy sources generated from food industry waste have become attractive and viable due to the potential and variety of possibilities for using different sources of biomass. The present review was carried out through careful bibliographical research in the literature and in scientific journals for the current discussion of concepts, production methodologies and challenges for the energy sector considering second-generation ethanol (2G ethanol). Several 2G ethanol production methodologies have been implemented as a potential low-cost alternative energy production that follows the principles of Green Chemistry.

CONTENTS

Eclética Química, vol. 48, n. 2, 2023, 22-34
ISSN: 1678-4618
DOI: 10.26850/1678-4618eqj.v48.2.2023.p22-34

1. Introduction

Sugarcane originated in the Southeast Asian region, near India. This desired product that passed through lands such as Genoa, Venice and Sicily had contact with Brazilian lands through Portuguese colonization, being brought by settlers from Madeira Island, famous for being the largest producer of sugarcane in the 15th century. During the Portuguese colonization, the province of Pernambuco, in a short period of time, became one of the most important and profitable lands in Portuguese possession. In addition to its coastal location, Pernambuco was ideal for planting sugarcane, with geographical (intense solar radiation) and natural (soil and climate) conditions favoring its exploitation and use in mills throughout the region. The mills produced not only sugar, but also one of the biggest by-products of sugarcane, ethanol, which was essential for the Portuguese rise in the world.

Nowadays, six centuries later, occupying the second largest producer and consumer of ethanol in the world, only behind the USA (UNEM, 2021), Brazil is responsible for producing about 31.6 billion liters of ethanol in 2019, according to the website of Agency of Brazil and Conab (National Supply Company of Brazil) (Agência Brasil, 2019). Hydrated ethanol sold at gas stations reaches 18.9 billion liters and anhydrous ethanol, used in the mixture with gasoline sold at gas stations, reaches 10.5 billion liters. In addition, the Midwest region is the one that most uses cereals for the production of ethanol in the national territory, about 1.27 billion liters in 2019.

The production of ethanol in abundance has an equivalent generation of residues that presents difficult decomposition, causing damage to the environment due to the accumulation of these materials (Herrera-Ruales and Arias-Zabala, 2014); therefore, techniques have been developed that use residues that are usually discarded from the main processes in the production of ethanol, but which are rich in cellulose, hemicellulose and lignin that, after undergoing pretreatments, steps and chemical processes, are converted into biofuels.

2. Second-generation (2G) ethanol

The USA occupies the position of one of the largest emitters of carbon dioxide on the planet; 2019 data record about 6,558 million tons of emission (US EPA, 2021). On the other hand, we celebrate the encouraging return of the USA, in 2020, to the Paris Climate Agreement proposed by COP21-2015 (21st Conference of Parties to the United Nations Framework Convention on Climate Change), which aimed to bring positive climate change, in order to reduce the environmental impacts resulting from the drastic increase in the temperature of the planet.

The matter is urgent for our planet, as it triggers other problems for all of us, such as the low yield of food production, the constant threat to biodiversity, compromised water quality in rivers and seas, and the possibility of extreme natural events as well.

Solutions that can minimize the effects mentioned above are frequently studied and developed around the world. The idea that has drawn the attention of many researchers is the use of discarded matter in agriculture, known as biomass or lignocellulosic biomass and confirmed as the most abundant renewable resource in nature (Yu *et al.*, 2018). One of the ideas that has been gaining strength is the use of biomass from sugarcane bagasse to produce 2G ethanol.

Raízen, a joint venture between Cosan and Shell, announced in 2022 the construction of four industrial plants to produce 2G ethanol using biomass from sugar cane, becoming the only one in the world to operate with a greater number of cellulosic ethanol plants on an industrial scale (Boechat *et al.*, 2022).

Most of the raw biomass, after pretreatment, are composed of hemicellulose (~28%), cellulose (~40%), lignin (~33%), extracts (~2%) and ash (< 1%), as shown in Fig. 1. The extracts are low molar mass chemical compounds. They consist mainly of terpenes, fats, waxes, and phenolics, and their content and composition vary among species, location and season (Jönsson and Martín, 2016). These components are associated with different types of cellular organization and biochemical processes of biomass, which makes their composition relative from one species to another. The use of lignocellulosic biomass discarded in biorefineries has been surprisingly positive. Recent study showed the possibility of obtaining monomers for polymers, high-value fuels and pharmaceutical intermediates that have a wide variety of structural complexity (Bender *et al.*, 2018).

Eclética Química, vol. 48, n. 2, 2023, 22-34
ISSN: 1678-4618
DOI: 10.26850/1678-4618eqj.v48.2.2023.p22-34

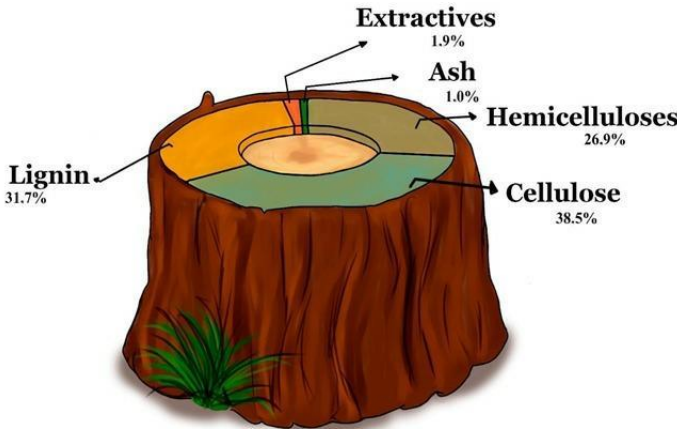

Figure 1. Representation of lignin, hemicellulose, cellulose, extractives and ash sources from plant biomass.
Source: Adapted from Jönsson and Martín (2016).

Regarding the issue mentioned above, the alternative of using 2G ethanol fits as a sustainable option for reducing greenhouse gases, in addition to increasing ethanol production per area of land. This alternative envisages being able to reduce the exploitation of other resources that are sources of high emission of gases, such as fossil fuels.

However, the production of 2G ethanol is not consolidated as it presents economic and technological obstacles (Elias *et al.*, 2021). The process of obtaining 2G ethanol needs to be detailed, because every type of raw material needs a pretreatment to successfully release the sugars contained in cellulose fibers that are incorporated into the bases of plant cell walls (Agbor *et al.*, 2011).

The main steps listed for the manufacture of 2G ethanol consist of pretreatment, hydrolysis and fermentation, those of which require greater care for each type of biomass exploited. The general model for representing the transformation of biomass is shown in Fig. 2.

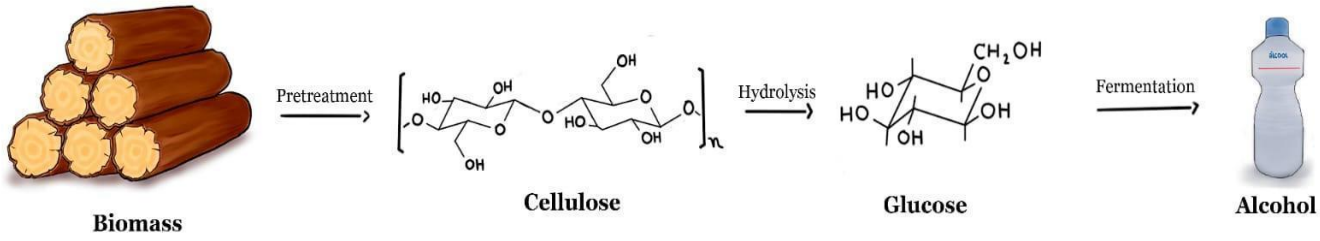

Figure 2. Representation of 2G ethanol production from lignocellulosic material.
Source: Adapted from Santos *et al.* (2012).

2.1 Pretreatment

Jönsson and Martín (2016) stated that pretreatment is an important step in the process that aims to eliminate the physical and chemical barriers that make native biomass recalcitrant and cellulose accessible for enzymatic hydrolysis, which is a fundamental step in the biochemical processing of lignocellulose based on the sugar platform concept. The efficiency of the process comes from increasing the surface of accessible cellulose through the solubilization of lignocellulosic residues such as lignin or/and hemicelluloses that cover the biomass.

Usually, pretreatment is carried out with the objective of reducing the degree of crystallinity of the cellulose, increasing the contact surface of the material leaving them porous, thus facilitating the conversion of sugars, eliminating hemicelluloses and lignins, which in contact with the hydrolysis step form monomeric sugars not fermentable by yeast (Beig *et al.*, 2021). The breakage of the lignocellulosic wall is schematized in Fig. 3.

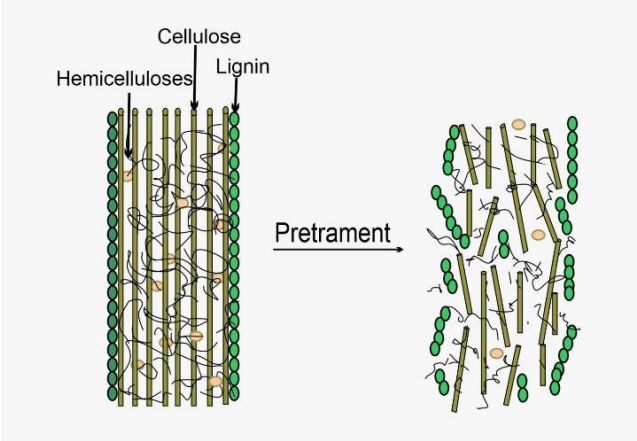

Figure 3. Biomass submitted to pretreatment, with the elimination of hemicellulose and lignins.
Source: Adapted from Santos *et al.* (2012).

Eclética Química, vol. 48, n. 2, 2023, 22-34
ISSN: 1678-4618
DOI: 10.26850/1678-4618eqj.v48.2.2023.p22-34

The concept of lignin-carbohydrate complex is well accepted in biomass chemistry, which is a cross-linked structure formed by the interconnection of polysaccharides (cellulose and hemicellulose) (Cui *et al.*, 2022). Lignin is a highly branched aromatic macromolecule composed of guaiacyl propane (methoxy-3-hydroxy-4-phenylpropane), syringyl-propane (dimethoxy-3-5-hydroxy-4-phenyl-propane) and hydroxyphenyl propane units that bind cellulose and hemicellulose together (Yu *et al.*, 2018).

Due to the complex matrix of lignocellulosic biomass and the peculiarity of recalcitrance of the material, we are faced with the obstacle of water-insoluble matter and the impossibility of being directly hydrolyzed to produce sugars. Therefore, the pretreatment step is mandatory.

Often, the reactions involved in pretreatment result in products derived from lignocellulosic materials that are inhibitors to the biochemical process, mainly because the lignin dissolved in the solution can be attached to the biomass surface, leading to decreased access of enzymes to cellulose and lignin, which can also cause inhibition of cellulase activity due to nonproductive adsorption through hydrophobic, electrostatic and hydrogen bonding interactions (Huang *et al.*, 2022), which become significant in large quantities of products. Hitherto, pretreatment records cannot be quantified, as we have numerous different sources of biomass, each with its own particularities and cellular organizations. However, some techniques show good results with different types of biomass and are therefore more commonly used and are routine procedures.

Some studies are investigating the interaction between lignin and cellulase, which is aimed to understand how lignin inhibits the enzymatic hydrolysis efficiency of cellulose (Cui *et al.*, 2022; Lu *et al.*, 2016; Zhao *et al.*, 2022). They also provide new evidence for the structural information between cellulose and lignin in poplar using ^{13}C NMR, ^{1}H NMR and 2D NMR analyses.

Pretreatment methods can be divided into categories including, physical (milling, microwave, ultrasound, and pyrolysis), chemical (acid, alkali, ozonolysis, and organic solvent, ionic liquids), physicochemical (hot water, steam explosion, ammonia based, wet oxidation, and carbon dioxide, CO_2) and biological (microbial and enzymatic). For each material, there may be more than one pretreatment considering that the most efficient methods may not be according to availability, there are adaptations of pretreatments or substitutions to arrive at the desired material (Meenakshisundaram *et al.*, 2021; Silva *et al.*, 2022; Zanivan *et al.*, 2022).

2.1.1 Acid-based methods

Acid hydrolysis is one of the most promising pretreatment methods regarding industrial implementation, due to the low methodological complexity. Acid-based methods are divided into weak acid and strong hydrolysis (Karatzos *et al.*, 2012).

The dilute acid treatment (e.g., maleic and fumaric acids) is one of the most effective pretreatment methods for lignocellulosic biomass. In general, there are two types of weak acid hydrolysis: High temperature ($T > 160$ °C) and continuous flow process for low-solids loading (5–10 wt% substrate concentration) and low temperature ($T < 160$ °C) and batch process for high-solids loading (10–40% substrate concentration) (Harmsen *et al.*, 2010).

Concentrated strong acids, such as H_2SO_4 and HCl, have been widely used for treating lignocellulosic materials because they are powerful agents for cellulose hydrolysis, but organic acids and sulfur dioxide are also used to a lesser extent (Assumpção *et al.*, 2016; Harmsen *et al.*, 2010).

This type of pretreatment results in high recovery of hemicellulosic sugars in the pretreatment liquid and a solid cellulose fraction with enzymatic convertibility. Acid pretreatment also has some disadvantages, such as high cost of materials used for reactor construction, gypsum formation during neutralization after sulfuric acid treatment, and formation of inhibitory by products (Jönsson and Martín, 2016). In addition, acid pretreatment can also lead to increased toxicity of the waste generated during the process.

2.1.2 Chemical pulping processes

Sulfite pretreatments are well-known and use acids, alkalis or neutral sulfite that show high recovery of hemicellulose sugars and enhance the susceptibility of the cellulose to enzymatic hydrolysis efficiency (Huang *et al.*, 2022). Despite being a technique that delivers satisfactory results, its execution is expensive due to the materials used in the construction of the reactors and can result in the production of inhibitory by-products after their neutralization (Jönsson and Martín, 2016).

2.1.3 Alkaline methods

Alkali pretreatment is based on saponification of intermolecular ester bonds crosslinking xylan hemicelluloses and other components such as lignin. This method removes acetyl and the various uronic acid substitutions on hemicellulose that lower the

Eclética Química, vol. 48, n. 2, 2023, 22-34
ISSN: 1678-4618
DOI: 10.26850/1678-4618eqj.v48.2.2023.p22-34

accessibility of the enzyme to the hemicellulose and cellulose surface (Harmsen *et al.*, 2010).

Alkaline pretreatment with heating results in lignin dehydration processes, promoting the formation of reactive compounds such as furfural and hydroxy-methyl-furfural, which are inhibitors of the metabolism of ethanol producing microorganisms. For this reason, it is important to control the temperature so that these reactions are not promoted. On the other hand, cleavage of acetyl groups may contribute to the formation of more reactive compounds such as furfural. Thus, alkaline pretreatments are highly efficient for the degradation of lignin and hemicellulose, which can increase bioethanol. However, it is important to control the temperature to avoid the formation of undesirable compounds (Carrillo *et al.*, 2005).

2.1.4 Oxidative methods

The crystallinity index can be reduced in pretreatment by adding oxidants to the biomass using alkali metal peroxide, wet oxidation and ozonolysis (Jönsson and Martín, 2016). The feasibility of the method is due to hemicelluloses solubilized and recovered as oligosaccharides in wet oxidation, which are of great interest to the pharmaceutical industry and the food sector since they have prebiotic agent and body agent properties (Maugeri Filho *et al.*, 2019). The combination of wet oxidation with alkaline compounds reduces the formation of phenolic aldehydes and furans.

2.1.5 Chemical pulping processes

Chemical pulping pretreatment is a method that targets lignin and to some extent hemicelluloses. This method can be applied to both soft and hard biomass. The major technologies used are Kraft (based on NaOH and Na_2S) and sulfite pulping. In sulfite pulping, which is based on an aqueous mixture of bisulfite (HSO_3^-) and sulfite (SO_3^{2-}), the hemicelluloses are hydrolyzed and removed to the spent sulfite liquor, while the cellulose is maintained almost intact (Mboowa, 2021).

Sulfite pretreatments are well-known and use acids, alkalis or neutral sulfite that show high recovery of hemicellulose sugars and enhance the susceptibility of the cellulose to enzymatic hydrolysis efficiency (Huang *et al.*, 2022). Despite being a technique that delivers satisfactory results, its execution is expensive due to the materials used in the construction of the reactors and can result in the production of inhibitory by products after their neutralization (Jönsson and Martín, 2016).

2.1.6 Hydrothermal processing

One alternative procedure is the hydrothermal processing, which consists of water in the vapor phase or liquid phase used in the biomass, being positive because it does not require the use of a catalyst and does not present significant corrosion problems. The key to the method is to control the pH around neutral values, which minimizes the formation of fermentation inhibitors, since in the process the water penetrates the biomass, hydrating the cellulose and removing part of the hemicelluloses and a small portion of the lignin (Jönsson and Martín, 2016).

Hydrothermal pretreatment was developed for cellulose recovery processes for conversion into ethanol. It is an energy-efficient, economical and eco-friendly technique because it employs water as a solvent in high temperature and pressure ranges. The conditions of the reaction medium can be divided based on the specific critical point of water (374 °C and 22.1 MPa), which separates into subcritical or supercritical hydrothermal pretreatment (HTP) (Ilanidis *et al.*, 2021; Saritpongteeraka *et al.*, 2020).

In addition, the systemic organization of the hemicellulosic matrix and the strong association of hemicellulose with the other components of the lignocellulosic complex confer resilience to the biomass cell wall. HTP stimulates the direct dissolution of hemicellulose into its sugars (arabinose, xylose, galactose, glucose, mannose), resulting in the synthesis of industrially attractive by-products, such as xylooligosaccharides, furfural and 5-hydroxymethylfurfural, and levulinic, acetic and formic acids (Ilanidis *et al.*, 2021).

The expansion and strengthening of multiproduct biorefineries have highlighted HTP, and it has been adapted for biomass fractionation through hemicellulose solubilization and lignin redistribution. The significant diffusion of HTP is a result of numerous advantages, such as competitive cost, limited use of catalysts, and sustainable and environmentally friendly properties (Scapini *et al.*, 2021).

Despite all the benefits of hydrothermal pretreatment, there are still some disadvantages of the process, such as high costs, the need for equipment that can withstand high pressures and temperatures, and the degradation of some compounds. In addition, the complexity of the reaction and the need for strict monitoring of the operating parameters also represent challenges for the commercial application of the process.

Eclética Química, vol. 48, n. 2, 2023, 22-34
ISSN: 1678-4618
DOI: 10.26850/1678-4618eqj.v48.2.2023.p22-34

2.1.7 Ionic liquid

A variety of ionic liquids (ILs), such as ammonium, pyridinium, imidazolium, and phosphonium-based cations, attached to alkyl or allyl side chains coupled to various anions, such as chloride, acetate, and phosphonate, has been used in the pretreatment of lignocellulosic biomass and presents an attractive method for presenting promising results; however, the final product presents potentially toxic by-products for fermentation microorganisms (Karatzos *et al.*, 2012).

ILs present high thermal stabilities and negligible vapor pressures; they do not release toxic or explosive gas when used, giving environmentally friendly characteristics (Karatzos *et al.*, 2012).

There are reports lignin removal from biomass, 29% total lignin removal from triticale straw using 1-ethyl-3-methylimidazolium acetate ([Emim]Ac) as a pretreated solvent at 150 °C for 1.5 h (Fu and Mazza, 2011). 1-Butyl-3-methylimidazolium chloride ([Bmim]Cl) was investigated as an IL solvent for pretreatment of legume straw at 150 °C for 2 h and observed 30% lignin removal (Wei *et al.*, 2012). Currently, studies (Asakawa *et al.*, 2015; Li *et al.*, 2007) have been conducted regarding lignin yield, as lignin is a potential renewable source for valuable products. Pretreatment of corn stalks with [Emim]Ac at 125 °C for 1 h resulted in a lignin yield of 44% (Li *et al.*, 2007). Bagasse fractionation was performed at 110 °C for 16 h with choline acetate, and 20% of the lignin was fractionated as lignin-rich material (Asakawa *et al.*, 2015).

ILs such as [Emim]Cl, [Bmim]Cl and [Emim]Ac have been widely advertised for the pretreatment of lignocelluloses; however, high pretreatment temperatures and long processing times are always required (Wang *et al.*, 2017).

Although the pretreatments appear separate, there is a way to use them in collaboration with other methods to obtain and investigate better results, as done by Yu *et al.* (2018), who used ultrasound pretreatment with ionic liquid at frequencies of 20, 28, 35, 40 and 50 kHz with 100 W power.

2.2 Hydrolysis

Hydrolysis is the step in which the cellulose and hemicellulose present in the biomass matrix, partially free from the lignin envelope, can be converted into pentoses and hexoses to be fermented, as schematically shown in Fig. 4 (Harmsen *et al.*, 2010; Grasel *et al.*, 2017). Despite expressing the acid hydrolysis process, the idea can be extended to the general concept of cellulose hydrolysis, since there are two varieties of possibilities widely used for this step: enzymatic hydrolysis or acid hydrolysis.

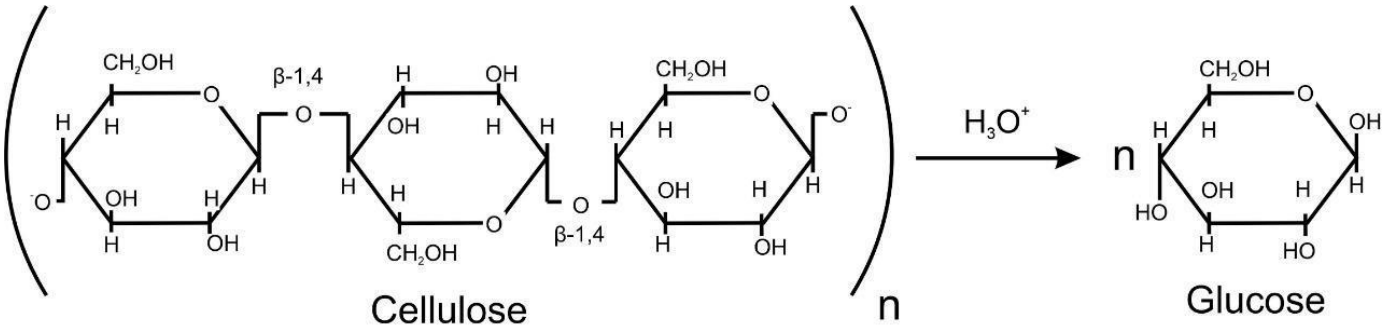

Figure 4. Cleavage of the β-1,4 glycosidic bonds of cellulose in an acidic medium and obtaining glucose.
Source: Adapted from Grasel *et al.* (2017).

2.2.1 Enzymatic hydrolysis

Enzymatic hydrolysis is carried out mainly by using the enzyme cellulase and hemicellulose, which breaks down cellulose and some other polysaccharides while keeping the lignin intact. Several factors can affect the yield and rate of enzymatic hydrolysis as well as limit the duration of the process depending on the substrate and enzyme. Substrate-related factors are cellulose crystallinity, degree of polymerization, available surface area, porosity, lignin barrier, hemicellulose content, particle size, cell wall thickness and capacity access to glucan, while enzyme-related factors are cellulase activity, reducing the cost and composition of the cocktail (Martins *et al.*, 2015).

Hemicellulose can also be attacked at intermediate positions along its skeleton, releasing oligomers made of many sugar molecules; these oligomers can be successively broken down into even smaller oligomers before a single sugar molecule can be formed. However, the breakdown of the released sugars can be moderate

Eclética Química, vol. 48, n. 2, 2023, 22-34
ISSN: 1678-4618
DOI: 10.26850/1678-4618eqj.v48.2.2023.p22-34

enough to recover about 80–90% of the maximum possible sugars (Ogeda and Petri, 2010).

The enzymatic hydrolysis of cellulose to produce 2G ethanol is a good alternative as it has temperature conditions of 40–59 °C at atmospheric pressure. However, as it is a process that takes 48 to 72 h, including catalytic deactivation by inhibiting enzymatic activity, as well as the use of enzymes such as cellulase, which have less environmental impact compared to acid hydrolysis (Cunha *et al.*, 2012), the process has a high cost to be accomplished. The residual lignin has an affinity for enzymatic adsorption, making it difficult for the enzymes to hydrolyze lignocellulosic matter, drastically increasing the amount of enzymes necessary for the glucose conversion to cellulose, increasing the cost of procedure (Florencio *et al.*, 2016).

The costs can be solved with methodologies that aim not only to reduce the number of enzymes used in the process, but also to improve the yield of saccharification and fermentation reactions, which consequently have a greater number of sugars to be fermented. A method that can reduce the total cost of enzymatic hydrolysis is the addition of lignin blocking agents at this stage, these blockers indicate increases in the alcoholic conversion rate, as the study by Kristensen *et al.* (2007) in the evaluation of the use of Tween 80 (Polysorbate 80) in Abies, which showed a 58% increase in the rate of conversion of biomass into available glucose. It is worth noting that the effect of the increase varies according to the type of biomass and pretreatment used.

2.2.2 Acid hydrolysis

Acid hydrolysis has inorganic acids, mostly sulfuric acid under high pressure conditions, for the cleavage or separation of the cellulose glycosidic bonds to obtain glucose (Harmsen *et al.*, 2010).

Although the two options are the most widespread in the sphere of the study on biomass, there are procedures used together that can meet the demand for breaking down cellulose, such as the one used by Tsubaki *et al.* (2017), who investigated the use of polyoxometalates with activated carbon support to the acceleration of hydrolysis under microwave irradiation.

Following these fundamental steps, sugars produced in the hydrolysis will be the direct source to produce ethanol; monosaccharides, which are simple carbohydrates with 4 to 6 carbons in their structure (Allinger *et al.*, 1976). These sugars are found in different proportions after hydrolysis of cellulose and hemicellulose; although it is not possible to predict the exact amounts of the sugars obtained, it is possible to have a projection of what they will be based on the type of material chosen.

Some examples: Pentoses (xylose and arabinose) are major monosaccharides in the hydrolysis of biomass from hardwoods (cane sugar, ipê tree and andiroba) and annual plants (corn and soybean). Hexose (glucose, mannose, galactose rhamnose) are major monosaccharides in the hydrolysis of softwood biomass (cane sugar and Paraná pine) (Agbor *et al.*, 2011; Jönsson and Martín, 2016; Rabemanolontsoa and Saka, 2013). It is important to point out that these statements are of major monosaccharides in these species, it does not mean that a species is devoid of one or another sugar. Such sugars will serve as an energy source for fermentation.

2.3 Fermentation

Fermentation is the step in which a microorganism (fungus or bacteria) transforms carbohydrates and produces ethanol. The options depend on what is worked on, considering that in many cases different rates of yield are obtained for different raw materials. This fact is given by the different types of sugars obtained, and the limitations of microorganisms (Tse *et al.*, 2021).

Due to their ease of acquisition and handling, the fungus *Saccharomyces cerevisiae* and the bacterium *Zymomonas mobilis* are the most used microorganisms in biomass fermentations, as they have high yields of ethanol rates. Values around 70–80% and higher at converting hexoses can be reached, despite their inactivity with xylose—the main pentose of hemicellulose (Hasner *et al.*, 2015). There are other types of microorganisms popular for being able to ferment hexoses and pentoses, such as *Scheffersomyces stipitis* and *Candida shehatae*; however, with limitations such as low consumption of sugars (Mengesha *et al.*, 2022).

The knowledge of species that ferment pentoses is still limited. Among the main species that ferment xylose, it can be mentioned *Pachysolen tannophilus, S. stipitis, Scheffersomyces shehatae, Kluyveromyces marxianus, Candida guilliermondii, Candida tenuis, Brettanomyces naardenensis, Scheffersomyces segobiensis* have been studied in the fermentation processes of pentoses. There are still challenges to controlling the fermentation of pentoses to ethanol, such as the low tolerance to ethanol by pentose fermenting yeasts. Also, the presence of glucose in hemicellulosic hydrolysates may act as a repressor of genes responsible for xylose utilization (Tse *et al.*, 2021).

Fermentations can occur using only one type of yeast (monoculture) or the combination of two or more yeasts (coculture). Regarding this topic, cocultures with

Eclética Química, vol. 48, n. 2, 2023, 22-34
ISSN: 1678-4618
DOI: 10.26850/1678-4618eqj.v48.2.2023.p22-34

genetically modified microorganisms have drawn attention in more recent studies, as their exception can supply the needs that isolated cultures have. Fermentation is a delicate step, as it requires the stability of factors such as temperature, reaction time, pH, bacterial contamination and organic and inorganic nutrients, which vary in quantity and type according to the material and microorganism chosen (Mengesha *et al.*, 2022).

3. Cellulose sources for ethanol production

The agricultural environment faces adversities due to demands that are not expected and supported by cycles of nature. In view of this, the negative impacts on the environment are almost inevitable, and if they are not minimized, they may be irreversible, as reinforced by Marques *et al.* (2007). These researchers stated that, given the great demand required by a socioeconomic system of society, the self-cleaning capacity of the aquatic cycle is compromised. Therefore, the importance of methodologies that have the ability to decelerate or reduce environmental degradation is no longer a small attraction to become a major priority.

It is important to mention that Brazil, as one of the largest holders of biological diversity, whether fauna or flora, has a variety of resources from unexplored sources for the conversion of sources of lignocellulosic materials. Moreover, we are faced with the use of various parts of a plant. As mentioned below, the cases range from studies involving parts of the same *Musa cavendishii* plant to the use of waste, such as the fiber present in the green coconut husk. The summarized list of the cases presented below are shown in Table 1.

Table 1. Different methodologies used in recent studies of 2G ethanol production through the purchase of biomass source, pretreatment, microorganism and yield results of pulp fermentation.

Cellulosic source	Pretreatment	Microorganism	Yield results
Cavendish banana (*Musa cavendishii*)	acid hydrolysis	*Saccharomyces cerevisiae*	34%
Orange albedo	acid hydrolysis	N.F*	49.7%
Elephant grass (*Pennisetum purpureum*)	acid hydrolysis	*Saccharomyces cerevisiae*	79%
Citrus pulp bran and orange pomace	enzymatic hydrolysis	*E.C* (Xanthomonas axonopodis, Saccharomyces cerevisiae)*	Monoculture: 50-99%
		Candida parapsilosis (IFM 48375 and NRRL Y-12969)	Coculture: 74-100%
Avocado seed (*Persea americana* Mill.)	enzymatic hydrolysis	*Yeast*	33.8%
Banana pseudostem	acid hydrolysis	*Saccharomyces* and *Zymomonas mobilis*	60%
		Scheffersomyces stipitis and *Pachysolen tannophilus*	
Green coconut husk fibers	Alkaline pretreatment and enzymatic hydrolysis	*Saccharomyces cerevisiae*	30.5%

*N.F. (not fermented), E.C (enzyme cocktail).
Source: Elaborated by the authors using data from Souza *et al.* (2012), Montagnoli *et al.* (2018), Antunes *et al.* (2015), Grasel *et al.* (2017), Cypriano *et al.* (2017), Cabral *et al.* (2016), Kowalski *et al.* (2017).

The growing agricultural production contributes to the increase of agricultural waste. Thus, this provides a diverse and encouraging variety of unexplored lignocellulosic materials to be selected and used.

Having this potential in mind, Souza *et al.* (2012) conducted a study that used banana pulp to produce 2G ethanol. Thus, the authors analyzed the potential of using the bark and pulp of *Musa cavendishii*, known in Brazil as banana in nature, previously hydrolyzed by enzymes and acid as a substrate for alcoholic fermentation. Two series of tests were carried out containing 18 pretreatments for each case of residue evaluated, using the isolated yeast *S. cerevisiae* for fermentation. The values of total ethanol yield (Qp) obtained using banana pulp and peel were, respectively, 3.04 and 1.32 g L^{-1} h^{-1}.

Eclética Química, vol. 48, n. 2, 2023, 22-34
ISSN: 1678-4618
DOI: 10.26850/1678-4618eqj.v48.2.2023.p22-34

The results showed superior yield when compared to sources such as wheat bran, corn flour and wood chips.

Proving again to be an excellent source of biomass, the banana and its plant was also approached by Montagnoli *et al.* (2018). They used the banana pseudostem to produce 2G ethanol, using different types of microorganisms for the fermentation of pentoses and hexoses: *S. cerevisiae* and *Z. mobilis*, *S. stipitis* and *P. tannophilus*. Despite the routine used in the steps, there was an application of the use of active charcoal for the detoxification of the banana pseudostem juice, which showed an increase of up to 60% in yield.

Considering that potential, Brazil is a country with high worldwide production and consumption of citrus fruits, with oranges being the one with the highest expressive numbers for the ranking. Accordingly, Antunes *et al.* (2015) dedicated to studies of better results from fruit byproducts. Then, they aimed to study the pretreatment of orange albedo with sulfuric, nitric, hydrochloric and phosphoric acids, with concentrations of 0.5% and 1%, for the determination of reducing sugars and total reducing sugars (TRS). The acid that generated the highest values of sugars was sulfuric acid, even at a concentration of 1%. However, the quantity of sugars obtained in the form of TRS were higher only when 0.5% acid was used, regardless of the acid chosen, indicating that higher concentrations of acid can degrade the sugars generated in secondary products. Consequently, an inhibitory effect on other steps in the production of 2G ethanol, such as fermentation and hydrolysis, may occur.

Another study developed by Grasel *et al.* (2017) used the biomass from elephant grass (*Pennisetum purpureum*). Unlike other biomasses, such as runny banana, corn and sugarcane, which are seasonal crops, elephant grass can yield up to four crops in a 1-year period. In addition to the advantage of being a crop that has a short production period, elephant grass does not need specific climates or soils for cultivation. For production, the material was previously treated to separate the cellulose from other components of the plant biomass, then acid hydrolysis was used to produce glucose and, finally, the alcoholic fermentation was carried out with the unisolated *S. cerevisiae* yeast. The result of sugarcane was 96 g of ethanol 100 g^{-1} of dry biomass compared to 79 g of ethanol 100 g^{-1} of dry biomass of elephant grass.

Using a cocktail of enzymes isolated from Gram-negative, *Xanthomonas axonopodis* and *S. cerevisiae* yeasts, and two strains of the *Candida* genus (*Candida parapsilosis* IFM 48375 and NRRL Y-12969), the conversion of biomass from citrus pulp bran was evaluated: 74.8 to 100% of 1 g of industrial orange pomace was converted into 2G ethanol in fermentations, while in monocultures the conversion was from 50 to 99.0%. The production of 2G ethanol corresponded to 51.1% of fermentable sugars. Based on the data, the study developed by Cypriano *et al.* (2017) stated that 6.69 to 130.7 thousand tons of 2G ethanol could be obtained annually. In addition to the production of 2G ethanol, the author was successful in the extraction of nanocellulose—managing the combination of chemical, enzymatic, defibrillation or partial hydrolysis processes, from the orange biomass. Nanocellulose has advantages over synthetic nanofibers such as improved thermal, biodegradability and mechanical properties in addition to its renewable character (Machado *et al.*, 2014).

Another fact that has caused concern is the inadequate disposal of green coconut husk. This situation presents a set of problems to the environment, such as the difficult degradation of coconut husk, which can take from 8 to 12 years and the production of methane gas, when it is inadequately disposed of in sanitary landfills. Taking this into account, Cabral *et al.* (2016) investigated the use of green coconut husk fiber to produce reducing sugars and conversion into ethanol. Despite a significant 17.9% loss in cellulose content, enzymatic hydrolysis was successful in converting about 87% of the sugars and the fermentation consumed 81% of the hydrolyzed matter, resulting in 22.34 g TRS per 100 g of coconut fiber.

Kowalski *et al.* (2017) studied enzymatic hydrolysis processes in avocado seeds to produce second generation ethanol. The ethanol obtained was characterized and the results showed that the raw material used is excellent for biofuel production, with 1.0579 g/L of starch producing 44 L of ethanol per ton of seed, 33.8% of yield ethanol.

The constant investigation of agricultural residues has proved to be extremely advantageous and ecological, due to the global concerns as a result of population growth, global warming and the rising of oil prices (Rosa and Garcia, 2009). The number of supplies to satisfy the energy needs of the society considering the constant exponential population growth will require an increase outside the natural capacity of cropland used as sources of raw material for consumable goods, increases that compromise food production, as they require significant growth in arable land.

4. Final considerations

Evidencing the potential of different sources of biomass to produce 2G ethanol, the exploitation of these resources showed multiple possibilities of use such as obtaining biogas and the value of cellulosic nanofibers for being biodegradable, expressing properties of higher performance and superiors to synthetic nanofibers. In addition, the exploitation of 2G ethanol not only

Eclética Química, vol. 48, n. 2, 2023, 22-34
ISSN: 1678-4618
DOI: 10.26850/1678-4618eqj.v48.2.2023.p22-34

combines with the current appeal of green chemistry, but also brings low-cost materials available in abundance in the nature of photosynthesis (Cypriano *et al.*, 2017).

Even in some cases of biomass, pretreatments require more expensive methodologies, the use of biomass becomes not only an excellent alternative for a cleaner future, but also a set of affordable solutions. Although the Brazilian Company Raízen is one of the few that includes 2G ethanol in its production sphere, the 50% increase in production after the implementation of the use of biomass may encourage others to join the method. These reservations and initiatives show the positive impact that can be caused by the global implementation of 2G ethanol.

The 2G ethanol production methodologies are diverse and have difficulties in implementing projects that are sufficiently attractive for large corporations, however, there are expansion projects for Asia, India and Thailand as they are sugarcane producers. Even with the possibility of expanding to new 2G ethanol producing countries, Brazil will still be the largest producer of this alternative energy due to its enormous agricultural potential and available biomass.

Authors' contribution

Conceptualization: Medeiros, P. V. C.; Theophilo, P. H. M.; Ribeiro, L. P. D.; Lopes, G. S.
Data curation: Medeiros, P. V. C.; Theophilo, P. H. M.
Formal Analysis: Medeiros, P. V. C.; Theophilo, P. H. M.
Funding acquisition: Ribeiro, L. P. D.; Lopes, G. S.
Investigation: Medeiros, P. V. C.; Theophilo, P. H. M.
Methodology: Medeiros, P. V. C.; Theophilo, P. H. M.
Project administration: Ribeiro, L. P. D.; Lopes, G. S.
Resources: Ribeiro, L. P. D.; Lopes, G. S.
Software: Not applicable.
Supervision: Ribeiro, L. P. D.; Lopes, G. S.
Validation: Ribeiro, L. P. D.; Lopes, G. S.
Visualization: Ribeiro, L. P. D.; Lopes, G. S.
Writing – original draft: Medeiros, P. V. C.; Theophilo, P. H. M.; Ribeiro, L. P. D.; Lopes, G. S.
Writing – review & editing: Ribeiro, L. P. D.; Lopes, G. S.

Data availability statement

All data sets were generated or analyzed in the current study.

Funding

Instituto Nacional de Ciências e Tecnologias Analíticas Avançadas (INCTAA) – Conselho Nacional de Desenvolvimento Científico e Tecnológico (CNPQ). Process No: 465768/2014-8.

Acknowledgments

Not applicable.

References

Agbor, V. B.; Cicek, N.; Sparling, R.; Berlin, A.; Levin, D. B. Biomass pretreatment: fundamentals toward application. *Biotechnol. Adv.* **2011**, *29* (6), 675–685. https://doi.org/10.1016/j.biotechadv.2011.05.005

Agência Brasil. *Brasil deve produzir 31,6 bilhões de litros de etanol este ano*. Agência Brasil, 2019. https://agenciabrasil.ebc.com.br/economia/noticia/2019-08/brasil-deve-produzir-316-bilhoes-de-litros-de-etanol-este-ano (accessed 2020-08-20).

Allinger, N. L.; Cava, M. P.; Jongh, D. C.; Johnson, C. R.; Lebel, N. A.; Stevens, C. L. *Química orgânica*, 2nd. Livros Técnicos e Científicos; 1976.

Antunes, D. P. C.; Viana, V. L.; Santos, M. C. S.; Soares, E. L. S.; Barbosa, K. L.; Moura, K. L.; Vieira, R. C.; Almeida, R. M. R. G. Produção de bioetanol de segunda geração a partir do hidrolisado do albedo da laranja como fonte de biomassa lignocelulósica. *Blucher Chem. Eng. Proc.* **2015**, *1* (2), 305–312. https://doi.org/10.5151/chemeng-cobeq2014-0206-26537-171359

Asakawa, A.; Kohara, M.; Sasaki, C.; Asada, C.; Nakamura, Y. Comparison of choline acetate ionic liquid pretreatment with various pretreatments for enhancing the enzymatic saccharification of sugarcane bagasse. *Ind. Crops Prod.* **2015**, *71*, 147–152. https://doi.org/10.1016/j.indcrop.2015.03.073

Assumpção, S. M. N.; Pontes, L. A. M.; Carvalho L. S.; Campos, L. M. A.; Andrade, J. C. F.; Silva, E. G. Pré-tratamento combinado H_2SO_4/H_2O_2/NaOH para obtenção das frações lignocelulósicas do bagaço da cana-de-açúcar. *Rev. Virt. Quim.* **2016,** *8* (3), 803–822. https://doi.org/10.5935/1984-6835.20160059

Beig, B.; Riaz, M.; Naqvi, S. R.; Hassan, M.; Zheng, Z.; Karimi, K.; Pugazhendhi, A.; Atabani, A. E.; Chi, N. T. L. Current challenges and innovative developments in pretreatment of lignocellulosic residues for biofuel production: A review. *Fuel*. **2021**, *287*, 119670. https://doi.org/10.1016/j.fuel.2020.119670

Bender, T. A., Dabrowski, J. A.; Gagné, M. R. Homogeneous catalysis for the production of low-volume, high-value

Eclética Química, vol. 48, n. 2, 2023, 22-34
ISSN: 1678-4618
DOI: 10.26850/1678-4618eqj.v48.2.2023.p22-34

chemicals from biomass. *Nat. Rev. Chem*. **2018**, *2* (5), 35–46. https://doi.org/10.1038/s41570-018-0005-y

Boechat, C. A.; Pitta, F. T.; Toledo, C. A. National State territoriality pattern and capital autonomization in Brazilian sugar-energy agribusiness: from the Ometto family's heritage to professionalization and financialization of Cosan. *Revista NERA*. **2022**, *25* (63), 67–95.

Cabral, M. M. S.; Abud, A. K. S.; Silva, C. E. F.; Almeida, R. M. R. G. Bioethanol production from coconut husk fiber. *Cienc. Rural.* **2016**, *46* (10), 1872–1877. https://doi.org/10.1590/0103-8478cr20151331

Carrillo, F.; Lis, M. J.; Colom, X.; López-Mesas, M.; Valldeperas, J. Effect of alkali pretreatment on cellulase hydrolysis of wheat straw: Kinetic study. Process Biochem. **2005**, *40* (10), 3360–3364. https://doi.org/10.1016/j.procbio.2005.03.003

Cui, S.; Xie, Y.; Wei, X.; Zhang, K.; Chen, X. Exploration of the chemical linkages between lignin and cellulose in poplar wood with 13C and Deuterium dual isotope tracer. *Ind. Crops Prod.* **2022**, *187* (Part. B), 115452. https://doi.org/10.1016/j.indcrop.2022.115452

Cunha, F. M.; Bacchin, A. L. G.; Horta, A. C. L.; Zangirolami, T. C.; Badino, A. C.; Farinas, C. S. Indirect method for quantification of cellular biomass in solids containing medium used as pre-culture for cellulase production. *Biotechnol Bioproc E.* **2012**, *17* (1), 100–108. https://doi.org/10.1007/s12257-011-0405-z

Cypriano, D. Z.; Silva, L. L.; Mariño, M. A.; Tasic, L. A Biomassa da laranja e seus subprodutos. *Rev. Virtual Quim.* **2017**, *9* (1), 176–191. https://doi.org/10.21577/1984-6835.20170014

Elias, A. M.; Longati, A. A.; Giordano, R. C.; Furlan, F. F. Retro-techno-economic-environmental analysis improves the operation efficiency of 1G-2G bioethanol and bioelectricity facilities. *Appl. Energy*. **2021**, *282* (Part. A), 116133. https://doi.org/10.1016/j.apenergy.2020.116133

Florencio, C.; Badino, A. C.; Farinas, C. S. Soybean protein as a cost-effective lignin-blocking additive for the saccharification of sugarcane bagasse. *Bioresour. Technol.* **2016**, *221*, 172–180. https://doi.org/10.1016/j.biortech.2016.09.039

Fu, D.; Mazza, G. Aqueous ionic liquid pretreatment of straw. *Bioresour. Technol*. **2011**, *102* (13), 7008–7011. https://doi.org/10.1016/j.biortech.2011.04.049

Grasel, F. S.; Stiehl, A. C. R.; Bernardi, L. P.; Herpich, T. L.; Behrens, M. C.; Andrade, J. B.; Schultz, J.; Mangrich, A. S. Inovação em biorrefinarias I. Produção de etanol de segunda geração a partir de capim-elefante (*Pennisetum purpureum*) e bagaço de cana-de-açúcar (*Saccharum officinarum*). *Rev. Virtual Quim.* **2017**, *9* (1), 4–14. https://doi.org/10.21577/1984-6835.20170003

Harmsen, P. F. H.; Huijgen, W. J. J.; Bermudez López, L. M.; Bakker, R. R. C. Literature Review of Physical and Chemical Pretreatment processes for Lignocellulosic Biomass. Report of the BioSynergy project, **2010**.

Hasner, C.; Santos, D. A.; Lima, A. A. Etanol no Brasil: Evolução do patenteamento de tecnologias de fermentação para a produção de etanol combustível de cana-de-açúcar no período de 2007 a 2014. *Cad. Prospec.* **2015**, *8* (1), 133–141. https://doi.org/10.9771/S.CPROSP.2015.001.015

Herrera-Ruales, F. C.; Arias-Zabala, M. Bioethanol production by fermentation of hemicellulosic hydrolysates of African palm residues using an adapted strain of *Scheffersomyces stipitis*. *Dyna*. **2014**, *81* (185), 204–210. https://doi.org/10.15446/dyna.v81n185.38552

Huang, C.; Li, R.; Tang, W.; Zheng, Y.; Meng, X. Improve Enzymatic Hydrolysis of Lignocellulosic Biomass by Modifying Lignin Structure via Sulfite Pretreatment and Using Lignin Blockers. *Fermentation.* **2022**, *8* (10), 558. https://doi.org/10.3390/fermentation8100558

Ilanidis, D.; Wu, G.; Stagge, S.; Martín, C.; Jönsson, L. J. Effects of redox environment on hydrothermal pretreatment of lignocellulosic biomass under acidic conditions. *Bioresour. Technol.* **2021**, *319*, 124211. https://doi.org/10.1016/j.biortech.2020.124211

Jönsson, L. J.; Martín, C. Pretreatment of lignocellulose: formation of inhibitory by-products and strategies for minimizing their effects. *Bioresour. Technol*. **2016**, *199*, 103–112. https://doi.org/10.1016/j.biortech.2015.10.009

Karatzos, S. K.; Edye, L. A.; Doherty, W. O. S. Sugarcane bagasse pretreatment using three imidazolium-based ionic liquids; mass balances and enzyme kinetics. *Biotechnol. Biofuels*. **2012**, *5*, 62. https://doi.org/10.1186/1754-6834-5-62

Kowalski, R. L.; Schneider, V. S.; Moretto, J.; Gomes, L. F. S. Produção de etanol de segunda geração a partir de caroço de abacate (*Persea americana* Mill.). *Revista Brasileira de Energias Renováveis*. **2017**, *6* (4), 665–677. https://doi.org/10.5380/rber.v6i4.49073

Kristensen, J. B.; Börjesson, J.; Bruun, M. H.; Tjerneld, F.; Jørgensen, H. Use of active surface additives in enzymatic hydrolysis of wheat straw lignocellulose. *Enzyme Microb. Technol.* **2007**, *40* (4), 888–895. https://doi.org/10.1016/j.enzmictec.2006.07.014

Li, Q.; He, Y.; Xian, M.; Jun, G.; Xu, X.; Yang, J.; Li, L. Improving enzymatic hydrolysis of wheat straw using ionic liquid 1-ethyl-3-methyl imidazolium diethyl phosphate pretreatment. *Bioresour. Technol*. **2007**, *100* (14), 3570–3575. https://doi.org/10.1016/j.biortech.2009.02.040

Lu, X.; Zheng, X.; Li, X.; Zhao, J. Adsorption and mechanism of cellulase enzymes onto lignin isolated from corn stover pretreated with liquid hot water. *Biotechnol. Biofuels*. **2016**, *9*, 118. https://doi.org/10.1186/s13068-016-0531-0

Eclética Química, vol. 48, n. 2, 2023, 22-34
ISSN: 1678-4618
DOI: 10.26850/1678-4618eqj.v48.2.2023.p22-34

Machado, B. A. S.; Reis, J. H. O.; Silva, J. B.; Cruz, L. S.; Nunes, I. L.; Pereira, F. V.; Druzian, J. I. Obtenção de nanocelulose da fibra de coco verde e incorporação em filmes biodegradáveis de amido plastificados com glicerol. *Quím. Nova* **2014**, *37* (8), 1275–1282. https://doi.org/10.5935/0100-4042.20140220

Marques, M. N.; Cotrim, M. B.; Pires, M. A. F.; Beltrame Filho, O. Avaliação do impacto da agricultura em áreas de proteção ambiental, pertencentes à bacia hidrográfica do rio Ribeira de Iguape, São Paulo. *Quím. Nova* **2007**, *30* (5), 1171–1178. https://doi.org/10.1590/S0100-40422007000500023

Martins, L. H. S; Rabelo, S. C.; Costa, A. C. Effects of the pretreatment method on high solids enzymatic hydrolysis and ethanol fermentation of the cellulosic fraction of sugarcane bagasse. *Bioresour. Technol.* **2015**, *191*, 312–321. https://doi.org/10.1016/j.biortech.2015.05.024

Maugeri Filho, F.; Goldbeck, R.; Manera, A. P. Produção de oligossacarídeos. In *Biotecnologia Industrial-Vol. 3: Processos fermentados e enzimáticos*, 2nd ed; Vol. 3, Blucher, 2019; pp 253.

Mboowa, D. A review of the traditional pulping methods and the recent improvements in the pulping processes. *Biomass Conv. Bioref.* **2021**. https://doi.org/10.1007/s13399-020-01243-6

Meenakshisundaram, S.; Fayeulle, A.; Leonard, E.; Ceballos, C.; Pauss, A. Fiber degradation and carbohydrate production by combined biological and chemical/physicochemical pretreatment methods of lignocellulosic biomass – A review. *Bioresour. Technol.* **2021**, *331*, 125053. https://doi.org/10.1016/j.biortech.2021.125053

Mengesha, Y.; Tebeje, A.; Tilahun, B. A Review on Factors Influencing the Fermentation Process of *Teff* (*Eragrostis teff*) and Other Cereal-Based Ethiopian Injera. *Int. J. Food Sci.* **2022**, *2022*, 4419955. https://doi.org/10.1155/2022/4419955

Montagnoli, M. S.; Souza, O.; Furigo Junior, A. Produção de etanol 2G de pseudocaule de bananeira por cocultura microbiana. *Blucher Chem. Eng. Proc*. **2018**, *1* (5),160–163. https://doi.org/10.5151/cobeq2018-PT.0049

Ogeda, T. L.; Petri, D. F. S. Hidrólise Enzimática de Biomassa. *Quim. Nova*. **2010**, *33* (7), 1549–1558. https://doi.org/10.1590/S0100-40422010000700023

Rabemanolontsoa, H.; Saka, S. Comparative study on chemical composition of various biomass species. *RSC Advances*. **2013**, *3* (12), 3946–3956. https://doi.org/10.1039/C3RA22958K

Rosa, S. E. S.; Garcia, J. L. F. O etanol de segunda geração: limites e oportunidades. *Revista do BNDES*. **2009**, *32*, 117–156.

Santos, F. A.; Queiróz, J. H.; Colodette, J. L.; Fernandes, S. A.; Guimarães, V. M.; Rezende, S. T. Potencial da palha de cana-de-açúcar para produção de etanol. *Quím. Nova* **2012**, *35* (5), 1004–1010. https://doi.org/10.1590/S0100-40422012000500025

Saritpongteerak, K.; Kaewsung, J.; Charnnok, B.; Chaiprapat, S. Comparing Low-Temperature Hydrothermal Pretreatments through Convective Heating versus Microwave Heating for Napier Grass Digestion. *Processes*. **2020**, *8* (10), 1221. https://doi.org/10.3390/pr8101221

Scapini, T.; Santos, M. S. N.; Bonatto, C.; Wancura, J. H. C.; Mulinari, J.; Camargo, A. F.; Klanovicz, N.; Zabo, G. L.; Tres, M. V.; Fongaro, G.; Treichel, H. Hydrothermal pretreatment of lignocellulosic biomass for hemicellulose recovery, *Bioresource Technology* **2021**, *342*, 126033. https://doi.org/10.1016/j.biortech.2021.126033

Silva, V. T. F.; Ruschoni, U. C. M.; Ferraz, A.; Milagres, A. M. F. Xylan, Xylooligosaccharides, and Aromatic Structures with Antioxidant Activity Released by Xylanase Treatment of Alkaline-Sulfite-Pretreated Sugarcane Bagasse. *Front. Bioeng Biotechnol*. **2022**, *10*, 940712. https://doi.org/10.3389/fbioe.2022.940712

Souza, O.; Schulz, M. A.; Fischer, G. A. A.; Wagner, T. M.; Sellin, N. Energia alternativa de biomassa: bioetanol a partir da casca e da polpa de banana. *Rev. Bras. de Eng. Agric. Ambient.* **2012,** *16* (8), 915–921. https://doi.org/10.1590/S1415-43662012000800015

Tse, T. J.; Wiens, D. J.; Reaney, M. J. T. Production of Bioethanol—A Review of Factors Affecting Ethanol Yield. *Fermentation*. **2021**, *7* (4), 268. https://doi.org/10.3390/fermentation7040268

Tsubaki, S.; Oono, K.; Onda, A.; Ueda, T.; Mitani, T.; Hiraoka, M. Microwave-assisted hydrolysis of biomass over activated carbon supported polyoxometalates. *RSC Adv*. **2017**, *7* (20), 12346–12350. https://doi.org/10.1039/C6RA28778F

União Nacional do Etanol de Milho (UNEM). *A Hegemonia do Etanol*. 2021. http://etanoldemilho.com.br/2020/02/03/a-hegemonia-do-etanol/ (accessed 2021-06-21).

United States Environmental Protection Agency (US EPA). I*nventory of U.S. Greenhouse Gas Emissions and Sinks*. 2021. https://www.epa.gov/ghgemissions/inventory-us-greenhouse-gas-emissions-and-sinks (accessed 2021-06-20).

Wang, F.-L.; Lo, S.; Sun, Y.-X.; Han, H.-Y.; Zhang, B.-X.; Hu, B.-Z.; Gao, Y.-F.; Hu, X.-M. Ionic liquids as efficient pretreatment solvents for lignocellulosic biomass. *RSC Adv*. **2017**, *7* (76), 47990–47998. https://doi.org/10.1039/C7RA08110C

Wei, L.; Li, K.; Ma, Y.; Hou, X. Dissolving lignocellulosic biomass in a 1-butyl-3-methylimidazolium chloride–water mixture. *Ind. Crops Prod*. **2012**, *37* (1), 227–234. https://doi.org/10.1016/j.indcrop.2011.12.012

Eclética Química, vol. 48, n. 2, 2023, 22-34
ISSN: 1678-4618
DOI: 10.26850/1678-4618eqj.v48.2.2023.p22-34

Yu, X.; Bao, X.; Zhou, C.; Zhang, L.; Yagoub, A. E.-G. A.; Yang, H.; Ma, H. Ultrasound-ionic liquid enhanced enzymatic and acid hydrolysis of biomass cellulose. *Ultrason. Sonochem.* **2018**, *41*, 410–418. https://doi.org/10.1016/j.ultsonch.2017.09.003

Zanivan, J.; Bonatto, C.; Scapini, T.; Dalastra, C.; Bazoti, S. F.; Alves Júnior, S. L.; Fongaro, G.; Treichel, H. Avaliação da produção de bioetanol a partir de resíduos mistos de frutas por *Wickerhamomyces* sp. UFFS-CE-3.1.2. *Bioenergia. Res.* **2022**, *15* (1), 175–182. https://doi.org/10.1007/s12155-021-10273-5

Zhao, X.; Huang, C.; Lin, W.; Bian, B.; Lai, C.; Ling, Z.; Yong, Q. A structure–activity understanding of the interaction between lignin and various cellulase domains. *Bioresource Technology*. **2022**, *351*, 127042, https://doi.org/10.1016/j.biortech.2022.127042

Eclética Química, vol. 48, n. 2, 2023, 22-34
ISSN: 1678-4618
DOI: 10.26850/1678-4618eqj.v48.2.2023.p22-34

Eclética Química

Original article

revista.iq.unesp.br

| Vol. 48 | n. 2 | 2023 |

Detection of dopamine using glassy carbon electrodes modified with AgNPs synthetized with *Monteverdia ilicifolia extract*

Francielle Schremeta Humacayo[1], Joel Toribio Espinoza[2], Josiane de Fátima Padilha de Paula[2], Luma Clarindo Lopes[1], Christiana Andrade Pessoa[1], Cássia Gonçalves Magalhães[1+]

1. State University of Ponta Grossa, Department of Chemistry, Ponta Grossa, Brazil.
2. State University of Ponta Grossa, Department of Science, Ponta Grossa, Brazil.

+Corresponding author: Cássia Gonçalves Magalhães, **Phone:** +55 42 3220-3062, **Email address:** cgmagalhaes@uepg.br

ARTICLE INFO

Article history:
Received: August 31, 2022
Accepted: December 05, 2022
Published: April 01, 2023

Section Editors: Assis Vicente Benedetti

Keywords:
1. *M. ilicifolia*
2. Dopamine
3. silver nanoparticles
4. green synthesis

ABSTRACT: This work reports a new application for a well-known medicinal plant used in Brazil. The green synthesis of silver nanoparticles (AgNPs) using the aqueous extract of *Monteverdia ilicifolia* (MI) leaves as stabilizing and reducing agent is described. The AgNPs-MI obtained were characterized by UV-VIS, FTIR, and Raman spectroscopies, DLS, zeta potential and FEG-SEM, which demonstrated that *M. ilicifolia* was effective at capping the AgNPs, yielding stable suspensions. These nanoparticles were deposited on glassy carbon electrodes, and they were efficiently applied as electrochemical sensors for the determination of dopamine (DA) using square wave voltammetry (SWV). The AgNPs-MI improved the electrochemical properties of the electrodes and enhanced their electroanalytical performance. The developed sensing device presented detection and quantification limits equal to 0.52 and 1.74 μmol L^{-1}, respectively, towards DA determination. The proposed electrochemical sensor quantified this neurotransmitter successfully, confirming its potential as a new promising analytical detection tool for DA quality control.

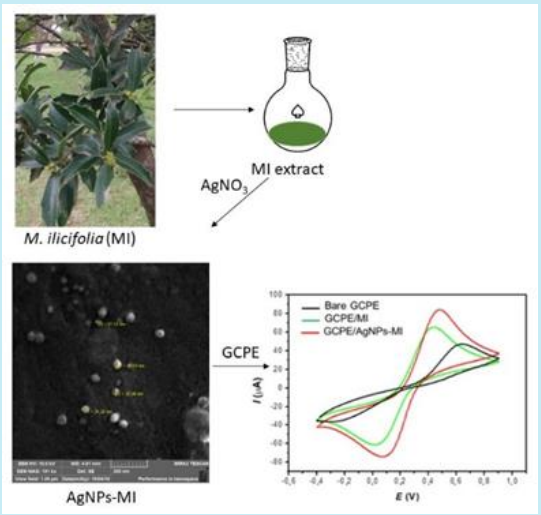

Eclética Química, vol. 48, n. 2, 2023, 35-48
ISSN: 1678-4618
DOI: 10.26850/1678-4618eqj.v48.2.2023.p35-48

1. Introduction

The green synthesis of metal nanoparticles shows many advantages when it is compared to conventional methods, since natural compounds make these syntheses environmentally friendly, as well as cheaper processes (Huq *et al*., 2022). Among the materials used in the biosynthesis of metal nanoparticles, the use of plants as reducing agents is widely explored, because it shows lower risks and provides a fast and stable product (Ahmad *et al*., 2016a; Jadoun *et al*., 2021). Considering the huge Brazilian biodiversity, it is possible to justify the interest of using the natural resource for the biosynthesis of metal nanoparticles, where species belonging to Celastraceae family constitute a good source for this technological application. For example, the extract of the root of *Monteverdia salicifolia* (syn. *Maytenus salicifolia)* was used as a stabilizing and reducing agent in the production of silver nanoparticles (AgNPs), with size in the range of 48–80 nm (Grzygorczyk *et al*., 2021). The extract of *M. royleanus* leaves was useful in the synthesis of gold nanoparticles (AuNPs) with particles size of approximately 30 nm, which exhibited relevant antileishmanial activity (Ahmad *et al*., 2016a). Moreover, the extract of the stems of this species lead to the synthesis of AgNPs associated to amphotericin B, with an approximate particle size of 15 nm. They exhibited higher antifungal activity than the nanomaterial that was not conjugated (Ahmad *et al*., 2016b). According to the evidence, the research that aim to study the capacity of plant extracts in the synthesis of nanoparticles as well as the evaluation of these biological properties are very relevant.

The most known species from this genus is *Monteverdia ilicifolia*, popularly known in Brazil as *espinheira santa* and *espinho-de-deus*. It is endemic to southern Brazil, Argentina, Paraguay, and Uruguay. This species is largely used in the traditional medicine in the treatment of gastritis, ulcers, and other gastric disorders (Périco *et al*., 2018; Zhang *et al*., 2020). The use of this extract exhibited advantages when compared to the commercial drugs that acts inhibiting the proton pump, such as omeprazole, that leads to side effects (Tabach *et al*., 2017).

The AgNPs also have attractive characteristics such as chemical stability, high surface area and relevant electrical and optical properties, being very versatile materials for different applications (Jadoun *et al*., 2021). They can be applied specially in the modification of electrodes, to improve electroanalytical techniques, where they can allow new electrochemical properties to them, increasing their selectivity, sensibility and stability. In consequence, they become a useful tool for determination of specific compounds in biological samples and for the control of quality of drugs (Lima Filho *et al*., 2019). In this context, many investigations highlighting the potential of plants improving the electrochemical properties of the electrodes have been reported. Screen-printed electrodes modified with Ag-NPs, which were biosynthesized using an extract aqueous of grape stalk waste, were tested for the simultaneous stripping voltammetric determination of Pb(II) and Cd(II). The results indicated good reproducibility, sensitivity and limits of detection around 2.7 μg L^{-1} for both metal ions (Bastos-Arrieta *et al*., 2018). The extract of *Araucaria angustifolia* was effective as a reducing and stabilizing agent in the synthesis of AgNPs. These nanomaterials were applied to a glassy carbon electrode used for the determination of paracetamol in drugs (Zamarchi and Vieira, 2021). Besides, carbon paste electrode modified with banana tissue was effective for determination of catechol in green tea (Broli *et al*., 2019). This evidence emphasizing the importance of the development of studies involving plants in order to extend their technological applications.

Dopamine (DA) is a neurotransmitter of the central and peripheral nervous system, responsible for physiological activities, such as behavior, memory, and movement. Abnormal levels of this catecholamine can lead to many neurological diseases, such as schizophrenia, Parkinson's disease and hyperactivity (Blum *et al*., 2021). Thus, the development of very selective and sensitive techniques for monitoring the level of DA in the organism are very important. This neurotransmitter has a known voltammetric behavior which enables its determination by electrochemical methods (Selvolini *et al*., 2019; Yu *et al*., 2018). As an example, the detection of DA was made with a screen-printed carbon electrode modified by AuNPs derived from *Rhanterium suaveolens* flowers extract (Chelly *et al*., 2021). A biosensor modified with AgNPs obtained from aqueous leaf extract of *Ziziphus mauritiana* was successfully applied for DA detection in real urine samples (Memon *et al*., 2021).

At the best of our knowledge, the biosynthesis of AgNPs using the extract of *M. ilicifolia* leaves is not reported. Therefore, considering the significant therapeutic value of *M. ilicifolia* (RENISUS, 2009; Tabach *et al*., 2017) the aim of this study was performing the green synthesis of AgNPs using the aqueous extract of its leaves and their application in the modification of glassy carbon electrodes, applied in the electroanalytical determination of DA.

Eclética Química, vol. 48, n. 2, 2023, 35-48
ISSN: 1678-4618
DOI: 10.26850/1678-4618eqj.v48.2.2023.p35-48

2. Experimental

2.1 Plant extract

M. ilicifolia leaves were collected from a specimen located at campus of the Universidade Estadual de Ponta Grossa (UEPG, 25°5'23"S 50°6'23"W), in Ponta Grossa, Paraná, Brazil. A voucher specimen was deposited at UEPG Herbarium, under number HUPG 21178. This species was insert on SISGEN platform under register A8E6438.

The leaves (20.17 g) were dried, ground and mixed with 300 mL of distilled water. The mixture was submitted to heat to boiling. After this, the sample was filtered, getting to the aqueous extract, which was stored at 4 °C.

2.2 Synthesis and characterization of silver nanoparticles

The green synthesis of the AgNPs was performed with the addition of 1.0 mL of the aqueous extract collected of a stock solution (extract diluted in distilled water in the proportion of 1:10), to 19.0 mL of $AgNO_3$ 1.0×10^{-3} mol L^{-1}. This mixture was heated at 60 °C and stirred for 10 min. The AgNPs with *M. ilicifolia* (AgNPs-MI) synthetized were kept in light-protected vials.

The nanocomposites were characterized by ultraviolet-visible spectrophotometry (UV-VIS) (in a Cary 50 Varian spectrophotometer) by scanning the wavelengths in the range of 200–800 nm. FTIR spectra were recorded in attenuated total reflectance (ATR) mode in the scanning range of 4000–400 cm^{-1} (scan rate of 10 cm^{-1}) for AgNPs-MI and *M. ilicifolia* (10 mg mL^{-1} solution) KBr tables after lyophilization of the extract, at room temperature. Raman spectral analysis were obtained in a spectrometer Xplora Plus (HORIBA scientific) in a range of 100 to 2,000 cm^{-1}. A laser of 532 nm was chosen for the measurements.

Field emission gun-scanning electron microscopy (FEG-SEM) was done in a Myra 3 LMH Tescan microscope (15 mV: 356 mA). The particle diameter was obtained by dynamic light scattering (DLS) measurements on a Malvern NanoZ590 equipment.

2.3 Preparation of glassy carbon paste electrodes

The unmodified glassy carbon paste electrode (GCPE) was prepared by mixing 50.0 mg of glassy carbon powder with 10.0 µL of mineral oil until homogenization. After this, a portion of this mixture was inserted into the cavity of a Teflon tube. For the construction of the modified electrodes with -MI, different amounts of this nanocomposite (10.0, 25.0, 50.0, 75.0 and 100 µL) was mixed with 50.0 mg of glassy carbon powder. After homogenization, at this mixture 10.0 µL of mineral oil was added. Similarly, to the bare GCPE, the modified glassy carbon paste was packed into Teflon tubes. A carbon paste electrode modified with the plant extract was also prepared (GCPE/MI), using 50.0 µL of the aqueous extract of *M. ilicifolia* leaves, diluted with distilled water (1:10) with 50.0 mg of glassy carbon powder. In this case, the mixture was homogenized and dried under air flow, followed by the addition of 10.0 µL of mineral oil. After a new homogenization step, this modified carbon pastes were separately inserted into Teflon tubes, similarly to the others. The electrode surfaces were renewed by smoothing the resulting electrodes on a soft paper and then on a glass plate.

2.4 Electrochemical characterization

Electrochemical measurements were carried out at room temperature, using a conventional three-electrode cell system. The carbon paste electrodes (modified or unmodified), Ag/AgCl/KClsat electrode and a platinum spiral wire were used as working electrodes, reference and auxiliary, respectively. In order to characterize the modified electrodes, cyclic voltammetry (CV) and electrochemical impedance spectroscopy (EIS) experiments were performed in an Autolab PGSTAT 100 potentiostat/galvanostat, by employing 0.15 mol L^{-1} PBS solution containing 10.0 mmol L^{-1} $K_4Fe(CN)_6/K_3Fe(CN)_6$ as supporting electrolyte.

For DA determination with the GCPE/MI and GCPE/AgNPs-MI, CV and square wave voltammetry (SWV) measurements were conducted in a PalmSens potentiostat (Palm Instruments BV) in 0.04 mol L^{-1} BR buffer, in the pH range of 2.0 to 7.0; DA = 1.0 mmol L^{-1}. Analytical parameters such as sensitivity, repeatability, reproducibility, limit of detection (LOD), limit of quantification (LOQ), and accuracy were determined for the modified electrodes following the Brazilian Health Surveillance Agency (ANVISA (2003) and International Conference on Harmonization (ICH, 2005) guidelines. In appropriate conditions, the CPE/AgNPs-MI was studied in different scan rates (10–100 mV s^{-1}) to determine the type of mass transport that guide the oxidation of DA on the modified electrode.

Eclética Química, vol. 48, n. 2, 2023, 35-48
ISSN: 1678-4618
DOI: 10.26850/1678-4618eqj.v48.2.2023.p35-48

3. Results and discussion

3.1 Synthesis and characterization of the AgNPs-MI

The biosynthesis of AgNPs using the aqueous extract of *M. ilicifolia* leaves was indicated by the color changing of the solution, from colorless to orange, which is a characteristic color of AgNPs in suspension. This show that the extract was able to reduce the cations Ag^{+} in Ag^{0} nanoparticles. It is important to emphasize that the advantage of using this extract in the nanoparticle synthesis is that it provides their both reduction and stabilization, and it is also an environmentally friendly and cheap reagent. Moreover, the AgNPs obtained were very stable, maintaining their size for about three months.

The color changing is due to the surface plasmon effect (Grzygorczyk *et al.*, 2021), exhibited for the AgMPs-MI. It is worth highlighting that the reaction time was very short, only 10 min, without the need to change the pH of the solution. The extract can act as both reducing agent and stabilizer simultaneously.

Studies about the phytochemical profile of *M. ilicifolia* show a great variety of secondary metabolites, such as pentacyclic triterpenes (friedelinol, friedelin, lupeol), phenolic acids and the flavonoids kaempferol, quercetin, epigallocatechin, among others (Périco *et al.*, 2018; Zhang *et al.*, 2020). Phenolic compounds, such as gallic acid and tannic acid, were useful as stabilizing and reducing agents in the synthesis of bimetallic Au@AgNPs (Orlowski *et al.*, 2020). The participation of phenolic compounds and flavonoids from *Elaeis guineensis* in the biosynthesis of gold nanoparticles was demonstrated by the reduction of the content of these metabolites quantified by Ahmad *et al.* (2019). Quercetin was also an effective reductant agent in the green synthesis of silver and gold nanoparticles (Karuvantevida *et al.*, 2022). Then, it is possible to relate the occurrence of these two classes of compounds to the capping and reducing action of the extract.

It could be observed an absorption band in 280 nm in the UV-VIS spectrum (Fig. 1), which is related to the flavonoids (Tošović and Marković, 2017) present the extract (Fig. A1 of the Appendix). Besides, a strong absorption band at 423 nm was observed for AgNPs-MI solution, which can be attributed to the surface plasmon resonance phenomena that is typical for AgNPs. An absorption band around 400 nm also characterizes spherical nanoparticles (Grzygorczyk *et al.*, 2021; Tošović and Marković, 2017).

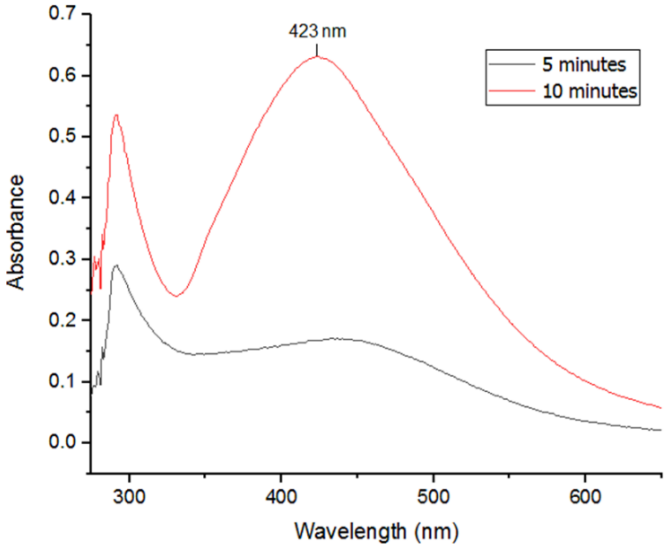

Figure 1. UV-VIS spectra of a freshly-prepared AgNPs-MI suspension after 5 min (—) and 10 min (—) of reaction.

By using DLS, it was verified that a bimodal size distribution was found for AgNPs-MI, corresponding to the average hydrodynamic diameters of 4.0 to 342.0 nm (Fig. A2a of the Appendix). The large particle sizes observed by using this technique can be explained by the fact that DLS measurements provides hydrodynamic sizes (Bojko *et al.*, 2020). In consequence, the diameter includes the molecules that stabilize the nanoparticles, which leads to an observation of a value higher than the real (Lin *et al.*, 2013). Zeta potential of the nanocomposite suspension was found to be –21.8 mV (Fig. A2b of the Appendix), which indicates that the nanoparticles were suitably capped with anionic extract metabolites. Despite the found value had been lower than typical potential range of stable colloids (–30.0 mV to +30.0 mV) (Efavi *et al.*, 2022), some research reported stable AgNPs with similar zeta potential values (Ahmad *et al.*, 2016a). Thus, such observations have proved the efficiency of *M. Ilicifolia* as a capping agent. The polydispersion index (PDI) was calculated for verifying the homogeneity in the AgNPs-MI size. The sample analyzed showed PDI = 0.516. Thus, the AgNPs-MI are polydispersive, since the PDI near to zero indicates monodispersive nanoparticles and PDI = 1 indicates a big variation in the particle size (Lin *et al.*, 2013).

The images obtained by FEG-MEV analysis confirm that the AgNPs-MI show homogeneous size and spherical shape, with just few aggregates observed (Figs. 2a–d). Besides, the high yield of the biosynthesis could be considered due to the high amount of AgNPs-MI detected (Fig. 2a), which showed particles sizes in the range of 20–80 nm.

Eclética Química, vol. 48, n. 2, 2023, 35-48
ISSN: 1678-4618
DOI: 10.26850/1678-4618eqj.v48.2.2023.p35-48

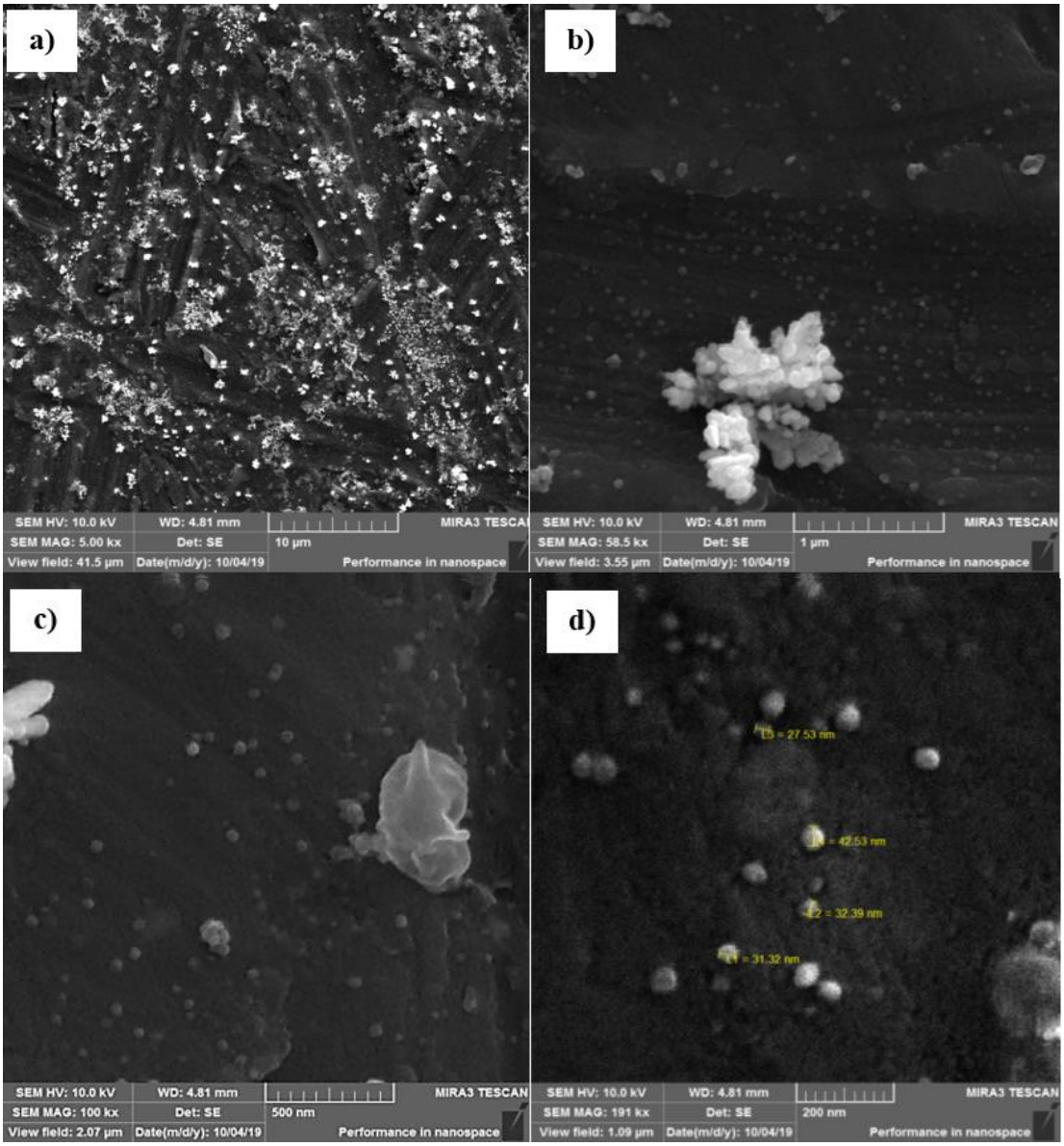

Figure 2. FEG-MEV Images obtained by analysis of AgNPs-MI with different magnifications **(a)** 5,00 kx; **(b)** 58,5 kx; **(c)** 100 kx, and **(d)** 191 kx.

Analyzing the AgNPs-MI FTIR spectra (Fig. 3), it is possible to observe that the bands intensity at 1641 (C=O stretching) and 3418 cm^{-1} (OH stretching) was decreased. This fact is probably related to their participation in the stabilization of the AgNPs. The absorption bands at 2848 (COO-H stretching) 1776 (C=O stretching) and 823 cm^{-1} (C-O stretching), were observed and they can be attributed to carboxylic groups (Haddad *et al.*, 2014). These bands suggest the occurrence of flavonoids and phenolic compounds from *M. ilicifolia* extract, which interacts with AgNPs through the electron donors oxygen atoms. Those biomolecules can be adsorbed on the metal ions surface, which is observed by the decreasing in the intensity of the bands observed. The band at 1776 cm^{-1} evidences the influence of the extracts in the formation of the AgNPs, considering the oxidation of this material and, in consequence, the reduction of Ag^{+} ions.

The AgNPs-MI were also analyzed by Raman spectroscopy (Fig. A3 of the Appendix). The Raman spectrum displayed a band at 236 cm^{-1} related to the vibration of stretching Ag-O bond (Barbosa, 2007). This band can be related to the interaction between Ag and carboxylate groups of the molecules of the extract, attached to the AgNPs-MI surface, which contribute to this stabilization. The peaks at 1365 e 1522 cm^{-1} were, respectively, attributed to the symmetric and asymmetric vibrations of C=O of carboxylate group (Barbosa, 2007).

Eclética Química, vol. 48, n. 2, 2023, 35-48
ISSN: 1678-4618
DOI: 10.26850/1678-4618eqj.v48.2.2023.p35-48

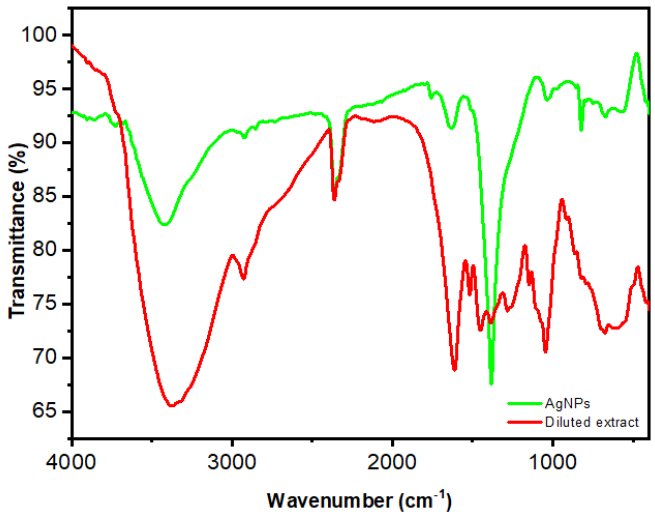

Figure 3. FTIR spectra of *M. ilicifolia* (—diluted aqueous extract) and (—AgNPs-MI).

3.2 Electrochemical characterization of GCPE, GCPE/MI and GCPE/AgNPs-MI

The electron transfer properties of bare GCPE, GCPE/MI and GCPE/AgNPs-MI were evaluated by CV and EIS techniques. The studies were carried out in the presence of 10.0 mmol L^{-1} $K_4Fe(CN)_6/K_3Fe(CN)_6$ as a redox probe, with 0.15 mol L^{-1} PBS buffer solution as supporting electrolyte, pH = 6.5. Analyzing the cyclic voltammograms (Fig. 4) and the data reported in the Table 1, it is possible to verify that both electrodes showed current peaks for the typical redox process of the electrochemical probe ($Fe(CN)_6^{4-} \rightleftharpoons Fe(CN)_6^{3-}$). However, GCPE/AgNPs-MI showed higher anodic peak (I_{pa}) and cathodic peak (I_{pc}) currents for both processes than bare GCPE. GCPE/AgNPs-MI also showed low peak potential separation values (ΔE_p). This suggest that the electronic transfer kinetic is more effective and show higher reversibility (C. Brett and A. Brett, 1993) when compared to bare GCPE.

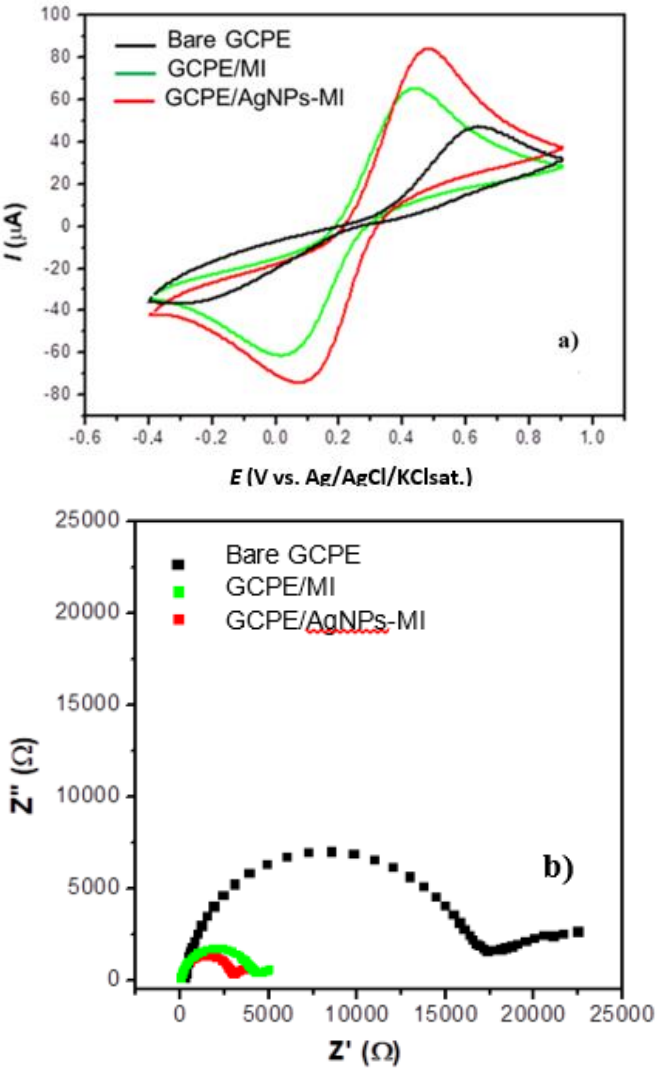

Figure 4. **(a)** Cyclic voltammograms (scan rate = 50.0 mV s^{-1}) and **(b)** electrochemical impedance spectra (Nyquist plots) of GCPE/AgNPs-MI, GCPE/MI and bare CPE (open circuit potential; frequency range: 5 kHz to 25 mHz; amplitude: 10 mV), in 0.15 mol L^{-1} PBS buffer solution (pH 6.5) containing 10.0 mmol L^{-1} $K_4Fe(CN)_6/K_3Fe(CN)_6$.

Table 1. I_{pa}, I_{pc}, ΔE_p and R_{ct} values obtained for bare GCPE, GCPE/MI and GCPE/AgNPs-MI.

Electrode	I_{pa} (µA)	- I_{pc} (µA)	E_{pa} (mV)	E_{pc} (mV)	ΔE_p	R_{ct} (Ω)
Bare GCPE	26.19	18.40	638	233	405	17389.99
GCPE/MI	58.27	49.50	431	19	412	4102.10
GCPE/AgNPs-MI 50 µL	71.64	65.13	477	81	396	2863.30

Since the diameter of the semicircle is related to the electronic transfer resistance (R_{ct}) (C. Brett and A. Brett, 1993; Van Der Horst *et al.*, 2015) it was observed that this parameter for bare GCPE was higher than for GCPE/AgNPs-MI and GCPE/MI. This suggests that GCPE/MI and GCPE/AgNPs-MI facilitates the electron transfer process in electrode-solution interface when compared to the bare GCPE. These results are in accordance with that obtained by CV. Besides, they can be better understood when evaluated together with the R_{ct} values obtained in each situation (Table 2). The higher current values, lower ΔE_p and lower R_{ct} exhibited

Eclética Química, vol. 48, n. 2, 2023, 35-48
ISSN: 1678-4618
DOI: 10.26850/1678-4618eqj.v48.2.2023.p35-48

by GCPE/AgNPs-MI can be attributed to the characteristics of AgNPs, such as high conductivity and big surface area (C. Brett and A. Brett, 1993). This suggest that the modification of the electrode with the nanocomposite obtained in this study is an advantage for its application as an electrochemical sensor.

In order to evaluate the influence in the amount of AgNPs-MI added in the GCPE electrochemical response, different volumes of AgNPs-MI (10, 25, 50, 75 and 100 µL) were added to 50.0 mg of powder glassy carbon. The electrodes response was analyzed in the presence of $[Fe(CN)_6]^{3-}/[Fe(CN)_6]^{4-}$ 10 mmol L^{-1} in PBS buffer 0.15 mol L^{-1} as electrolyte support.

Table 2. I_{pa}, I_{pc}, ΔE_p and R_{ct} values of bare GCPE and GCPE/AgNPs-MI in different volumes.

Electrode	I_{pa} (µA)	- I_{pc} (µA)	E_{pa} (mV)	E_{pc} (mV)	ΔE_p	R_{ct} (Ω)
Bare GCPE	26.19	18.40	638	233	405	17389.99
GCPE/AgNPs-MI 10 µL	72.73	64.60	481	33	448	3910.00
GCPE /AgNPs-MI 25 µL	62.00	61.16	485	58	427	4991.30
GCPE /AgNPs-MI 50 µL	**71.64**	**65.13**	**477**	**81**	**396**	**2863.30**
GCPE /AgNPs-MI 75 µL	49.4	41.52	514	5	509	6909.80
GCPE /AgNPs-MI 100 µL	64.18	56.02	415	94	321	3490.40

The anodic peak current (I_{pa}) was decreased until 25 µL, and, after this, a higher I_{pa} was observed with 50 µL (Fig. 5); then, the current decreased again. When GCPE/AgNPs-MI 10 µL and GCPE/AgNPs-MI 50 µL were compared, it was possible to verify that both showed similar current responses. However, the GCPE/AgNPs-MI with 50 µL exhibited a low ΔE_p as well as a lower R_{ct} values, suggesting that, for those conditions, the charge transfer process in the electrode-solution interface is fast. Moreover, it shows higher reversibility for the process (Van Der Horst *et al.*, 2015), when compared with GCPE/AgNPs-MI obtained with 10 µL. Hence, 50 µL of AgNPs-MI was chosen as the amount for the preparation of the modified CPE electrodes.

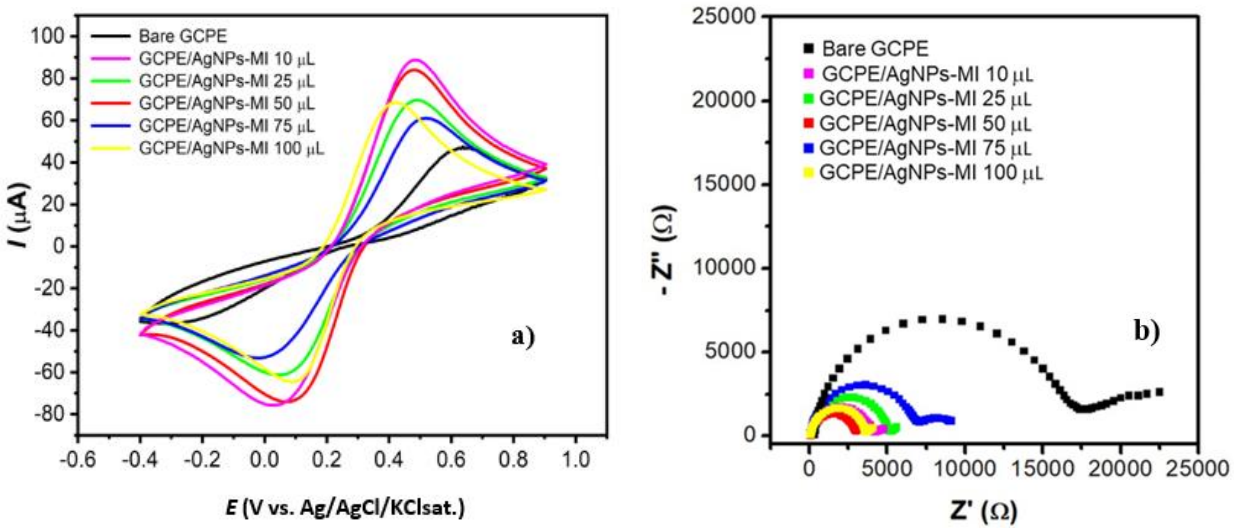

Figure 5. **(a)** Cyclic voltammograms and **(b)** electrochemical impedance spectra of GCPE/AgNPs-MI and bare GCPE, in an equimolar solution of $K_4Fe(CN)_6/K_3Fe(CN)_6$ 0.010 mol L^{-1} in PBS buffer solution 0.15 mol L^{-1} (pH 6.5).

3.3 Effect of pH

The pH of the supporting electrolyte is an important parameter for the analytical performance of the sensor. It can influence in the electrochemical response of the device during the detection of the analyte (Lima *et al.*, 2018). Since there are protons involved in the DA electrooxidation mechanism, the effect of pH of the supporting electrolyte on the electrochemical response of GCPE/AgNPs-MI (50 µL) for 1 × 10^{-2} mol L^{-1} of DA was evaluated. The voltammograms were obtained in 0.04 mol L^{-1} BR buffer with different pH values (pH 2.0–7.0) by employing the SWV technique (Fig. 6).

Eclética Química, vol. 48, n. 2, 2023, 35-48
ISSN: 1678-4618
DOI: 10.26850/1678-4618eqj.v48.2.2023.p35-48

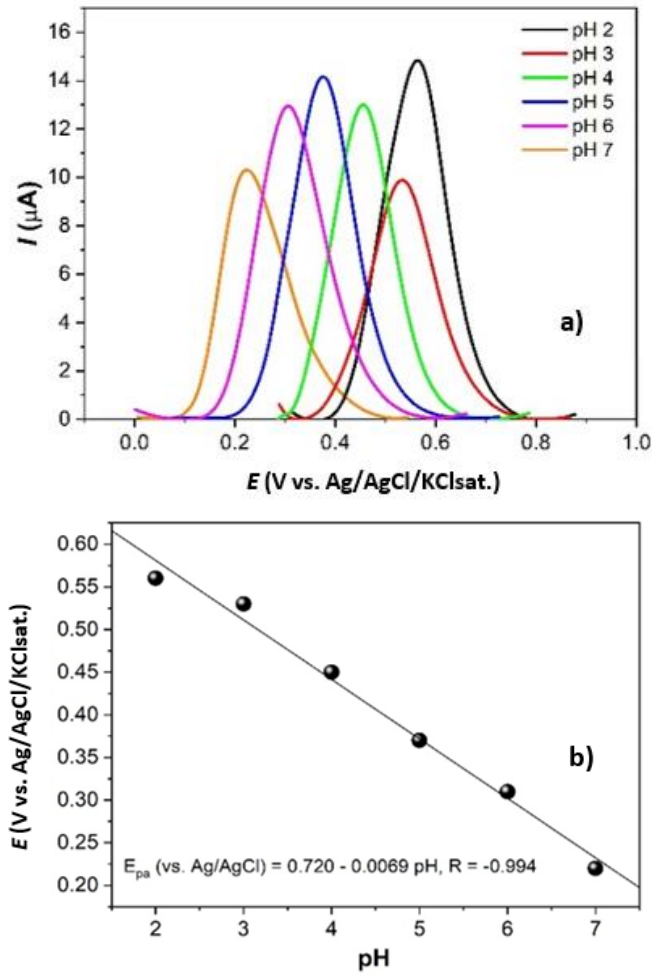

Figure 6. Effect of pH in the electrochemical response of DA. **(a)** Square wave voltammograms of 1.0×10^{-2} mol L^{-1} of DA on GCPE/AgNPs-MI in BR buffer 0.04 mol L^{-1}, at pH in the range of 2.0 to 7.0. **(b)** Relationship between de E_{pa} and pH obtained from the voltamograms.

The effect of pH in the current and potential values was also evaluated. The DA peak potential shifted negatively with the increase of the pH values (Fig. 6), since the electrooxidation of DA involves 2 protons and 2 electrons, leading to the DA quinone, which can be reduced in the reverse process (Sakthivel *et al.*, 2017). A linear relationship was verified between the anodic peak potential and the pH medium according to the following linear regression equation: (E_{pa} (vs. Ag/AgCl) = 0.720–0.069 pH, R = 0.994). The slope obtained was of −69.0 mV pH^{-1}, which was close to the theoretical Nernstian value of −59.0 mV pH^{-1}, suggesting that the number of electrons and protons transferred in the electrode reaction is the same (Lima *et al.*, 2018).

DA shows voltammetric response on the GCPE/AgNPs-MI for all pH range studied, and the highest current value was obtained in pH 2.0. However, pH 7.0 was chosen for further analysis, because a biological application for the sensor is intended.

3.4 Influence of scan rate

In order to determine the mechanism of mass transport in the redox reaction of DA on the GCPE/AgNPs-MI, the influence of the scan rate on the voltammetric profile was analyzed, by recording cyclic voltammograms for 1.0×10^{-2} mol L^{-1} of DA (fixed concentration) in the range of 10–100 mV s^{-1}. The supporting electrolyte was BR buffer 0.04 mol L^{-1} at pH 7.0. A linear relationship was noticed in the plot of log(Ip) vs. log(ν), corresponding to the equation $\log(I_{pa}) = 0.270 + 0.373 \log(\nu)$; R = 0.985 (Fig. 7).The slope value of 0.37 is close to 0.50, which is the theoretically expected value for a totally diffusion-controlled process. Therefore, it was concluded that the electrochemical oxidation of DA on GCPE/AgNPs-MI is mostly governed by diffusion (Lima *et al.*, 2018).

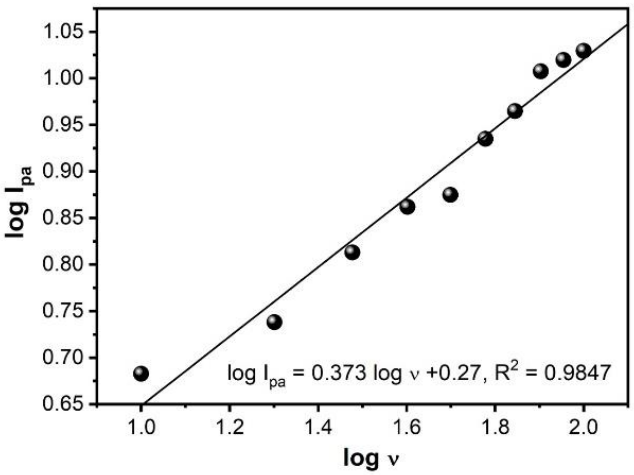

Figure 7. Relationship of log I_{pa} vs. log ν for DA.

3.5 Analytical curves

DA quantitative analysis employing the GCPE/AgNPs-MI were recorded by SWV (Fig. 8a). Analytical curves (Fig. 8b) were constructed under the optimum conditions in the range of 30 to 90 μmol L^{-1} of DA, by using 0.04 mol L^{-1} BR buffer solution as supporting electrolyte at pH 7.0. The regression equation obtained by the linear regression of the average of three analytical curves and the correlation coefficient are shown in Table 3.

The analytical curves indicated a linear increase of I_{pa} value with the increase of DA concentration in the concentration range studied. From this curve, it was

Eclética Química, vol. 48, n. 2, 2023, 35-48
ISSN: 1678-4618
DOI: 10.26850/1678-4618eqj.v48.2.2023.p35-48

possible to calculate the detection (LOD) and the quantification (LOQ) limits for the electrode evaluated. LOD and LOQ values were calculated as recommended by ANVISA (2003) and ICH (2005) guidelines: LOD = 3 SD/b and LOQ = 10 SD/b, where SD is the standard deviation of the intercepts (n = 3) and b is the slope of the analytical curve. The obtained results are shown in Table 3, along with the linear range, regression equation, standard error and correlation coefficient of each electrode.

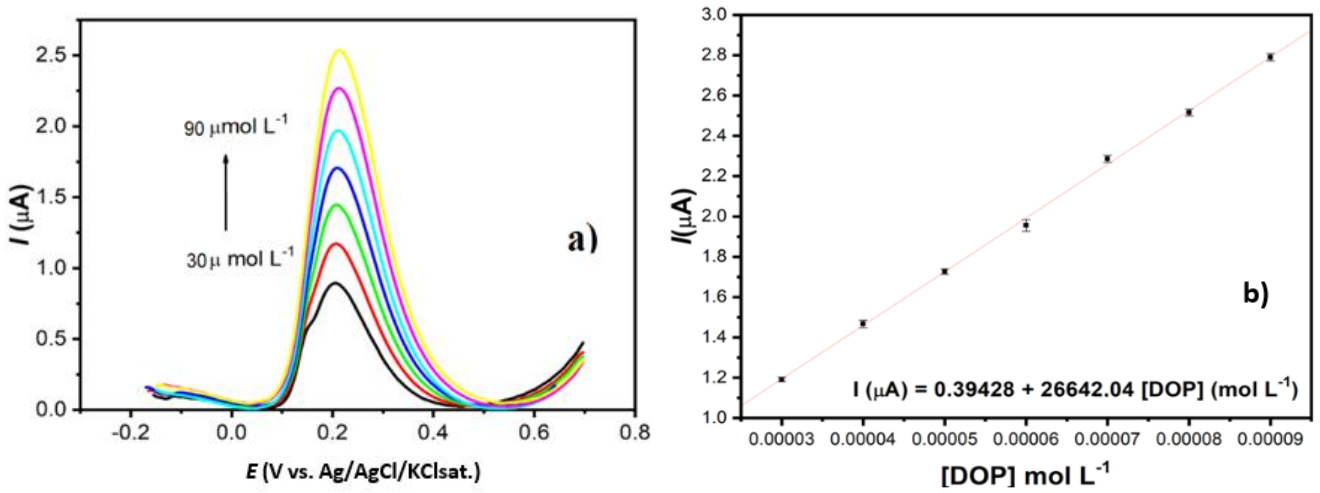

Figure 8. DA quantitative analysis using the GCPE/AgNPs-MI. **(a)** Square wave voltammograms obtained in the range of 30 to 90 µmol L^{-1} of DA, on GCPE/AgNPs-MI, in BR buffer 0.04 mol L^{-1} at pH 7.0, with a = 90 mV, f = 100 Hz e ΔEs = 8 mV. **(b)** Analytical curves obtained for GCPE/AgNPs-MI (average of three measurements).

Table 3. Analytical parameters obtained from the linear regression curves of GCPE/AgNPs-MI for DA determination by using SWV.

Parameter	GCPE/AgNPs-MI
Linear range (µmol L^{-1})	30.0 – 90.0
Regression equation	I (µA) = 0.39428 + 26642.04 [DOP] (µmol L^{-1})
Correlation coefficient	0.999
LOD (µmol L^{-1})	0.52
LOQ (µmol L^{-1})	1.74

Considering the low LOD (0.52 µmol L^{-1}**)** and LOQ (1.74 µmol L^{-1}) values obtained, it is possible to verify the good sensitivity of the modified electrode. Thus, those detection and quantification limits can be considered satisfactory for determination of DA in biological samples and pharmaceutical formulations. Besides, the values described in this work are comparable with other electrochemical methods previously reported in the literature (Table 4).

Table 4. Comparison of LOD values for DA detection using electrochemical and other analytical methods.

Technique	Working Electrode	LOD (µmol L^{-1})	Reference
DPV	Glassy carbon electrodes modified with CdTe quantum dots	0.30	Yu *et al.* (2018)
SWV	Gold electrode modified with a nanostructure of polypyrrole-mesoporous molecular silica film	0.70	Zablocka *et al.* (2019)
CV	AuNPs-modified screen-printed carbon electrode	0.20	Chelly *et al.* (2021)
CV	Glassy carbon electrodes modified with AgNPs using *Ziziphus mauritiana* extract	0.10	Memon *et al.* (2021)
SWV	CPE modified with iron oxide (Fe_2O_3) nanoparticle	0.79	Vinay and Nayaka (2019)
DPV	Electrode printed in graphite screen modified by nanocomposite film	0.86	Selvolini *et al.* (2019)
SWV	**GCPE/AgNPs-MI**	**0.52**	**This work**

DPV= differential pulse voltammetry.

Eclética Química, vol. 48, n. 2, 2023, 35-48
ISSN: 1678-4618
DOI: 10.26850/1678-4618eqj.v48.2.2023.p35-48

3.6 Accuracy, repeatability and recover assays

The accuracy of GCPE/AgNPs-MI for the determination of DA was evaluated by determination of the repeatability levels (intraday precision) of the voltammetric response generated by the sensor in the presence of the analyte, as well as considering the reproducibility level of preparation of the modified electrode. For this purpose, SWV measurements (n = 10) were carried out in the presence of 1.0×10^{-2} mol L^{-1} of the analyte, in the same day, and the results were expressed in terms of relative standard deviation (%RSD) between the found concentrations. For the evaluation of reproducibility, five independent GCPE/AgNPs-MI were prepared (n = 5) and tested in the same conditions, as mentioned above.

The results obtained for the accuracy and precision studies were expressed in terms of %RSD between the I_{pa} obtained. It was observed that the GCPE/AgNPs-MI presented satisfactory repeatability (%RSD = 3.66) and precision (%RSD = 4.47) levels for the determination of DA, since %RSD values were lower than 5.00%, that are in good agreement with the ANVISA (2003) and ICH (2005) guidelines. In order to verify the amount of DA, which could be quantified by GCPE/AgNPs-MI, assays of DA recovery were done by SWV, using the supporting electrolyte BR buffer 0.04 mol L^{-1} at pH 7.0).

These studies were performed by using the linear regression of the analytical curves for GCPE/AgNPs-MI (Fig. 8b) and the results obtained reveal the possibility of using the sensor in the determination of DA in real samples. For this, aliquots of DA (30, 50 and 70 µmol L^{-1}) stock solution were added to the electrochemical cell. For each addition, the current value was registered. After, the concentration of DA was obtained by the linear regression I (µA) = 0.39428 + 26642.04 [DA]. The experiments were carried out in triplicate (n = 3) by the standard addition method, and the results were expressed as percent recovery, as shown in Table 5. It could be observed that the percent recoveries were obtained in three different amounts of DA indicating that the matrix does not significantly affect the response of the modified electrode for DA detection. Therefore, these results clearly show that GCPE/AgNPs-MI may be efficiently applied for the quantification of DA in real samples, with good accuracy and precision.

Table 5. Results for the recovery of DA in injection with GCPE/AgNPs-MI by SWV.

Added (µmol L^{-1})	Found (µmol L^{-1})	(RSD%)	Recovery (%)
30.00	30.88 ± 0.07	2.22	102.93
50.00	50.9 ± 0.3	2.90	101.82
70.00	70.7 ± 0.4	3.05	101.04

4. Conclusions

In this review, recent literature on UV-blocking textiles have been reported to give an overview of their importance and prospects in sun-protective methods. UV-protective compounds incorporated, anchored, or coated textile fibers compose a useful class of UV-blocking materials for the development of smart fabrics as proved by the large number of scientific publications in the last years. Different UV-protective compounds, mainly TiO_2 and ZnO, are used to improve UV-blocking ability of fabrics and, often, they also impart to additional fabric properties, e.g., antibacterial, and self-cleaning activities. Analyzing from spectroscopic point of view, the elucidation of UV-blocking mechanisms gives an important information about electronic structure and optical properties of UV-protective textiles; therefore, it can be more investigated and discussed in the literature. A remarkable point is the reduced number of scientific papers that reported the use of organic filters in smart fabrics although these UV-protective compounds have high UV absorption capacity and, depending on their molecular structure, can interact to fiber surface without the presence of cross-linker compounds. UPF is a good parameter to indicate the UV-blocking ability of UV-protective compound-containing smart fabrics, however, some aspects must be considered in the analyses and interpretation of UPF results. Among them, (i) the amount of the UV-protective compound per textile area, (ii) textile thickness, and (iii) textile properties changed by the incorporation, coating and/or anchorage with UV-protective compounds, e.g., textile roughness. In this perspective, new scientific studies need to be undertaken to know the effective contribution of UV-protective compounds in the UPF values. Considering the growing requirement for simple, cheap, and practical sun-protective products, UV-blocking textiles are one of the best alternatives. Thus, scientific research in the field of smart fabric and/or UV-blocking textile, especially UV-protective compounds incorporated, anchored, or coated textile fibers, must be encourage in order to promote new

Eclética Química, vol. 48, n. 2, 2023, 35-48
ISSN: 1678-4618
DOI: 10.26850/1678-4618eqj.v48.2.2023.p35-48

insights in sun-protective clothing and future applications of multifunctional textiles.

Authors' contribution

Conceptualization: Humacayo, F. S.; Magalhães, C. G.
Data curation: Humacayo, F. S.; Espinoza, J. T.; Lopes, L. C.
Formal Analysis: Magalhães, C. G.; Paula, J. F. P.; Pessoa, C. A.
Funding acquisition: Not applicable.
Investigation: Humacayo, F. S.
Methodology: Humacayo, F. S.; Espinoza, J. T.; Lopes, L. C.
Project administration: Magalhães, C. G.; Paula, J. F. P.; Pessoa, C. A.
Resources: Not applicable.
Software: Not applicable.
Supervision: Magalhães, C. G.; Paula, J. F. P.; Pessoa, C. A.
Validation: Magalhães, C. G.; Paula, J. F. P.; Pessoa, C. A.
Visualization: Magalhães, C. G.; Paula, J. F. P.; Pessoa, C. A.
Writing – original draft: Humacayo, F. S.; Espinoza, J. T.; Lopes, L. C.
Writing – review & editing: Magalhães, C. G.; Paula, J. F. P.; Pessoa, C. A.

Data availability statement

The data will be available upon request.

Funding

Not applicable.

Acknowledgments

The authors are grateful to CLabMu – UEPG (Complexo de Laboratórios Multiusuários da UEPG) for providing the analysis.

References

Agência Nacional de Vigilância Sanitária (ANVISA), Guia para Validação de Métodos Analíticos e Bioanalíticos. Ministério da Saúde, Brasil (Resolução – RE nº 899, de 29 de maio de 2003), 2003. https://bvsms.saude.gov.br/bvs/saudelegis/anvisa/2003/res0899_29_05_2003.html (accessed 2021-03-21).

Ahmad, A.; Syed, F.; Imran, M.; Khan, A. U.; Tahir, K.; Khan, Z. U. H.; Yuan, Q. Phytosynthesis and antileishmanial activity of gold nanoparticles by Maytenus royleanus. J. Food Biochem. 2016a, 40 (4), 420–427. https://doi.org/10.1111/jfbc.12232

Ahmad, A.; Wei, Y.; Syed, F.; Tahir, K.; Taj, R.; Khan, A. U.; Hameed, M. U.; Yuan, Q. Amphotericin B-conjugated biogenic silver nanoparticles as an innovative strategy for fungal infections. *Microb. Pathog.* **2016b** *99*, 271–281. https://doi.org/10.1016/j.micpath.2016.08.031

Ahmad, T.; Bustam, M. A.; Irfan, M.; Moniruzzaman, M.; Asghar, H. M. A.; Bhattacharjee, S. Mechanistic investigation of phytochemicals involved in green synthesis of gold nanoparticles using aqueous *Elaeis guineensis* leaves extract: Role of phenolic compounds and flavonoids. *Biotech. Appl. Biochem.* **2019**, *66* (4), 698–708. https://doi.org/10.1002/bab.1787

Barbosa, L. C. A. Espectroscopia no Infravermelho na Caracterização de Compostos Orgânicos, Editora UFV, 2007.

Bastos-Arrieta, J.; Florido, A.; Pérez-Ràfols, C.; Serrano, N.; Fiol, N.; Poch, J.; Villaescusa, I. Green Synthesis of Ag Nanoparticles Using Grape Stalk Waste Extract for the Modification of Screen-Printed Electrodes. *Nanomaterials.* **2018**, *8* (11), 946. https://doi.org/10.3390/nano8110946

Blum, S. A.; Zahrebelnei, F.; Nagata, N.; Zucolotto, V.; Mattoso, L. H. C.; Pessoa, C. A.; K. Wohnrath, K. Experimental Design to Enhance Dopamine Electrochemical Detection Using Carbon Paste Electrodes. *Braz. J. Analytical Chem.* **2021**, *8* (32), 178–197. https://doi.org/10.30744/brjac.2179-3425.AR-31-2021

Bojko, L.; Jonge, G.; Lima, D.; Lopes, L. C.; Viana, A. G.; Garcia, J. R.; Pessôa, C. A.; Wohnrath, K.; Inaba, J. Porphyran-capped silver nanoparticles as a promising antibacterial agent and electrode modifier for 5-fluorouracil electroanalysis. *Carb. Res.* **2020**, *498*, 108193. https://doi.org/10.1016/j.carres.2020.108193

Brett, C. M. A.; Brett, A. M. O. Electrochemistry: Principles, Methods, and Applications, Oxford University Press, 1993.

Broli, N.; Vallja, L.; Shehu, A.; Vasjari, M. Determination of catechol in extract of tea using carbon paste electrode modified with banana tissue. *J. Food Process Preserv.* **2019**, *43* (6), e13838. https://doi.org/10.1111/jfpp.13838

Chelly, M.; Chelly, S.; Zribi, R.; Bouaziz-Ketata, H.; Gdoura, R.; Lavanya, N.; Veerapandi, G.; Sekar, C.; Neri, G. Synthesis of silver and gold nanoparticles from *Rumex roseus* plant extract and their application in electrochemical sensors. *Nanomaterials*. **2021**, *11* (3), 739. https://doi.org/10.3390/nano11030739

Efavi, J. K.; Nyankson, E.; Kyeremeh, K.; Manu, G. P.; Asare, K.; Yeboah, N. Monodispersed AgNPs Synthesized from the nanofactories of *Theobroma cacao* (cocoa) leaves and pod

husk and their antimicrobial activity. *Int. J. Biomat.* **2022**, *2022*, 4106558. https://doi.org/10.1155/2022/4106558

Grzygorczyk, S.; Ezpinoza, J. T.; Paula, J. F. P.; Boscardin, P. M. D.; Nunes, D. S.; Sandri, M. C. M.; Magalhães, C. G. Evaluation of the biotechnological potential of *Monteverdia salicifolia* (Mart ex. Reissek) Biral. *Orbital: Electron. J. Chem.* **2021**, *13* (2), 140–144. https://doi.org/10.17807/orbital.v13i2.1545

Haddad, Z.; Abid, C.; Oztop, H. F.; Mataoui, A. A review on how the researchers prepare their nanofluids. *Int. J. Therm. Sci.* **2014**, *76*, 168–189. https://doi.org/10.1016/j.ijthermalsci.2013.08.010

Huq, A.; Ashrafudoulla, M.; Rahman, M.; Balusamy, R.; Akter, S. Green synthesis and potential antibacterial applications of bioactive silver nanoparticles: A review. *Polymers.* **2022**, *14* (4), 742–764. https://doi.org/10.3390/polym14040742

International Conference on Harmonisation (ICH). Harmonised Tripartite Guideline. Validation of Analytical Procedures: Text and Methodology Q2 (R1). ICH Expert Working Group, 2005. https://database.ich.org/sites/default/files/Q2%28R1%29%20Guideline.pdf (accessed 2019-05-22).

Jadoun, S.; Arif, R.; Jangid, N. K.; Meena, R. K. Green synthesis of nanoparticles using plant extracts: A review. *Environ. Chem. Lett*. **2021**, *19* (1), 355–374. https://doi.org/10.1007/s10311-020-01074-x

Karuvantevida, N.; Razia, M.; Bhuvaneshwar, R.; Sathishkumar, G.; Prabukumar, S.; Sivaramakrishnan, S. Bioactive flavonoid used as a stabilizing agent of mono and bimetallic nanomaterials for multifunctional activities. *J. Pure Appl. Microbiol*. **2022**, *16* (3), 1652–1662. https://doi.org/10.22207/JPAM.16.3.03

Lima, D.; Calaça, G. N.; Viana, A. G.; Pessôa, C. A. Porphyran-capped gold nanoparticles modified carbon paste electrode: A simple and efficient electrochemical sensor for the sensitive determination of 5-fluorouracil. *Appl. Surf. Sci.* **2018**, *427* (Part B), 742–753. https://doi.org/10.1016/j.apsusc.2017.08.228

Lima Filho, M. M. S.; Correa, A. A.; Silva, F. D. C.; Carvalho, F. A. O.; Mascaro, L. H.; Oliveira, T. M. B. F. A glassy carbon electrode modified with silver nanoparticles and functionalized multi-walled carbon nanotubes for voltammetric determination of the illicit growth promoter dienestrol in animal urine. *Microchim. Acta.* **2019**, *186*, 525. https://doi.org/10.1007/s00604-019-3645-9

Lin, J.; Yeap, S. P.; Che, H. X.; Low, S. C. Characterization of magnetic nanoparticle by dynamic light scattering. *Nanoscale Res. Lett.* **2013**, *8*, 381. https://doi.org/10.1186/1556-276X-8-381

Memon, R.; Memon, A. A.; Nafady, A.; Sirajuddin; Sherazi, S. T. H.; Balouch, A.; Memon, K.; Brohi, N. A.; Najeeb, A. Electrochemical sensing of dopamine via bio-assisted synthesized silver nanoparticles. *Int. Nano Lett.* **2021**, *11* (3), 263–271. https://doi.org/10.1007/s40089-021-00339-9

Orlowski, P.; Zmigrodzka, M.; Tomaszewska, E.; Ranoszek-Soliwoda, K.; Pajak, B.; Slonska, A.; Cymerys, J.; Celichowski, G.; Grobelny, J.; Krzyzowska, M. Polyphenol-conjugated bimetallic Au@AgNPs for improved wound healing. *Int. J. Nanomed*. **2020**, *15*, 4969–4990. https://doi.org/10.2147/IJN.S252027

Périco, L. L.; Rodrigues, V. P.; Almeida, L. F. R.; Fortuna-Perez, A. P.; Vilegas, W.; Hiruma-Lima, C. A. *Maytenus ilicifolia* Mart. ex Reissek. In *Medicinal and Aromatic Plants of South America*. Albuquerque, U., Patil, U., Máthé, Á, Eds.; Springer, 2018; Vol. 5, 323–335. https://doi.org/10.1007/978-94-024-1552-0_29

Relação Nacional de Plantas Medicinais de Interesse ao SUS (RENISUS). Espécies vegetais. Ministério da Saúde, 2009. https://www.gov.br/saude/pt-br/composicao/sctie/daf/pnpmf/ppnpmf/arquivos/2014/renisus.pdf (accessed 2022-10-06).

Sakthivel, R.; Dhanalakshmi, S.; Chen, S.-M.; Chen, T.-W.; Selvam, V.; Ramaraj, S. K.; Weng, W.-H.; Leung, W.-H. A novel flakes-like structure of molybdenum disulphide modified glassy carbon electrode for the efficient electrochemical detection of dopamine. *Int. J. Electrochem. Sci*. **2017**, *12*, 9288–9300. https://doi.org/10.20964/2017.10.71

Selvolini, G.; Lazzarini, C.; Marrazza, G. Electrochemical nanocomposite single-use sensor for dopamine detection. *Sensors*. **2019**, *19* (14), 3097. https://doi.org/10.3390/s19143097

Tabach, R.; Duarte-Almeida, J. M.; Carlini, E. A. Pharmacological and toxicological study of *Maytenus ilicifolia* leaf extract. Part II—Clinical Study (Phase I). *Phytother. Res.* **2017**, *31* (6), 921–926. https://doi.org/10.1002/ptr.5816

Tošović, J.; Marković, S. Reproduction and interpretation of the UV–vis spectra of some flavonoids. *Chem. Pap*. **2017**, *71* (3), 543–552. https://doi.org/10.1007/s11696-016-0002-x

Van Der Horst, C.; Silwana, B.; Iwuoha, E.; Somerset, V. Bismuth–silver bimetallic nanosensor application for the voltammetric analysis of dust and soil samples. *J. Electroanal. Chem.* **2015**, *752*, 1–11. https://doi.org/10.1016/j.jelechem.2015.06.001

Vinay, M. M.; Nayaka, Y. A. Iron oxide (Fe_2O_3) nanoparticles modified carbon paste electrode as an advanced material for electrochemical investigation of paracetamol and dopamine. *J. Sci.-Adv. Mater. Dev.* **2019**, *4* (3), 442–450. https://doi.org/10.1016/j.jsamd.2019.07.006

Eclética Química, vol. 48, n. 2, 2023, 35-48
ISSN: 1678-4618
DOI: 10.26850/1678-4618eqj.v48.2.2023.p35-48

Yu, H.-W.; Zhang, Z.; Jiang, J.-H.; Pan, H.-Z.; Chang, D. Simple strategy for sensitive detection of dopamine using CdTe QDs modified glassy carbon electrode. *J. Clin. Lab. Anal.* **2018**, *32*, e22320. https://doi.org/10.1002/jcla.22320

Zablocka, I.; Wysocka-Zolopa, M.; Winkler, K. Electrochemical detection of dopamine at a gold electrode modified with a polypyrrole–mesoporous silica molecular sieves (MCM-48) film. *Int. J. Mol. Sci.* **2019**, *20* (1), 111. https://doi.org/10.3390/ijms20010111

Zamarchi, F.; Vieira, I. C. Determination of paracetamol using a sensor based on green synthesis of silver nanoparticles in plant extract. *J. Pharm. Biomed. Anal.* **2021**, *196*, 113912. https://doi.org/10.1016/j.jpba.2021.113912

Zhang, L.; Ji, M.-Y.; Qiu, B.; Li, Q.-Y.; Zhang, K.-Y.; Liu, J.-C.; Dang, L.-S.; Li, M.-H. Phytochemicals and biological activities of species from the genus *Maytenus*. *Med. Chem. Res.* **2020**, *29* (4), 575–606. https://doi.org/10.1007/s00044-020-02509-4

Appendix

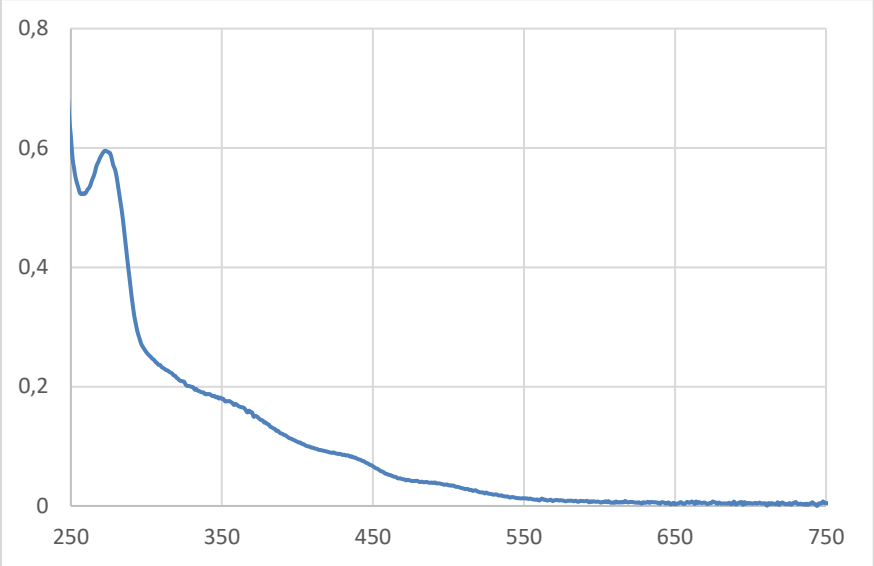

Figure A1. UV-Vis spectrum of aqueous extract of the leaves from *M. ilicifolia*.

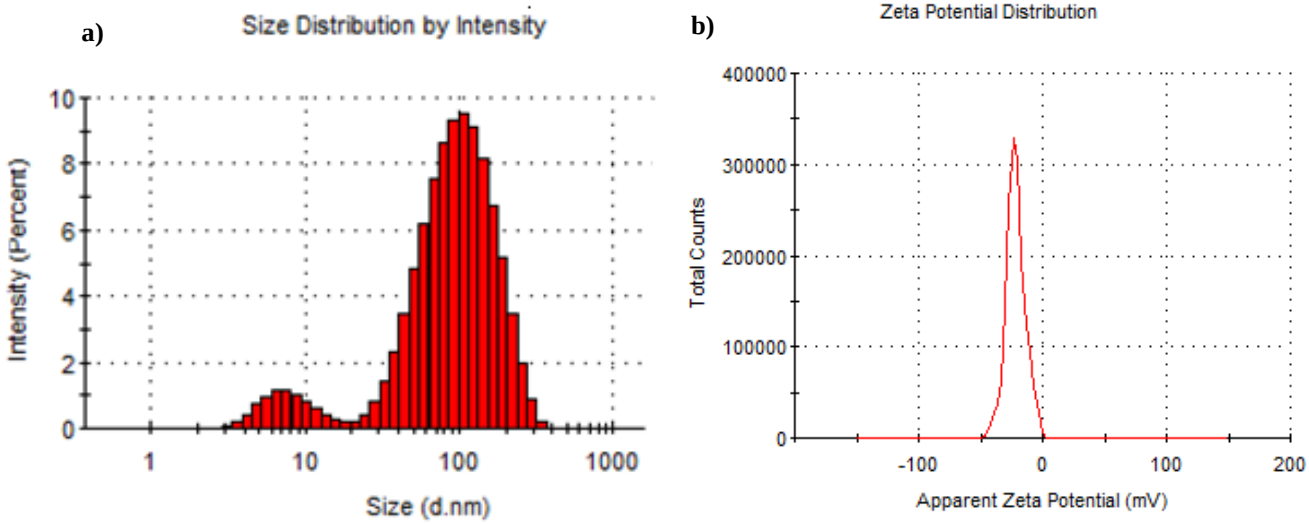

Figure A2. Distribution of particles size obtained by DLS **(a)** and Zeta potential **(b)** for AgNPs-MI.

Eclética Química, vol. 48, n. 2, 2023, 35-48
ISSN: 1678-4618
DOI: 10.26850/1678-4618eqj.v48.2.2023.p35-48

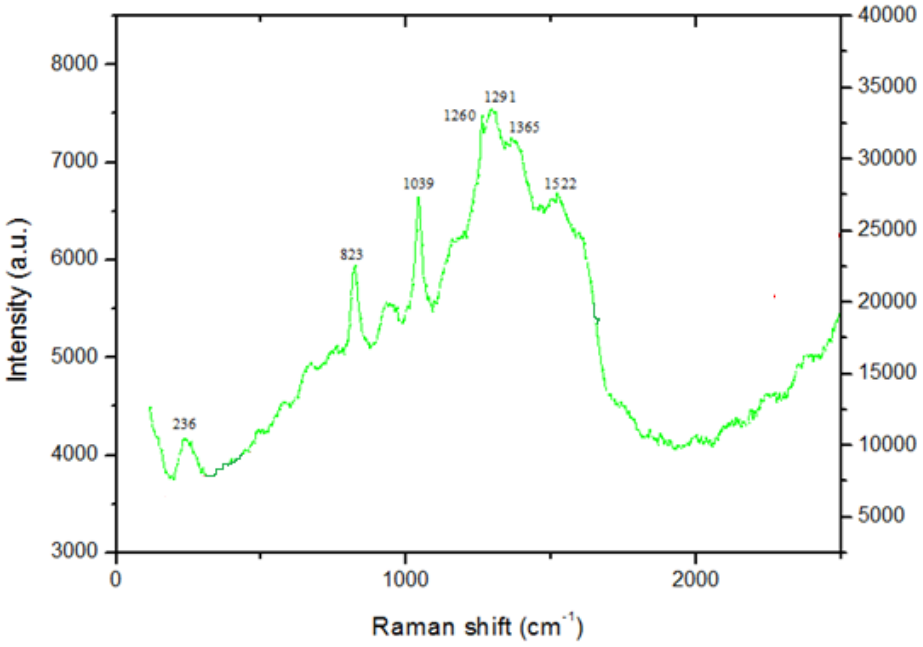

Figure A3. Raman spectra of AgNPs-MI.

Eclética Química, vol. 48, n. 2, 2023, 35-48
ISSN: 1678-4618
DOI: 10.26850/1678-4618eqj.v48.2.2023.p35-48

Eclética Química

Original article

revista.iq.unesp.br

| Vol. 48 | n. 2 | 2023 |

Synthesis of some new substituted imines from aldehydes and ketones derived from quinolinic acid

Anwar Abdulghani Fathi[1], Yassir Shakeeb Al Jawaheri[1+], Shaimaa Samir Ismaee[1]

1. Mosul University, College of Education and Pure Science, Mosul, Iraq.

+Corresponding author: Yassir Shakeeb Al Jawaheri, **Phone:** +964 7709210286, **Email address:** Yassir_chem71@uomosul.edu.iq

ARTICLE INFO

Article history:
Received: September 18, 2022
Accepted: January 02, 2023
Published: April 01, 2023

Section Editors: Assis Vicente Benedetti

Keywords:
1. imine
2. Schiff base
3. quinolinic acid
4. benzenesulfonyl chloride

ABSTRACT: In this paper, some substituted imines compounds have been prepared from quinolinic acid as a starting material. Firstly, the quinolinic acid was treated with acetic anhydride and acetic acid to form furo[3,4-b]pyridine-5,7-dione (1); the resulting compound was heated with urea to form 5H-pyrrolo[3,4-b]pyridine-5,7(6H)-dione (2). After that, it was treated with potassium hydroxide to give potassium 5,7-dioxo-5,7-dihydropyrrolo[3,4-b]pyridin-6-dione, which was directly and easily converted to 6-(2-([1,1'-biphenyl]-4-yl)-2-oxoethyl)-5H-pyrrolo[3,4-b]pyridine-5,7(6H)-dione (3) by the reaction with 1-([1,1'-biphenyl]-4-yl)-2-bromoethan-1-one. Finally, the resultant compound reacted with substituted aniline to give imines (4, 5). Secondly the quinolinic acid converted to 4-(5,7-dioxo-5,7-dihydro-6H-pyrrolo[3,4-b] pyridin-6-yl) benzenesulfonyl chloride according to our previous work, then treated with p-hydroxy acetophenone or p-hydroxy benzaldehyde to form 4-substituted bezyloxy 4-(5,7-dioxo-5,7-dihydro-6H-pyrrolo[3,4-b] pyridine-6-yl) benzenesulfonate (6, 7), which were finally treated with substituted aniline to form new substituted imines (8–12).

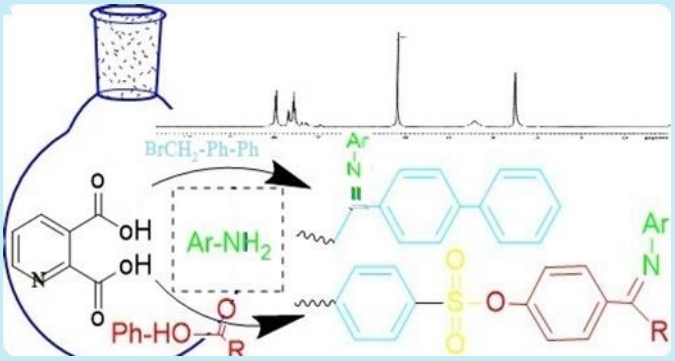

Eclética Química, vol. 48, n. 2, 2023, 49-65
ISSN: 1678-4618
DOI: 10.26850/1678-4618eqj.v48.2.2023.p49-65

1. Introduction

In recent years, imines have been the millstone of chemist research because they were easy to prepare and get various reactions. They can be prepared simply by the reaction of primary amines with carbonyl compound (usually aldehydes or ketones) in the presence of acid as catalyst. The functional group of these compounds is azomethane group C=N. Due to the electronegativity of the nitrogen atom, this group has four different reactions. Firstly, electrophilic, secondly nucleophilic, thirdly dienophile, and lastly, aza-diene reaction (Fig. 1) (Choudhury and Parvin, 2011).

There is a big similarity between carbonyl and the imine groups. Therefore, their reaction is very similar, but the reactivity of the carbonyl group is higher than the imine group because the electronegativity of oxygen is greater than nitrogen. To increase the reactivity, Lewis's acid was used as a catalyst in imine reactions (Chan *et al.*, 2019).

The imine compounds exhibit a wide range of useful biological activity, such as inflammatory, antimalarial, analgesic, antioxidant, antimicrobial, anthelmintic, antitubercular and anticancer (Fig. 2) (Bashiri *et al.*, 2020; Hania, 2009; Jasril *et al.*, 2020; Kajal *et al.*, 2013; Silva *et al.*, 2016).

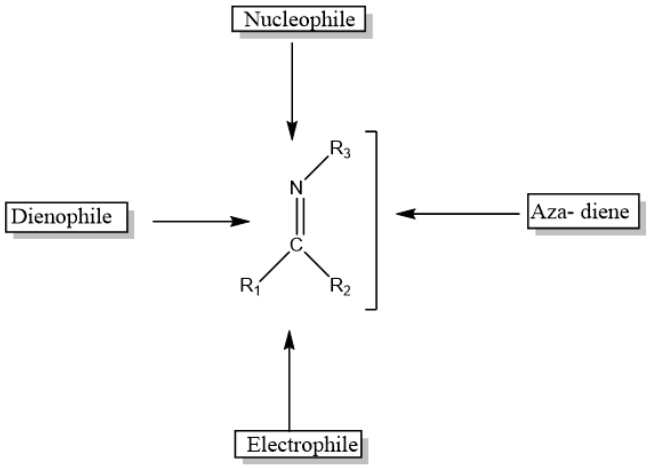

Figure 1. Imine reactivity.
Source: Retrieved from Choudhury and Parvin (2011).

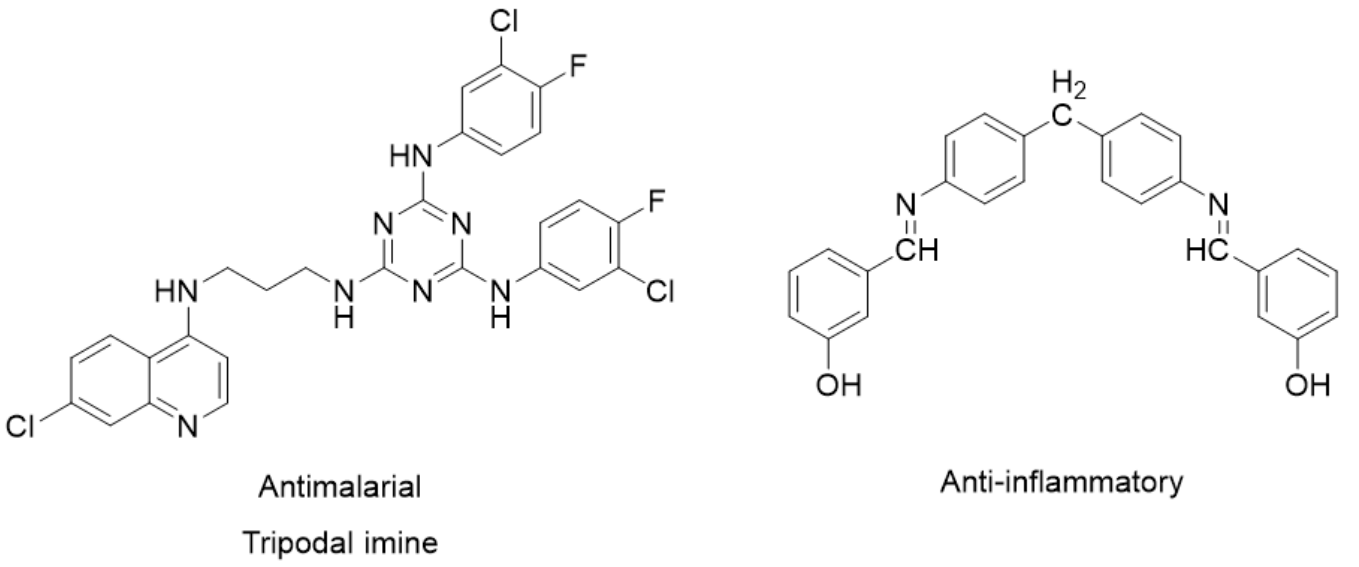

Figure 2. Some of the bioactive imine compounds.
Source: Adapted from Bashiri *et al.*, (2020) and Kajal *et al.*, (2013).

2. Experimental

All chemicals and solvents were purchased from commercially available known sources and used directly without more purification. IR spectra (*V*max in cm^{-1}) were verified utilizing a Shimadzu FT-IR 8400 spectrophotometer with KBr disc. ^{1}H-NMR Bruker at 300 MHz, using dimethyl sulfoxide-d^{6} and tetramethylsilane as a standard.

2.1 Synthesis of 5H-pyrrolo[3,4-b] pyridine-5,7(6H)-dione (2)

Furo [3,4-b] pyridine-5,7-dione (1) was prepared from quinolinic acid (Rapolu *et al.*, 2019) (0.15 mol, 9 g) from anhydride (1) was mixed with (0.3 mol, 2 g) of urea in 100 mL round and heated to (130 to 135 °C) with shaking for (10–20 min) until the reaction was noticed increasing in size. After this point, the product cooled to

Eclética Química, vol. 48, n. 2, 2023, 49-65
ISSN: 1678-4618
DOI: 10.26850/1678-4618eqj.v48.2.2023.p49-65

room temperature, then (10 mL) of water was added and mixed to destroy the amide (2); then, filtrate and recrystallisation from ethanol to give white crystal 83% (188–190 °C), IR, 3104, 1725, 1620, 1391 cm^{-1} (Cai, 2012).

2.2 6-(2-([1,1'-biphenyl]-4-yl)-2-oxoethyl)-5H-pyrrolo[3,4-b] pyridine-5,7(6H)-dione (3)

First step: Imides (0.01 mol, or 1.4 g) were dissolved in 20 mL of absolute ethanol, and the mixture was then heated in a water bath with a clear solid obtained. Ethyl alcohol was added to potassium hydroxide solution of 0.01 mol of KOH in 25 mL of pure ethanol while stirring and letting it cool. The precipitate that formed was then filtered and dried. The resultant compound was used in the next reaction without any further purification; 73% broke down at 230 °C.

In the second step, 0.01 mol (2.7 g) of 4-phenyl phenacyl bromide was dissolved in 25 mL of absolute ethanol in a round-bottomed flask. Then, 0.01 mol (1.8 g) was added. Imide salt, which was prepared in the first step, was added slowly while stirring. The resultant mixture was heated and stirred for 6 h, then cooled to room temperature. The precipitate was filtered, washed with distilled water, dried, and then recrystallized from ethanol to give a brown powder. 60% (120–124 °C), IR, 3104, 1715, 1680, 1676, 1620, 1391 cm^{-1}, 1HNMR δ 8.3–7.3 (m, 12H), 4.9 (s, 2H) (Fig. S1 – Supplementary Material) (Aliabadi *et al.*, 2013).

2.3 General procedure for synthesis of Schiff bases (4–5, 10–12)

For 6 h, 35 mL of absolute ethanol and 2-3 drops of glacial acetic acid were added to 0.01 mol of carbonyl compound and 0.01 mol of primary aromatic amine while stirring at a refluxing temperature. After cooling the reaction mixture to a room temperature, the precipitate was separated from the solvent by filtration, dried, and recrystallized from ethanol Fig. 3 (Altaee and Al-Sabawi, 2021; Yin *et al.*, 2020).

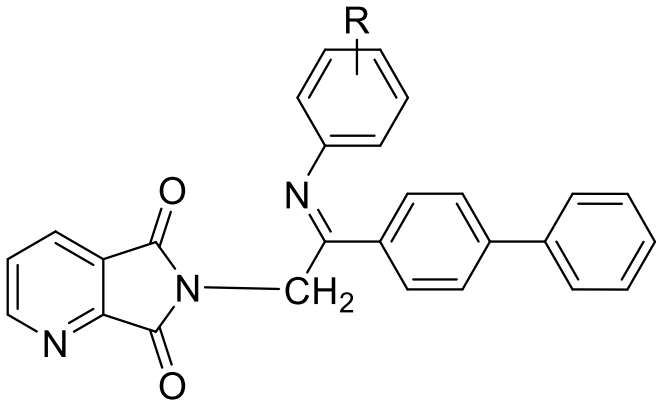

Figure 3. Substituted Schiff bases.

Compound 4 (R = P-hydroxy) is a yellow powder yield in 81% and m. p. 116–117 °C, IR, 3440, 3035, 1728, 1690, 1630 cm^{-1}, ^{1}HNMR δ 8.5 (s, 1H), 8.2–7.3 (m, 16H), 5.0 (s, 2H) Fig. S2 (Supplementary Material).

Compound 5 (R = m-nitro) is a red powder yield in 65% and m. p. 112–114 °C, IR, 2995, 1702, 1621, 1550 cm^{-1}, ^{1}HNMR δ 8.1–7.3 (m, 16H), 5.2 (s, 2H) Fig. S3 (Supplementary Material).

2.4 4-substituted benzyloxy 4-(5,7-dioxo-5,7-dihydro-6H-pyrrolo[3,4-b] pyridin-6-yl) benzenesulfonate (6-7)

A combination of 0.015 mol of 4-hydroxyacetophenone or 4-hydroxybenzaldehyde and 3 mL of pyridine was placed in three-necked flasks with a stirrer and thermostat. The temperature of the combination was lowered to 10 °C by the ice bath that surrounded the flask. During a 20-min period with constant stirring, the phthalimide sulfonyl chloride (Fathi and Al-Jawaheri, 2022) (0.01 mol, 3.2 g) was added gradually. After being refluxed for 2 h, the mixture was cooled to room temperature before being put into cold water and stirred till the oily layer solidified. The resultant solid was filtered, washed with cold, diluted HCl solution, then washed with distilled water before being dried. The desired chemicals were produced by recrystallizing the final product from ethanol Fig. 4 (Soyer *et al.*, 2017).

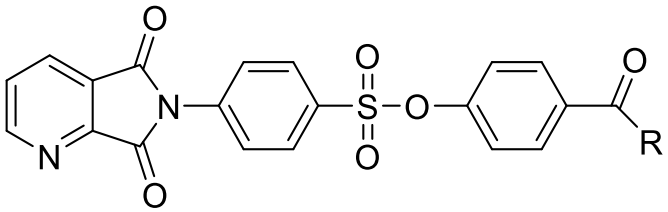

Figure 4. Substituted benzyloxy benzenesulfonate.

Eclética Química, vol. 48, n. 2, 2023, 49-65
ISSN: 1678-4618
DOI: 10.26850/1678-4618eqj.v48.2.2023.p49-65

Compound 6 (R=H) is a yellow powder yield in 70% and m. p. 170–172 °C, IR, 3100, 1720, 1690, 1205 cm^{-1}, ^{1}HNMR δ 10.0 (s, 1H), 8.2–7.7 (m, 9H), 7.4 (d, 2H) Fig. S4 (Supplementary Material).

Compound 7 (R=CH_3) is a yellow powder yield in 75% and m. p. 271–272 °C, IR, 3075, 1707, 1680, 1200 cm^{-1}, ^{1}HNMR δ 8.2–7.8 (m, 9H), 7.35 (d, 2H), 2.60 (s, 3H) Fig. S5 (Supplementary Material).

These compounds were prepared according to the general procedure for synthesis of Schiff bases (8–12) Fig. 5.

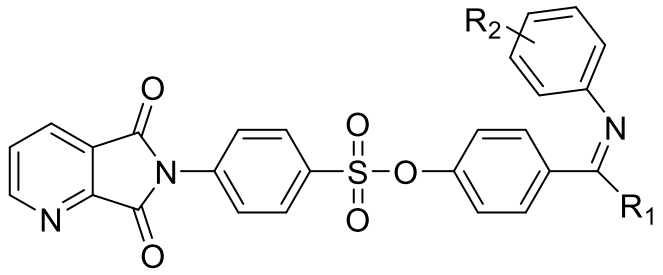

Figure 5. Substituted benzyloxy benzenesulfonate Schiff bases.

Compound 8 (R_1= CH_3/ R_2= O-methyl) is a yellow powder yield in 80% and m. p. 270–271 °C, IR, 3112, 2990, 1728, 1630 cm^{-1}, ^{1}HNMR δ 8.2–7.7 (m, 13H), 7.35 (d, 2H), 2.6 (s, 3H), 2.45 (s, 3H) Fig. S6 (Supplementary Material).

Compound 9 (R_1= CH_3/ R_2= P-methyl) is a light-yellow powder yield in 83% and m. p. 189–190 °C, IR, 3100, 2920, 1720, 1610 cm^{-1}, ^{1}HNMR δ 8.25-7.75 (m, 13H), 7.35 (d, 2H), 2.55 (s, 3H), 2.47 (s, 3H) Fig. S7 (Supplementary Material).

Compound 10 (R_1= CH_3/ R_2= 2-Nitro 4- chloro) is a white powder yield in 62% and m. p. 160–161 °C, IR, 3120, 2950, 1715, 1605 cm^{-1}, ^{1}HNMR δ 8.25–7.63 (m, 11H), 7.33(d, 2H), 2.55(s, 3H) Fig. S8 (Supplementary Material).

Compound 11 (R_1= H/ R_2= P-methyl) is a white powder yield in 90% and m. p. 226–228 °C, IR, 3099, 2925, 1710, 1600 cm^{-1}, ^{1}HNMR δ 8.7 (s,1H), 8.2- 7.7 (m, 11H), 7.55–7.2 (d,d, 4H), 2.05 (s, 3H) Fig. S9 (Supplementary Material).

Compound 12 (R_1= H/ R_2= 2,4-Dichloro) is a yellow powder yield in 83% and m. p. 190–191 °C, IR, 3090, 1725, 1600, 770 cm^{-1}, ^{1}HNMR δ 8.65 (s, 1H), 8.3- 7.7 (m, 13H), 7.6–7.3 (m, 3H) Fig. S10 (Supplementary Material).

3. Results and discussion

The synthesis of new compounds is a millstone in the field of organic chemistry and is the first step for the invention of new things that could improve our life. Quinolinic acid was used as the available starting material in this paper to convert to anhydride (1) (Fig. 6) using the dehydration agent acetic anhydride. The resultant compound (1) in 85% is regarded as a known compound and is confirmed by its physical properties as a beige solid powder and m.p. = 139–140 °C. The IR spectra gave strong signals at 3043 and 1765 cm^{-1} belonging to the C-H aromatic and carbonyl groups, respectively (Sigma Aldrich CAS Number 699-98-0).

The next step was to convert the anhydride (1) to pyrrole (2) by heating the anhydride with urea. The resultant compound was confirmed by its physical properties as a white crystal yield in 83%, m.p. = 188–190 °C. The IR spectra gave in cm^{-1} at 3104 for C-H aromatic, 1725 for carbonyl, 1620 for N-H.

Compound (3) was prepared in two steps. Firstly, compound (2) was treated with alcoholic potassium hydroxide to form organic salt to increase the nucleophilicity to react with 4-phenyl phenacyl bromide via one step SN2 mechanism (Fig. 6). The resultant compound was confirmed by physical properties as a brown powder resulting in 60% (m.p. 120–124 °C), IR 3104 cm^{-1} for aromatic C-H, 1715 cm^{-1} for amid carbonyl, 1680 cm^{-1} for ketonic. In addition, ^{1}HNMR δ chart gave signals at 8.21–7.32 (m, 12) and at 4.95 singlet belongs to two protons for CH_2 (Maimaris *et al.*, 2022).

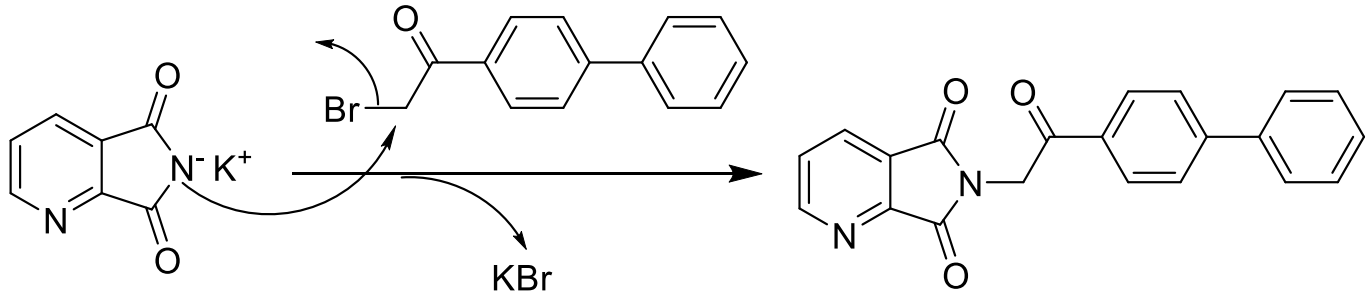

Figure 6. Mechanism of SN2 Reaction.

Eclética Química, vol. 48, n. 2, 2023, 49-65
ISSN: 1678-4618
DOI: 10.26850/1678-4618eqj.v48.2.2023.p49-65

Intermediate compounds were prepared according to our past paper (Fathi and Al-Jawaheri, 2022). Compounds (6-7) were prepared from phthalimide sulfonyl chloride by replacing the chlorin with the phenolic group from p-hydroxy benzaldehyde or p-hydroxy acetophenone throw SN2 mechanism. The resultant compounds were confirmed by their physical properties, for (6) was a yellow powder yield in 70%, melted at 170–171°C, IR 3100 cm^{-1} for C-H aromatic, 1720 and 1690 cm^{-1} for carbonyls, ^{1}HNMR δ chart have clear unique signals at 10 ppm singlet for aldehyde proton, 8.2–7.7 multiplet and at 7.4 doublet for aromatic protons. Compound (7) was a yellow powder yield in 75% and m.p. in 271–272°C, IR 3075 cm^{-1} for aromatic C-H, 1707 and 1680 cm^{-1} for carbonyls, ^{1}HNMR δ signals confirmed the structure at 8.2–7.8 ppm multiplet and at 7.35 doublet for aromatic protons and at 2.60 singlet belongs to three protons of CH_3 (Fadlelmoula *et al.*, 2022).

The final step was to form a Schiff base by choosing different primary amines to react with compound (3) to form (4, 5) and compounds (6, 7) to form (8–12). The mechanism of the reaction shows six steps in which the proton of the acid has been attacked by the electron pair of the carbonyl oxygen to increase the electrophilicity of the carbonyl of the carbon and form the oxonium ion. At this point, the electron pair of the amine nitrogen will be ready to attack the carbon of the carbonyl to form the zwitterion. The next steps included the release and addition of the proton, then dehydration (Fig. 7) (Choudhury and Parvin, 2011).

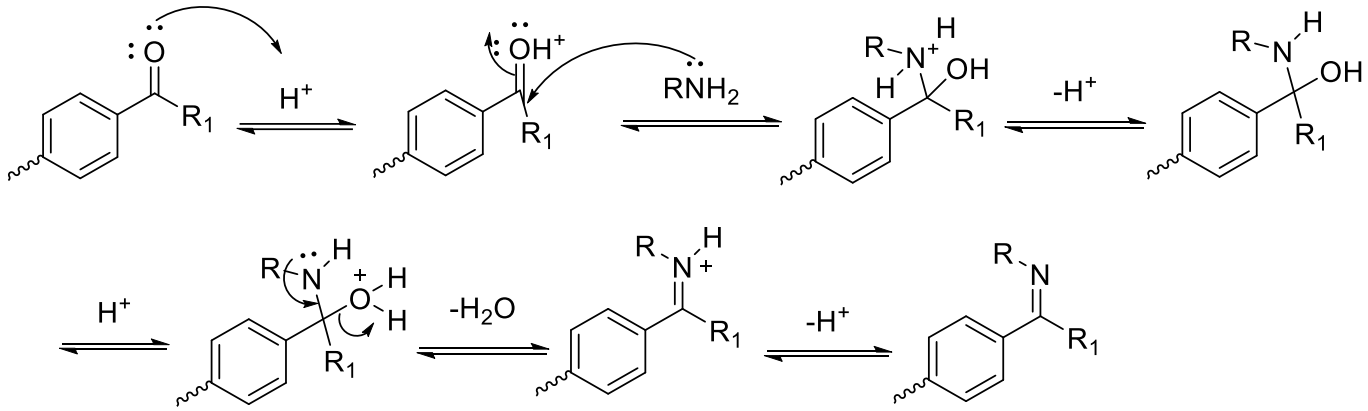

Figure 7. Mechanism of Schiff bases formations.

The structure of the resultant compounds (4, 5) was confirmed by physical properties, yellow powder and red powder yield 81% and 65%, m.p. 116–117 °C and 112–114 °C, respectively. Also, spectral data showed IR cm^{-1} 3440 belonging to the hydroxyl group in (4), 3112, 2995 for C-H aromatic, 1728, 1702 for the carbonyl group, 1690, 1621 for the C=N group, ^{1}HNMR δ ppm showed signals, 8.5 singlet for OH in (4), 8.2–7.3 and 8.1–7.3 multiplet for aromatic protons, 5.0, 5.2 singlet for CH_2 protons, respectively.

Compounds (8–12): Every compound has a unique ^{1}HNMR δ spectrum. For (8) the spectral data presented signals at 2.6 and 2.45 singlet for CH_3 protons, while (9) showed signals at 2.55, 2.47 singlet for CH_3 protons; for (10) at 2.55 singlet for CH_3 protons, for (11) and (12) at 8.7 singlet belonging to the proton attached to the C=N group and 2.05 for CH_3 protons. Finally, for (12) at 8.65 singlet belonging to the proton attached to the C=N group. (Fig. 8), find the attached Supplementary Material.

Eclética Química, vol. 48, n. 2, 2023, 49-65
ISSN: 1678-4618
DOI: 10.26850/1678-4618eqj.v48.2.2023.p49-65

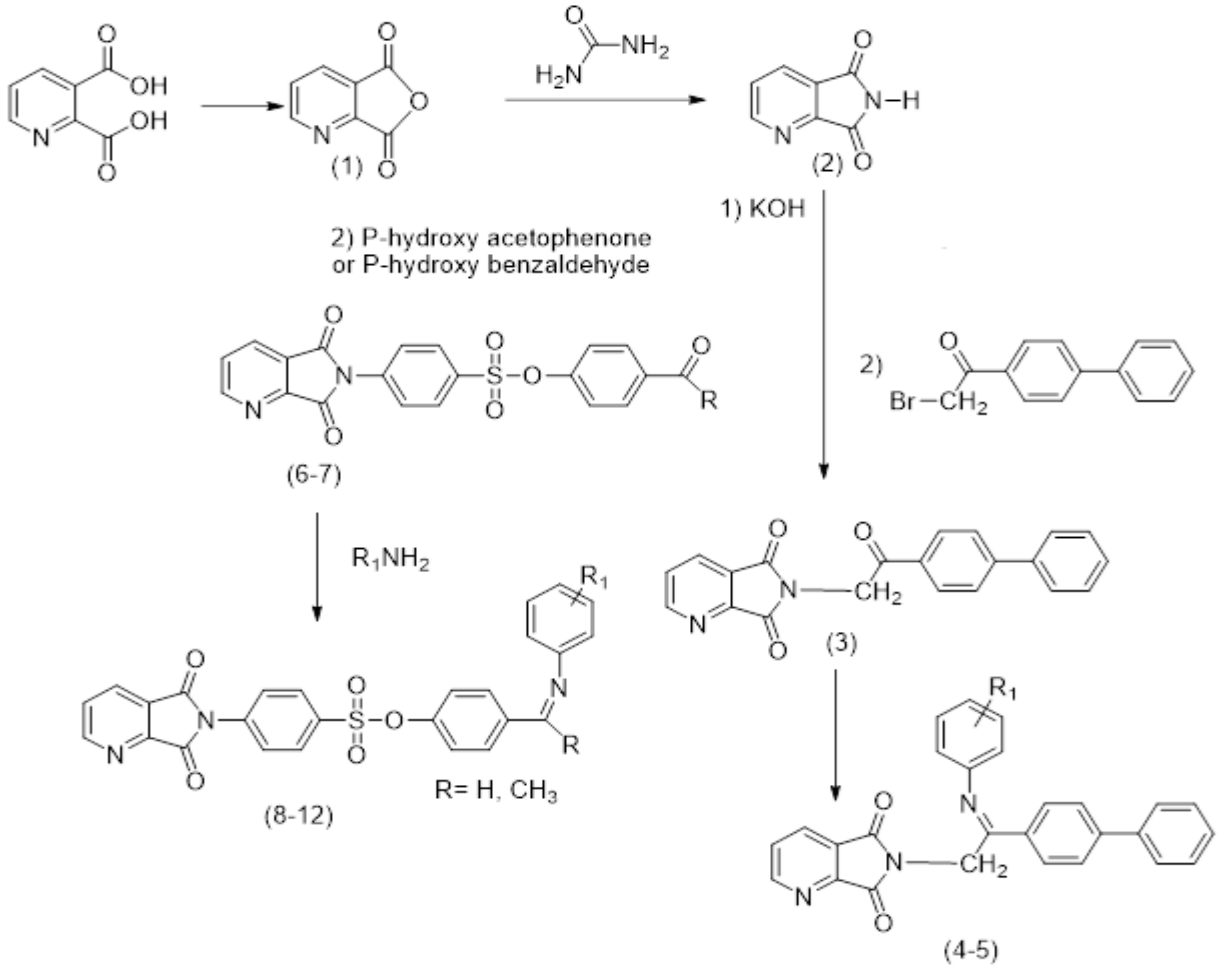

Figure 8. Scheme of the reactions.

4. Conclusions

In this study, we have successfully prepared several new substituted compounds derived from substituted nicotinic acid to enhance the library of organic chemistry. These compounds contain carbon and nitrogen double bond as an imine functional group, which can be used as starting material in many fields, such as organometal compounds.

Authors' contribution

Conceptualization: Fathi, A.; Al-Jawaheri, Y.
Data curation: Fathi, A.
Formal Analysis: Ismaeel, S.
Funding acquisition: Not applicable.
Investigation: Al-Jawaheri, Y.
Methodology: Fathi, A.; Al-Jawaheri, Y.
Project administration: Fathi, A.; Al-Jawaheri, Y.
Resources: Ismaeel, S.
Software: Not applicable.
Supervision: Fathi, A.
Validation: Fathi, A.; Al-Jawaheri, Y.; Ismaeel, S.
Visualization: Ismaeel, S.
Writing – original draft: Al-Jawaheri, Y.
Writing – review & editing: Fathi, A.; Al-Jawaheri, Y.

Data availability statement

All data set were generated or analyzed in the current study.

Funding

Not applicable.

Acknowledgments

The authors would like to thank the University of Mosul College of Education for Pure Science for their support and encouragement during this research project.

Eclética Química, vol. 48, n. 2, 2023, 49-65
ISSN: 1678-4618
DOI: 10.26850/1678-4618eqj.v48.2.2023.p49-65

References

Aliabadi, A.; Foroumadi, A.; Mohammadi-Farani, A; Mahvar, M. G. Synthesis and Evaluation of Anti-acetylcholinesterase Activity of 2-(2-(4-(2-Oxo-2-phenylethyl) piperazin-1-yl) ethyl)Isoindoline-1,3-dione Derivatives with Potential Anti-Alzheimer Effects. *Iran J. Basic Med. Sci.* **2013**, *16* (10), 1049–1054.

Altaee, E. A.; Al-Sabawi, A. H. Synthesis and Spectral Study of Some New 4-substituted but-2-enolide Derivatives. *Egypt. J. Chem*. **2021**, *64* (12), 7117–7122. https://doi.org/10.21608/ejchem.2021.80154.3957

Bashiri, M.; Jarrahpour, A.; Rastegari, B.; Iraji, A.; Irajie, C.; Amirghofran, Z.; Malek-Hosseini, S.; Motamedifar, M.; Haddadi, M.; Zomorodian, K.; Zareshahrabadi, Z.; Turos, E. Synthesis and evaluation of biological activities of tripodal imines and β-lactams attached to the 1,3,5-triazine nucleus. *Monatsh Chem*. **2020**, *151* (5), 821–835. https://doi.org/10.1007/s00706-020-02592-8

Cai, Y.-H. Solvent-Free Synthesis of Phthalimide Under Microwave Irradiation and Modification of Talc with Synthesized Phthalimide. *Asian J. Chem*. **2012**, *24* (2), 481–484.

Chan, K. K.; Wong, Y. F.; Yang, D.; Pettus, T. R. R. Nucleophilic Imines and Electrophilic *o*-Quinone Methides, a Three-Component Assembly of Assorted 3,4-Dihydro-2*H*-1,3-benzoxazines. *Org. Lett*. **2019**, *21* (19), 7746–7749. https://doi.org/10.1021/acs.orglett.9b02655

Choudhury, L. H.; Parvin, T. Recent advances in the chemistry of imine-based multicomponent reactions (MCRs). *Tetrahedron*, **2011**, *67* (43), 8213–8228. https://doi.org/10.1016/j.tet.2011.07.020

Fadlelmoula, A.; Pinho, D.; Carvalho, V. H.; Catarino, S. O.; Minas, G. Fourier Transform Infrared (FTIR) Spectroscopy to Analyse Human Blood over the Last 20 Years: A Review towards Lab-on-a-Chip Devices. *Micromachines*, **2022**, *13* (2), 187. https://doi.org/10.3390/mi13020187

Fathi, A. A.; Al-Jawaheri, Y. S. M. Synthesis and characterization of new N- Aryl sulfonyl hydrazone compounds. *Egypt. J. Chem*. **2022**, *65* (3), 179–183. https://doi.org/10.21608/ejchem.2021.90637.4320

Hania, M. M. Synthesis of Some Imines and Investigation of their Biological Activity. *J. Chem*. **2009**, *6* (3), 629–632. https://doi.org/10.1155/2009/104058

Jasril, J.; Ikhtiarudin, I.; Nurulita, Y.; Nurisma. Microwave-assisted synthesis and antioxidant activity of an imine, (*E*)-1-(3-bromobenzylidene)-2-phenylhydrazine. *AIP Conf. Proc*. **2020**, *2242*, 040041. https://doi.org/10.1063/5.0009374

Kajal, A.; Bala, S.; Kamboj, S.; Sharma, N.; Saini, V. Schiff Bases: A Versatile Pharmacophore. *J. Catal*. **2013**, *2013*, 893512. https://doi.org/10.1155/2013/893512

Maimaris, M.; Pettipher, A. J.; Azzouzi, M.; Walke, D. J.; Zheng, X.; Gorodetsky, A.; Dong, Y.; Tuladhar, P. S.; Crespo, H.; Nelson, J.; Tisch, J. W. G.; Bakulin, A. A. Sub-10-fs observation of bound exciton formation in organic optoelectronic devices. *Nat. Commun*. **2022**, *13*, 4949. https://doi.org/10.1038/s41467-022-32478-8

Rapolu, R. K.; Areveli, S.; Raju, V. V. N. K. V. P.; Navuluri, S.; Chavali, M.; Mulakayala, N. An Efficient Synthesis of Darunavir Substantially Free from Impurities: Synthesis and Characterization of Novel Impurities. *ChemistrySelect*. **2019**, *4* (14), 4422–4427. https://doi.org/10.1002/slct.201803825

Silva, E. T.; Araújo, A. S.; Moraes, A. M.; Souza, L. A.; Lourenço, M. C. S.; Souza, M. V. N.; Wardell, J. L.; Wardell, S. M. S. V. Synthesis and Biological Activities of Camphor Hydrazone and Imine Derivatives. *Sci. Pharm*. **2016**, *84* (3), 467–483. https://doi.org/10.3390/scipharm84030467

Soyer, Z.; Uysal, S.; Parlar, S.; Dogan, A. H. T.; Alptuzun, V. Synthesis and molecular docking studies of some 4-phthalimidobenzenesulfonamide derivatives as acetylcholinesterase and butyrylcholinesterase inhibitors. *J. Enzyme Inhib. Med. Chem*. **2017**, *32* (1), 13–19. https://doi.org/10.1080/14756366.2016.1226298

Yin, Y.; Zhao, X.; Jiang, Z. Advances in the Synthesis of Imine-Containing Azaarene Derivatives via Photoredox Catalysis. *ChemCatChem*. **2020**, *12* (18), 4471–4489. https://doi.org/10.1002/cctc.202000741

Eclética Química, vol. 48, n. 2, 2023, 49-65
ISSN: 1678-4618
DOI: 10.26850/1678-4618eqj.v48.2.2023.p49-65

Supplementary Material

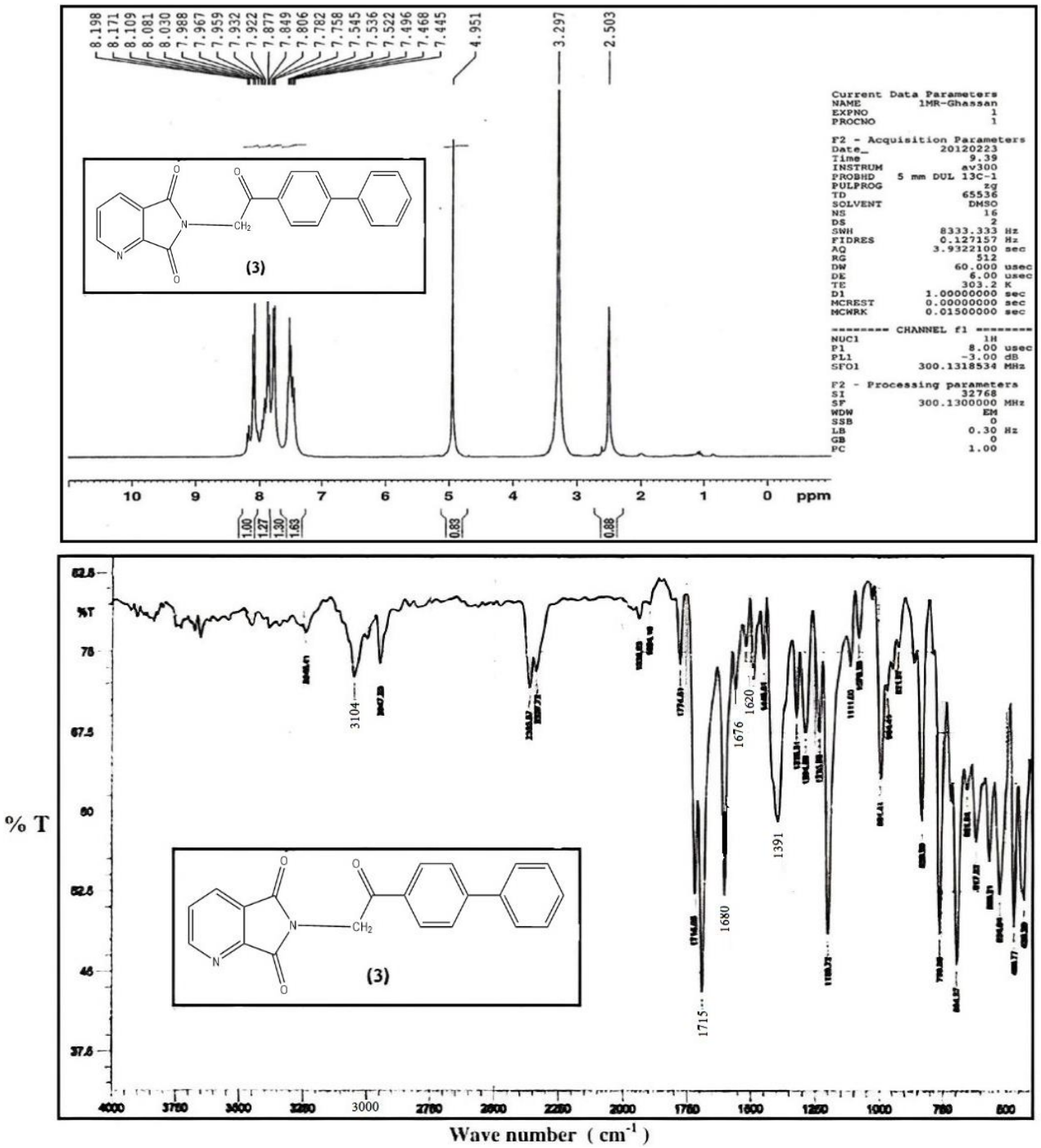

Figure S1. NMR and IR. Charts for compound 3.

Eclética Química, vol. 48, n. 2, 2023, 49-65
ISSN: 1678-4618
DOI: 10.26850/1678-4618eqj.v48.2.2023.p49-65

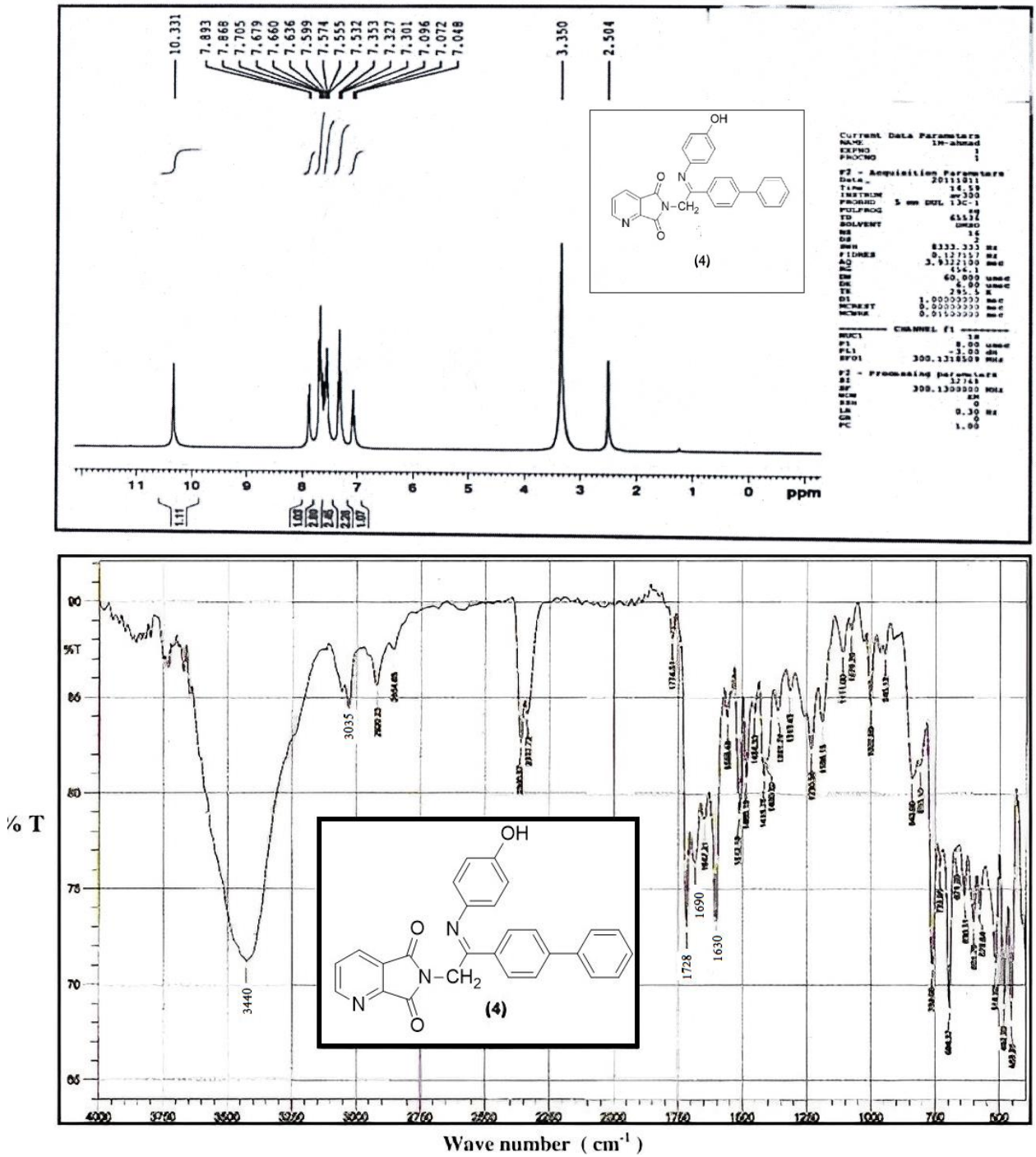

Figure S2. NMR and IR. Charts for compound 4.

Eclética Química, vol. 48, n. 2, 2023, 49-65
ISSN: 1678-4618
DOI: 10.26850/1678-4618eqj.v48.2.2023.p49-65

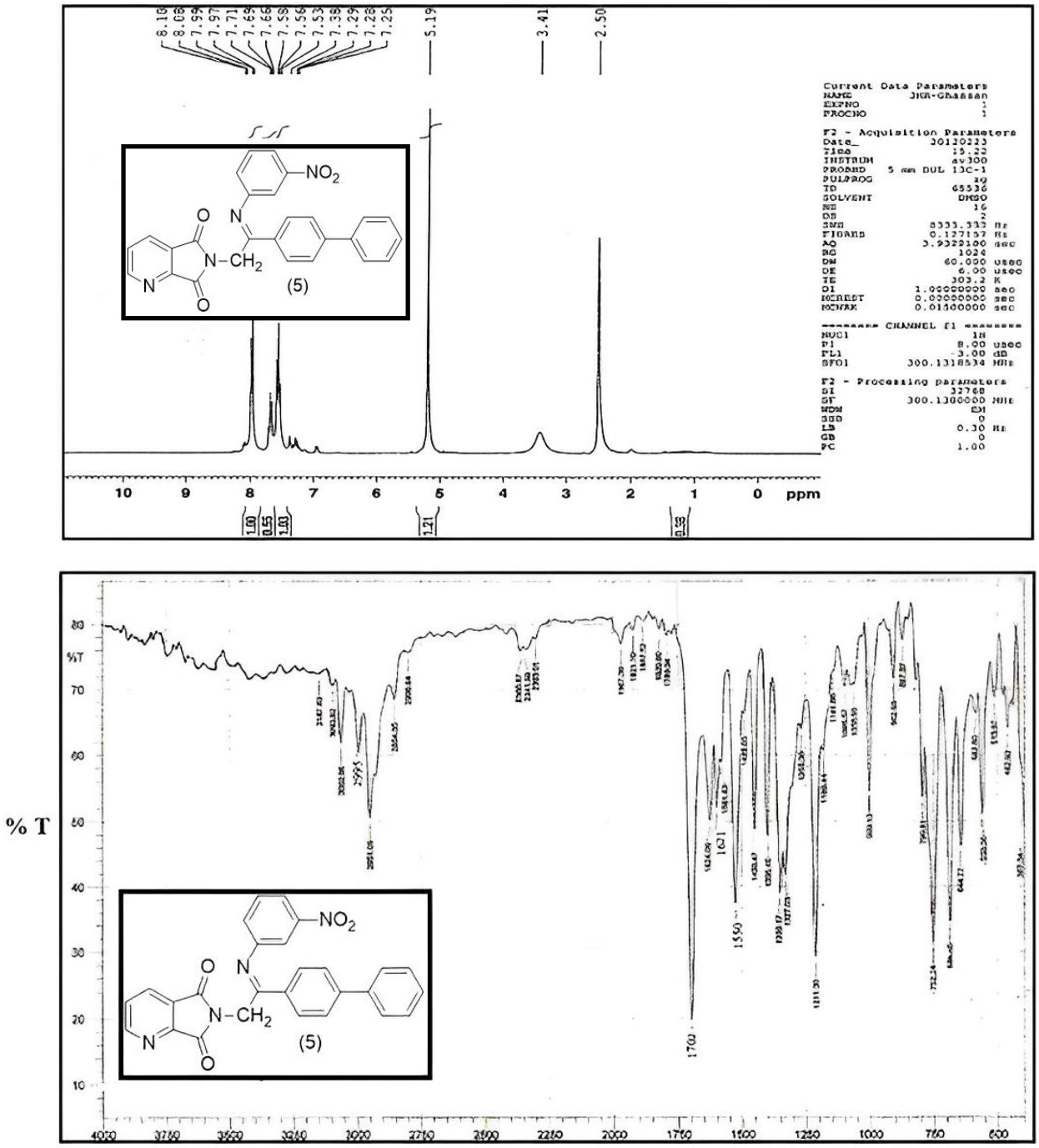

Figure S3. NMR and IR. Charts for compound 5.

Eclética Química, vol. 48, n. 2, 2023, 49-65
ISSN: 1678-4618
DOI: 10.26850/1678-4618eqj.v48.2.2023.p49-65

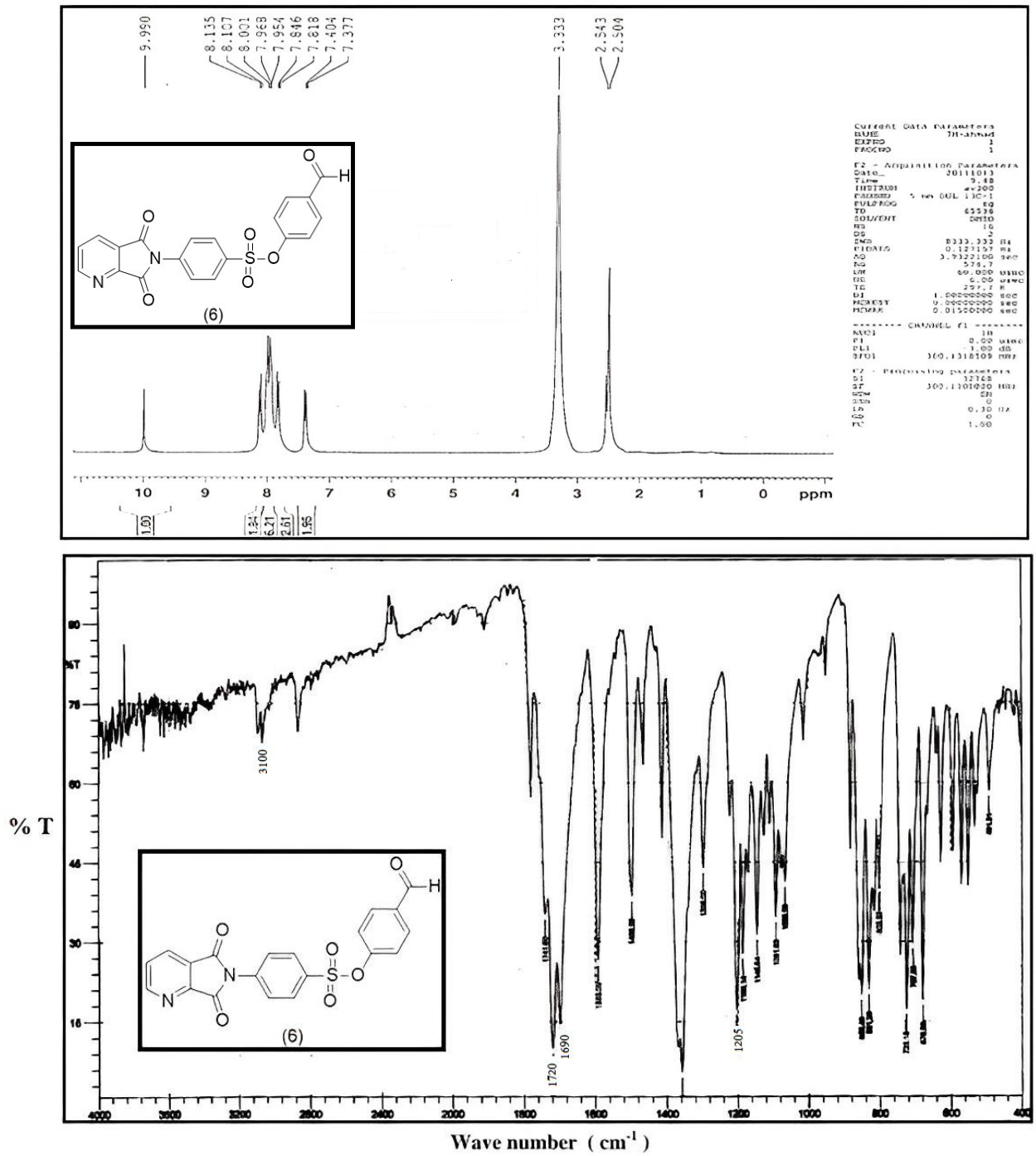

Figure S4. NMR and IR. Charts for compound 6.

Eclética Química, vol. 48, n. 2, 2023, 49-65
ISSN: 1678-4618
DOI: 10.26850/1678-4618eqj.v48.2.2023.p49-65

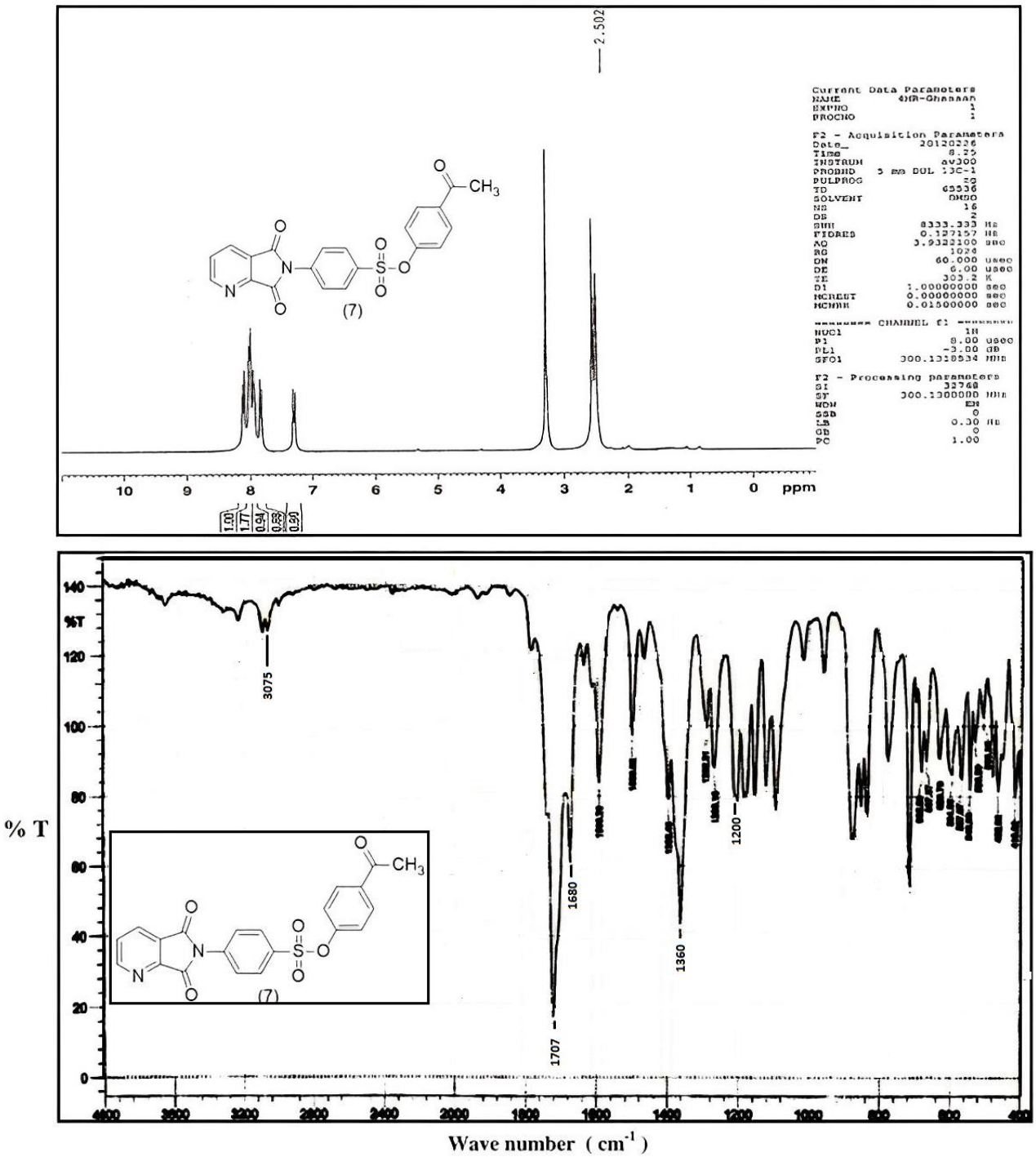

Figure S5. NMR and IR. Charts for compound 7.

Eclética Química, vol. 48, n. 2, 2023, 49-65
ISSN: 1678-4618
DOI: 10.26850/1678-4618eqj.v48.2.2023.p49-65

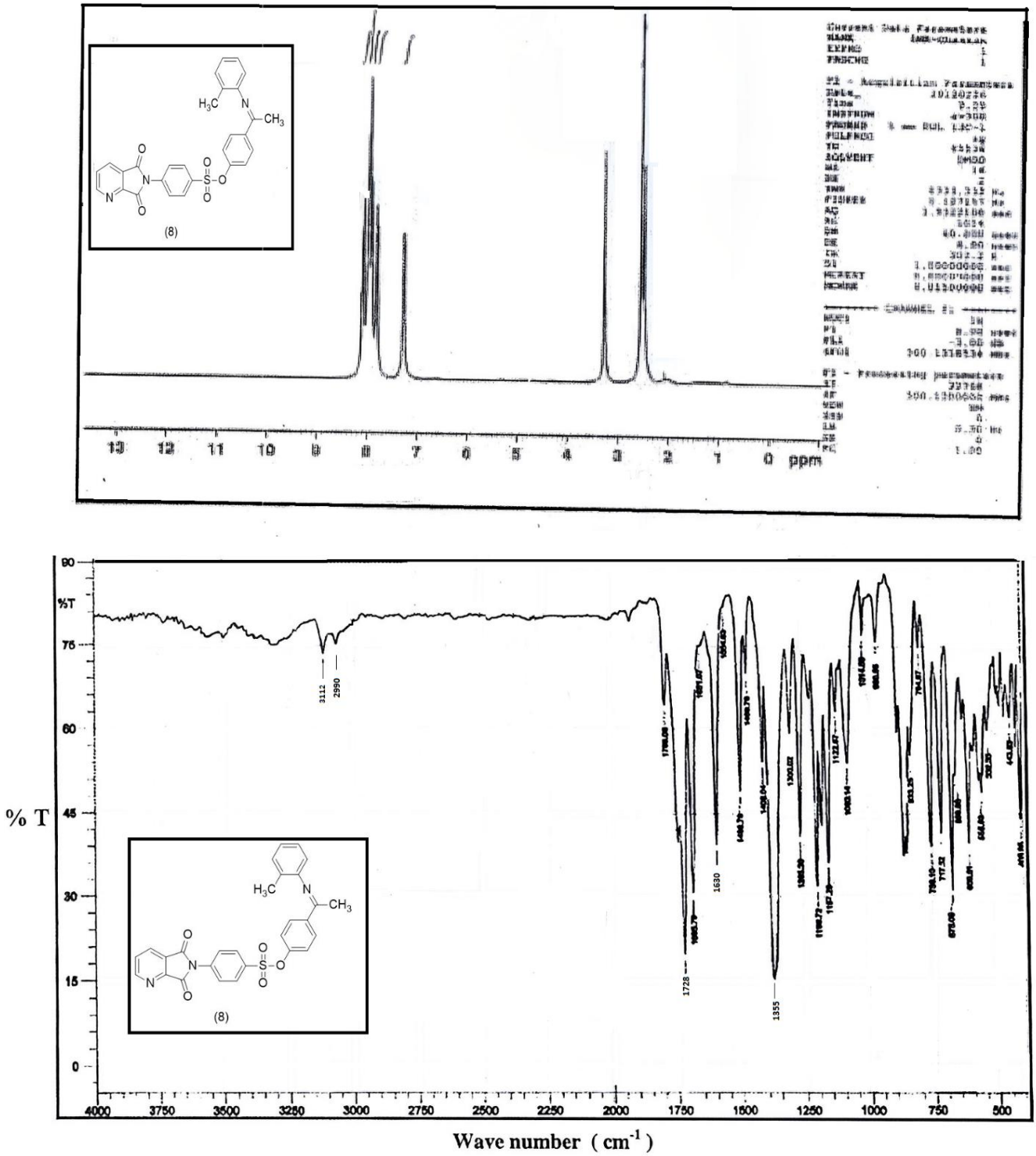

Figure S6. NMR and IR. Charts for compound 8.

Eclética Química, vol. 48, n. 2, 2023, 49-65
ISSN: 1678-4618
DOI: 10.26850/1678-4618eqj.v48.2.2023.p49-65

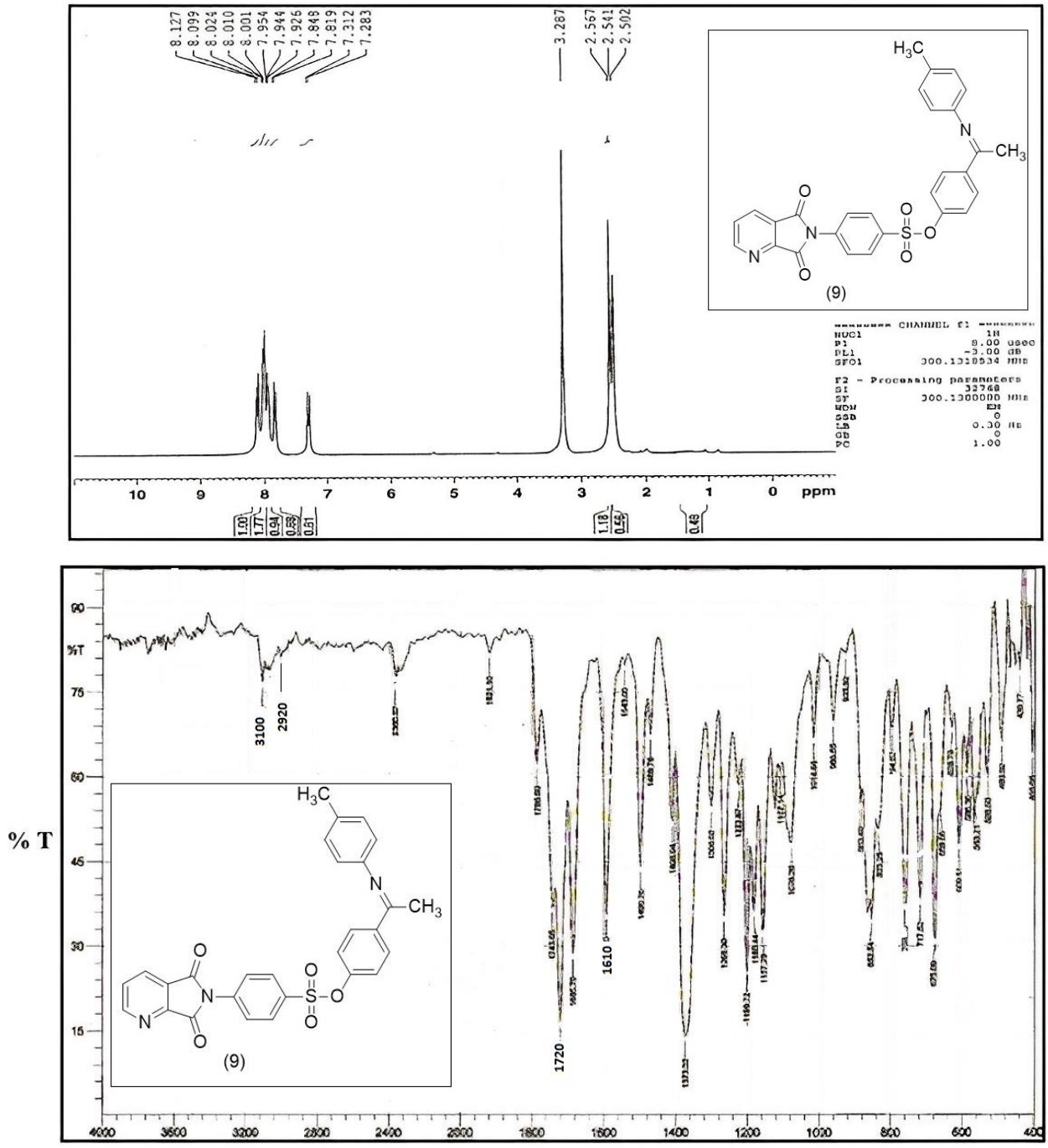

Figure S7. NMR and IR. Charts for compound 9.

Eclética Química, vol. 48, n. 2, 2023, 49-65
ISSN: 1678-4618
DOI: 10.26850/1678-4618eqj.v48.2.2023.p49-65

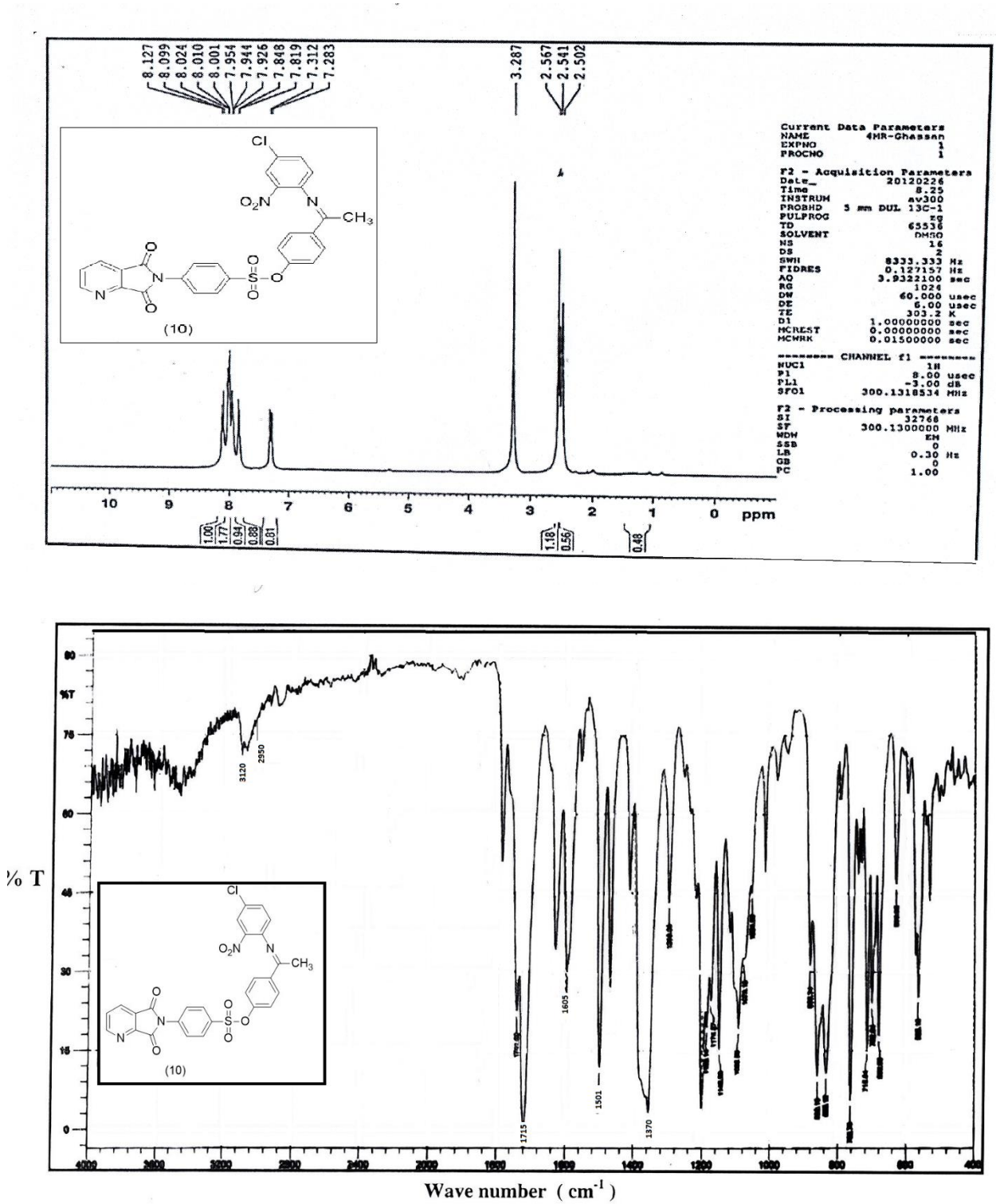

Figure S8. NMR and IR. Charts for compound 10.

Eclética Química, vol. 48, n. 2, 2023, 49-65
ISSN: 1678-4618
DOI: 10.26850/1678-4618eqj.v48.2.2023.p49-65

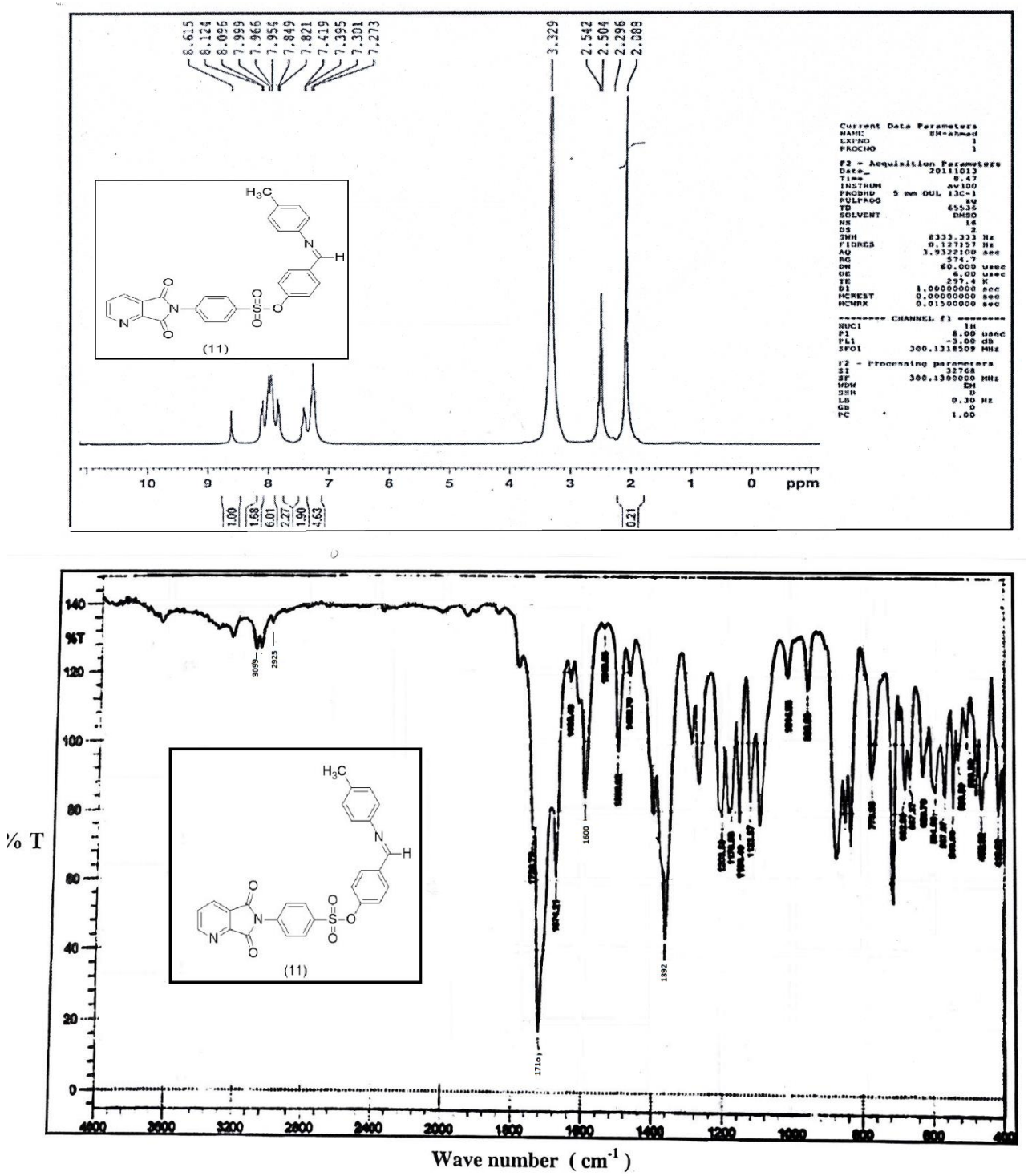

Figure S9. NMR and IR. Charts for compound 11.

Eclética Química, vol. 48, n. 2, 2023, 49-65
ISSN: 1678-4618
DOI: 10.26850/1678-4618eqj.v48.2.2023.p49-65

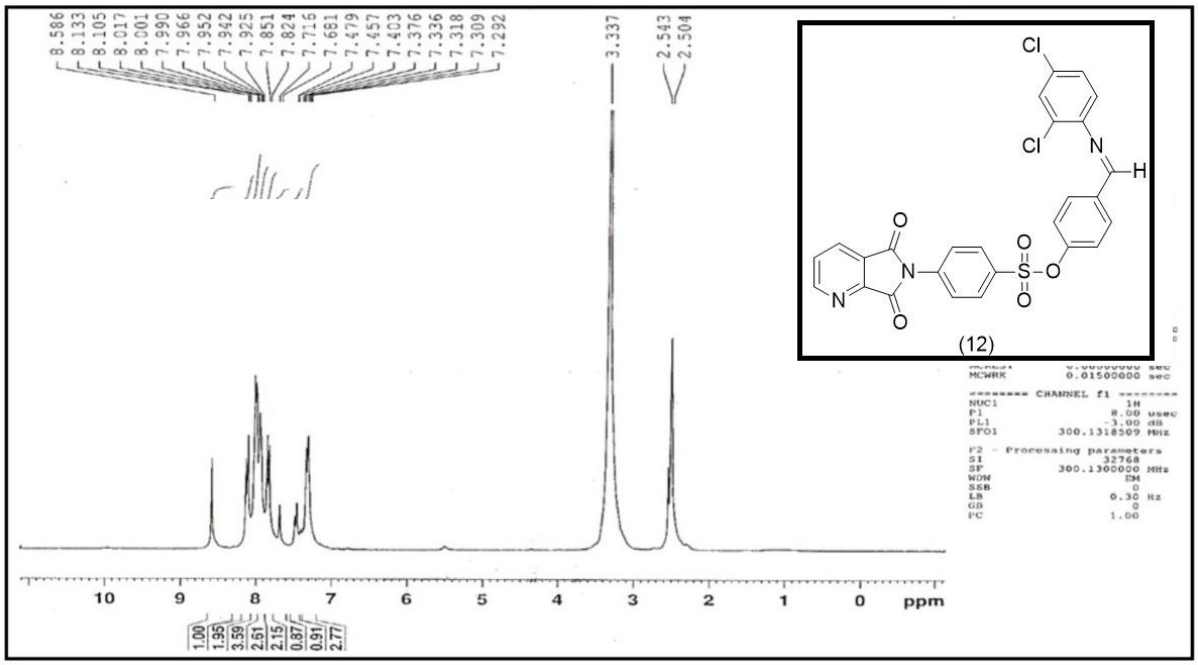

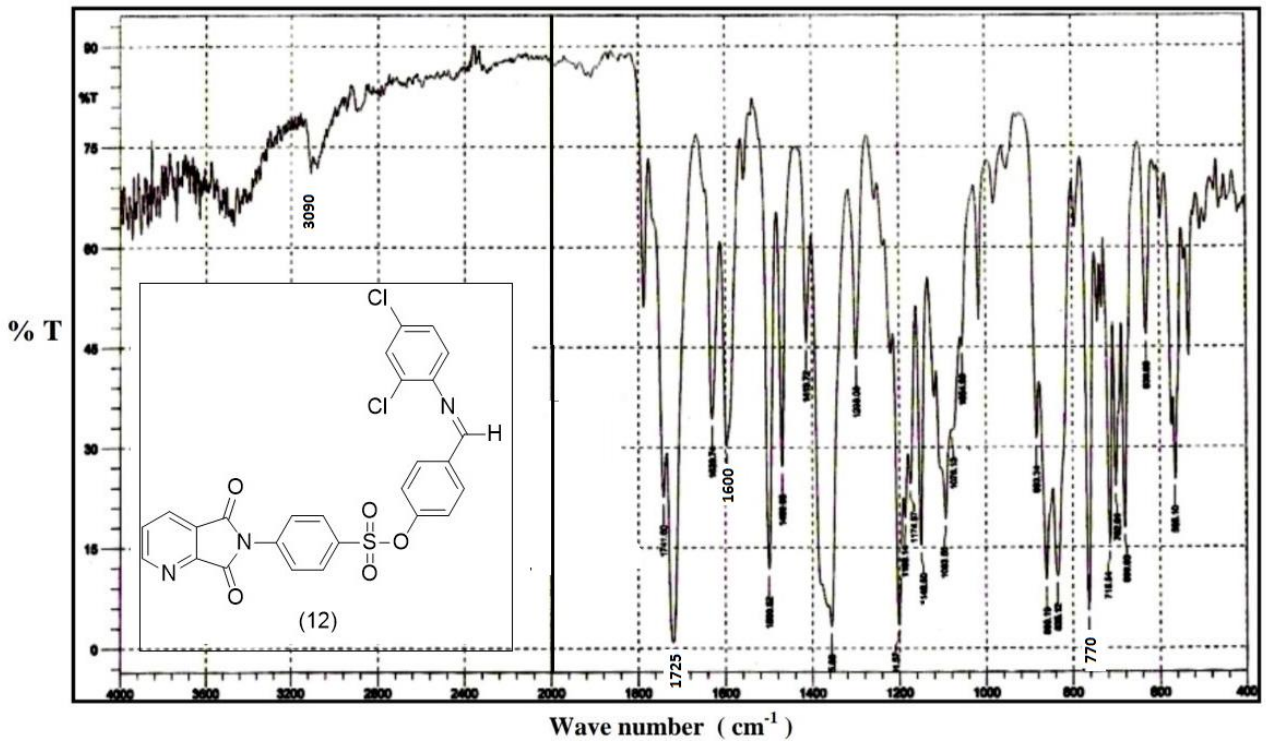

Figure S10. NMR and IR. Charts for compound 12.

Eclética Química, vol. 48, n. 2, 2023, 49-65
ISSN: 1678-4618
DOI: 10.26850/1678-4618eqj.v48.2.2023.p49-65

Eclética Química

Original article

revista.iq.unesp.br

| Vol. 48 | n. 2 | 2023 |

Synthesis, structural and spectroscopic properties of Co(II), Ni(II) and Cu(II) complexes with 2-((2-chlorobenzylidene)amino) acetohydrazide hydrate and their Antimicrobial and antioxidant activities

Fathi Mohammed Al-Azab[1], Yasmin Mosa'd Jamil[1+], Amani Ahmed Al-Gaadbi[1]

1. Sana'a University, Faculty of Science, Sana'a, Yemen.

+Corresponding author: Yasmin Mos'ad Jamil, **Phone:** +967-771952842, **Email address:** y.jamil@su.edu

ARTICLE INFO

Article history:
Received: November 14, 2022
Accepted: February 24, 2023
Published: April 01, 2023

Section Editors: Rogéria Rocha Gonçalves

Keywords:
1. Schiff base
2. powder X-ray diffraction
3. antioxidant activity

ABSTRACT: The current study was purposed to prepare Co(II), Ni(II) and Cu(II) complexes with the ligands derived from 2-chlorobenzaldehyde, glycine and hydrazine hydrate. The obtained compounds were characterized by different physicochemical studies such as elemental analysis, atomic absorption, molar ratio analysis, electronic absorption (UV-Vis spectroscopy), magnetic properties, FTIR spectroscopy, ^{1}H–NMR, ^{13}C-NMR, conductance measurements and XRD. Antimicrobial and antioxidant activities were also calculated. The antibacterial activity was evaluated by the diffusion method against two Gram-positive and two Gram-negative bacteria, while antifungal activity was assessed against two fungal strains by using the agar method. The ligand with Schiff base and hydrazide groups and its complexes showed better biological activity. The results showed that the most metal complexes have much higher antibacterial and antifungal activity compared to the parent ligand. The antioxidant activity of 3.7453 mg of the ligand exhibited excellent activity as the activity of 1 mg of ascorbic acid which is used as a standard antioxidant.

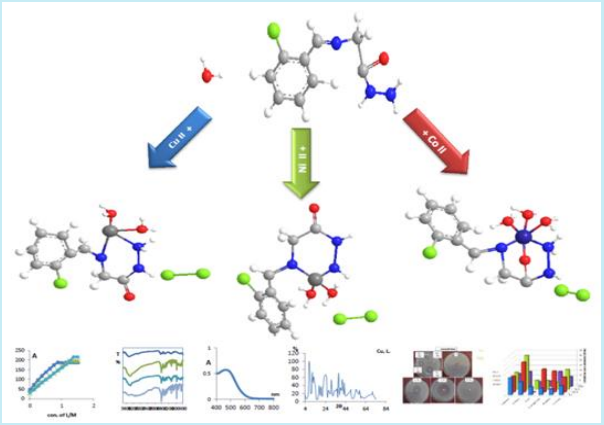

Eclética Química, vol. 48, n. 2, 2023, 66-82
ISSN: 1678-4618
DOI: 10.26850/1678-4618eqj.v48.2.2023.p66-82

1. Introduction

1.1 Schiff bases and hydrazides

Schiff bases are usually prepared by the condensation of a carbonyl compound with a primary amine (Malakyan *et al*., 2016). Imine or azomethine groups are present in various natural, natural-derived and nonnatural compounds (Safoura, 2014). They are used in many fields such as biological activities, analytical chemistry, corrosion inhibitors, fungicidal, agrochemical, electrical conductivity, magnetism, ion exchange, nonlinear optics, catalysis (Emriye, 2016), crystal engineering (Al Zoubi, 2013), and medical substrates (Savalia *et al*., 2013). Hydrazides include C(=O)NHNH$_2$ group, and were produced as far back as 1895 by Kurzius (Majumdar *et al*., 2014). Hydrazides have been used widely in medicine, catalysis, and analytical chemistry (Salawu *et al*., 2018), and are highly useful starting materials and intermediates in the synthesis of heterocyclic intermediates in the synthesis of heterocyclic molecules. They have been investigated due to their antitumor and biocidal activity, also they have been used widely as antituberculosis compounds because of their ability to form metal chelates (Mathew *et al*., 2006). A large number of different Schiff base ligands have been used for excellent selectivity, sensitivity, and stability for specific metal ions such as Ag(II) Al(III), Co(II), Cu(II), Gd(III), Hg(II), Ni(II), Pb(II), Y(III), and Zn(II) (Ashraf *et al*., 2011).

The aim of the present work is to synthesize new compounds containing derivatives of ligands via Schiff base with hydrazide which is derived from 2-chlorobenzaldehyde, glycine and hydrazine hydrate which reacted with Co, Ni and Cu ions to form new complexes.

2. Experimental

2.1 Reagents and solutions

All chemicals used are commercially available from BDH.

2.2 Instrumentation

The melting points were determined in glass capillary tubes in degrees Celsius. Molar conductance in dimethyl sulfoxide (DMSO) (10^{-3} mol L^{-1} solution at 25 °C) and molar ratio were measured on Jenway conductivity meter model 4510. The ligand and its complexes were characterized by comparison of spectroscopic data, infrared (IR) spectra of the ligand and metal complexes were measured using FT/IR – 140, Jasco, Japan in KBr pellets. ^{1}H and ^{13}C nuclear magnetic resonance (NMR) spectra were recorded in a Varian FT – 300 MHz spectrometer in d_6-DMSO solvent using tetramethylsilane as internal standard. Ultraviolet-visible (UV-Vis) spectra and antioxidant activity measurements (by ferric-bipyridine method) (Specord 200, Analytilk Jena, Germany) using DMSO and methanol as the reference and solvent, respectively. The magnetic susceptibilities of the complexes were measured at room temperature using Gouy's method by a magnetic susceptibility balance from Johnson Metthey and Sherwood model. Carbon, hydrogen, and nitrogen were estimated by Vario ELFab. Nr. 11042023. The X-ray powder diffraction patterns of the ligand and the solid complexes were obtained using XD-2 (Shimadzu ED-720), X-ray powder diffractometer at a voltage of 35 KV and current of 20 mA using CuKα radiation generator in the range $5° < 2\theta < 70°$ with a 1 min^{-1} scanning rate and a wavelength of 0.154056 nm. Microbiological analysis was carried out using the filter paper disc method.

2.3 Synthesis of Schiff base hydrazide ((2-chlorobenzylidene)amino)acetohydrazide hydrate = L

The solid ligand was prepared in 1:1:1 molar ratio as shown in Fig. 1 by adding dropwise of an ethanolic solution of glycine (0.01 mol) to an ethanolic solution of the aldehyde (0.01 mol) with stirring. The mixture was refluxed for 3 h with constant stirring and heating (Gao, 2013) until light brown solution of the Schiff base is formed. Then, addition of hydrazine hydrate drop by drop with constant stirring to the hot solution of the first part of the Schiff base until light brown precipitate is formed. The resulting precipitate was filtered off and washed with ethanol until the solution become clear then was left to dry.

2.4 Synthesis of the complexes

Generally, all the solid complexes were prepared as shown in Fig. 2 by adding dropwise of an methanolic solution of the hydrated metal chlorides (0.008 mol) to an methanolic solution of the ligand (Schiff base hydrazide 0.008 mol) with stirring. The mixture of each was refluxed for 4 to 6 h with constant stirring until colored precipitates are formed. All the materials solutions were in 1:1 molar ratio. The resulting precipitates were filtered off and washed with methanol even become a clear solution, then left them to dry.

Eclética Química, vol. 48, n. 2, 2023, 66-82
ISSN: 1678-4618
DOI: 10.26850/1678-4618eqj.v48.2.2023.p66-82

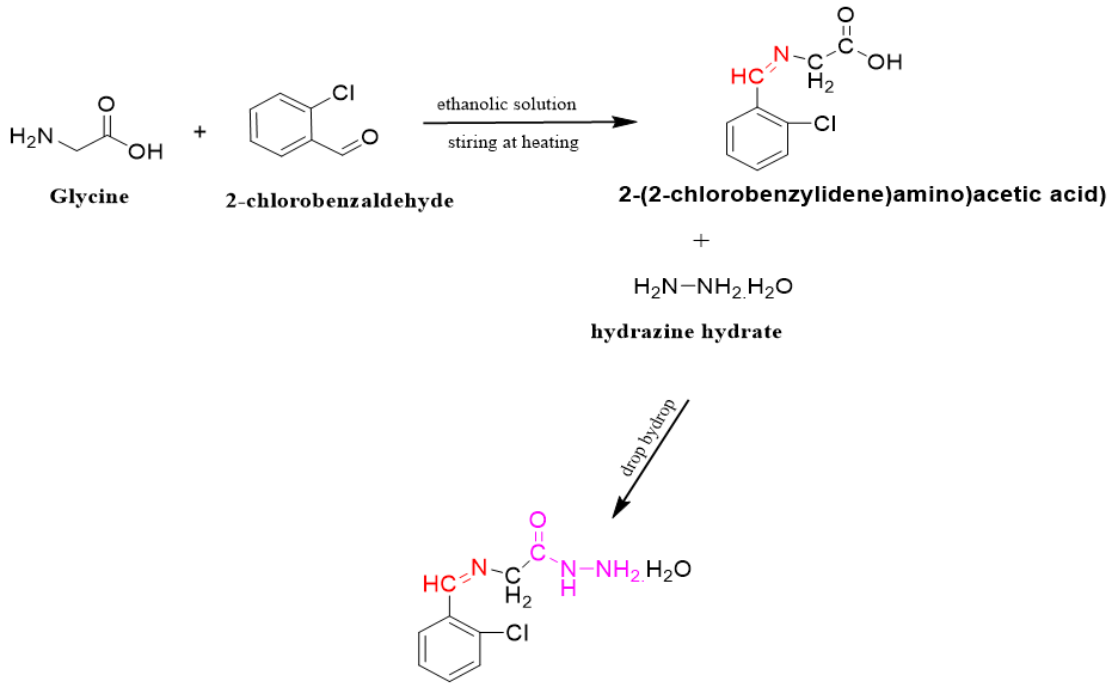

Figure 1. The schematic diagram of preparation of the ligand
Source: Elaborated by the authors using method from Gao (2013).

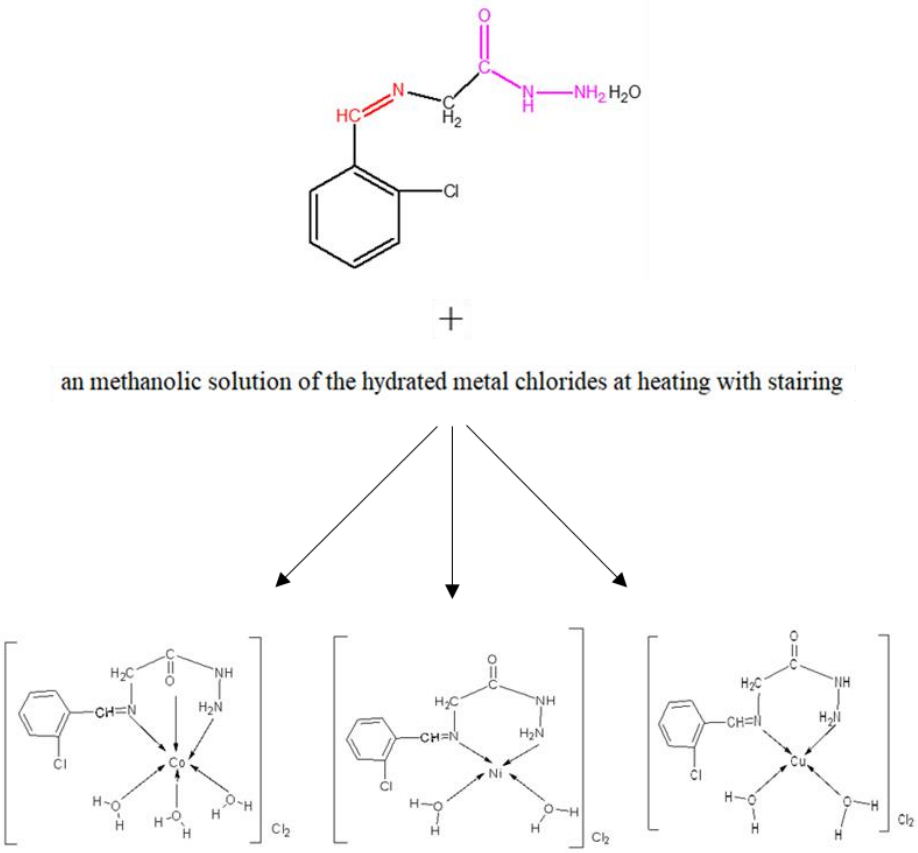

Figure 2. The schematic diagram of the synthesis method of the complexes.

Eclética Química, vol. 48, n. 1, 2023, 66-82
ISSN: 1678-4618
DOI: 10.26850/1678-4618eqj.v48.2.2023.p66-82

3. Results and discussion

All the compounds are colored solids and insoluble in common organic solvents except DMSO (Table 1). Molar conductance values of these compounds were in the range of 178–205 S cm^2 mol^{-1}, indicating their electrolytic nature (G. Mohamed *et al*., 2006) as recorded in Table 2.

Table 1. Some physical properties of the ligand and its complexes.

Complex Proposed Formula		L ($C_9H_{12}N_3O_2Cl$)	$[Co(L)(H_2O)_3]Cl_2$ $[Co(C_9H_{16}N_3O_4Cl)]Cl_2$	$[Ni(L)(H_2O)_2]Cl_2$ $[Ni(C_9H_{14}N_3O_3Cl)]Cl_2$	$[Cu(L)(H_2O)_2]Cl_2$ $[Cu(C_9H_{14}N_3O_3Cl)]Cl_2$
Color		Light brown	Purple	Green	Dark green
Melting point (°C)		142	160	285	295
Yield (%)		96.85	69.87	68.81	82.36
Solubility	dimethyl sulfoxide	soluble	soluble	soluble	soluble
	dimethylformamide	soluble	soluble	soluble	partially soluble
	diethyl ether	partially soluble	insoluble	insoluble	insoluble
	benzene	soluble	insoluble	insoluble	insoluble
	acetone	partially soluble	insoluble	insoluble	insoluble
	trichloromethane	soluble	insoluble	insoluble	insoluble
	tetrachloromethane	soluble	insoluble	insoluble	insoluble
	hexane	soluble	insoluble	insoluble	insoluble
	methanol	soluble	soluble	soluble	partially soluble
	ethanol	insoluble	soluble	partially soluble	partially soluble
	H_2O	insoluble	soluble	soluble	soluble

Table 2. Molecular weight, elemental analysis and molar conductance of the ligand and its complexes.

	Complex proposed formula	L	$[Co(L)(H_2O)_3]Cl_2$	$[Ni(L)(H_2O)_2]Cl_2$	$[Cu(L)(H_2O)_2]Cl_2$
Molecular weight	calc.	229.66	395.53	377.28	382.13
	found	229.69	395.56	377.29	382.14
%C	calc.	47.07	27.33	28.65	28.29
	found	47.07	27.33	28.65	28.29
%H	calc.	5.27	4.08	3.74	3.69
	found	5.28	4.09	3.74	3.70
%N	calc.	18.30	10.62	11.14	11
	found	18.29	10.62	11.14	11.02
%M	calc.	-	14.90	15.56	16.63
	found	-	14.90	15.56	16.64
%CI	calc.	15.43	26.89	28.19	27.83
	found	15.43	26.90	28.20	27.84
Molar Conductance (cm^2 mol^{-1} (Ω^{-1})	-	-	182	205	178

3.1 Molar ratio by conductivity measurements

Through the conductivity measurements of the ligand with the divalent metals Co(II), Ni(II) and Cu(II) in order to calculate the molar ratio between the ligand and these metals, the following was found:

1. The resulting values were high, indicating that these complexes have a conductive nature (Tulu and Yimer, 2018). This was also confirmed using silver nitrate;
2. The ratio between these metals and chloride ion was 1:2 (G. Mohamed *et al*., 2006), where the resulting values were located between 186.7–115.9 S cm^2 mol^{-1};
3. Through conductivity measurements for different concentrations of these complexes, conductivity readings were confirmed at a fixed molar value, which represents 1:1 between the ligand and these metals (Ghara *et al*., 2017) as show in Fig. 3.

Eclética Química, vol. 48, n. 1, 2023, 66-82
ISSN: 1678-4618
DOI: 10.26850/1678-4618eqj.v48.2.2023.p66-82

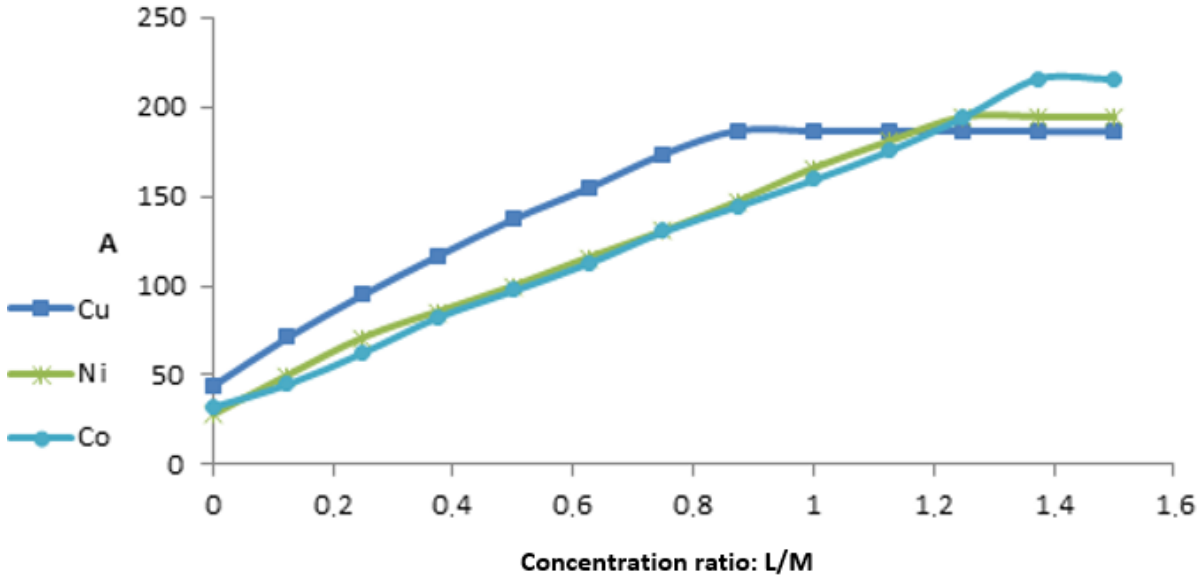

Figure 3. Curve of the mole ratio for the ligand and the metals.

3.2 IR spectra of the ligand and its complexes

Comparing the IR spectral data of the ligand and its complexes (Table 3 and Fig. 4) confirmed the complexation through the azomethine group $\upsilon_{C=N}$. The band at 1663 cm^{-1} assigned to $\upsilon_{C=N}$ in the free ligand was shifted to lower wave number in the complexes, indicating the participation of the azomethine nitrogen in coordination (Jamil *et al*., 2022; E. Mohamed *et al*., 2014). The IR spectra of the Co(II) complex showed a band at 1654 cm^{-1} which is characteristic of (C=O) group. This band is indicating coordination of this group through oxygen atom (Al-Salami *et al*., 2017). The band at 3106 cm^{-1} can be assigned to vibration of the NH_2 group in the ligand, which shifted to higher frequencies in the complexes, which identifies coordination of the amine nitrogen (Demirbaş *et al*., 2002).

The ligand and its complexes show additional broad bands in the range 3373–3436 cm^{-1} due to the OH stretching of the water molecule, which is confirmed by the elemental analysis and gravimetric studies (Al-Salami *et al*., 2017; Jamil *et al*., 2022). Low intensity bands observed in far-IR region in the range 528–591 cm^{-1} and 436–439 cm^{-1} which may probably be due to the formation M-O and M-N bonds, respectively (Alomari, 2010; Hossain *et al*., 2019).

Other absorption bands of v(N-N) (Ali *et al*., 1997; Dzulkifli *et al*., 2012), v(NH) (Ali *et al*., 1997; Ejelonu *et al*., 2018), v(Ar-Cl) (Emriye, 2016; Kapadnis *et al*., 2016), v(CH_2), v(C=C), (E. Mohamed *et al*., 2014), v(CH) (Al-Salami *et al*., 2017; E. Mohamed *et al*., 2014), v(NH_2) (Demirbaş *et al*., 2002) are given in Table 3.

Table 3. Significant IR spectral bands (cm^{-1}) of the ligand and its complexes.

Compounds	L	$[Co(L)(H_2O)_3]Cl_2$	$[Ni(L)(H_2O)_2]Cl_2$	$[Cu(L)(H_2O)_2]Cl_2$
C=N	1663^{w}	1616^{s}	1616^{s}	1617^{m}
C=O	1685^{w}	1654^{w}	1682^{w}	1685^{s}
C=C	1588^{m}	1588^{m}	1586^{m}	1580^{w}
C-N	1390^{m}	1412^{s}	1411^{s}	1411^{m}
NH	$3068^{w.br}$	$3068^{w.br}$	$3069^{w.br}$	3067^{w}
NH_2	3106^{br}	3347^{s}	3180^{w}	3250^{w}
=C-H	3033^{w}	3031^{w}	3032^{w}	$3030^{w.br}$
N-N	1047^{s}	1046^{s}	1045^{s}	1051^{m}
CH_2	1465^{s}	1464^{m}	1464^{m}	1458^{m}
Ph-Cl	869^{m}	868^{w}	863^{m}	870^{w}
OH	3432^{br}	3408^{br}	3373^{br}	3432^{br}
M-N	-	591^{m}	528^{m}	580^{w}
M-O	-	436^{m}	435^{m}	439^{w}

w = weak, m = medium, s = strong, br = broad.

Eclética Química, vol. 48, n. 1, 2023, 66-82
ISSN: 1678-4618
DOI: 10.26850/1678-4618eqj.v48.2.2023.p66-82

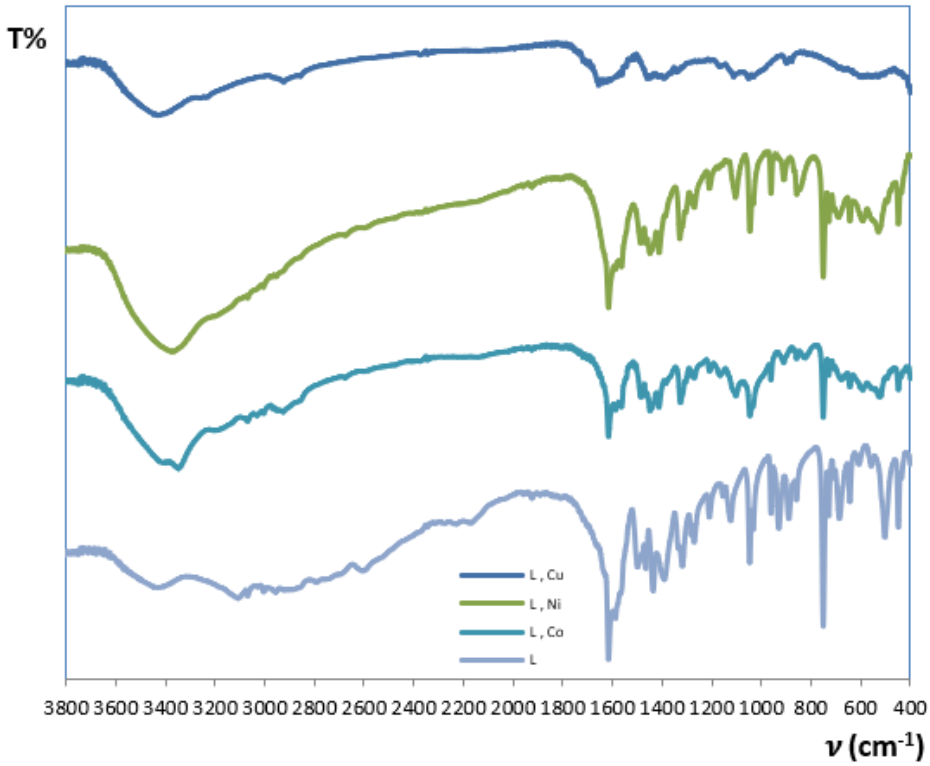

Figure 4. IR spectra of the ligand and its complexes.

3.3 NMR spectroscopy of the ligand

3.3.1 [1]HNMR

The resonance of protons has been assigned on the basis of their integration and multiplicity pattern. The [1]HNMR spectra of the ligand (Table 4 and Fig. 5) in DMSO exhibits signal at 8.55 ppm attributed to CH=N- proton (Al-Salami *et al*., 2015). The signals within the 6.85 and 6.88 ppm are assigned to the NH and NH_2 respectively (Mathew *et al*., 2006). Spectra of aromatic range was observed at 7.67–7.70 ppm (Sakhare *et al*., 2015). The signals appeared at 2.50 and 3.20 ppm were indicated the protons of CH_2 (Al-Garawi *et al*., 2012) and H_2O, respectively.

3.3.2 [13]C NMR

The [13]CNMR spectra provide further support for the structural characterization of the ligand (Table 4 and Fig. 6) [13]C NMR spectral data of the ligand has signal at 160.35 attributed to carbon of CH=N- (Neelofar *et al*., 2017). The aromatic carbon signals are present in the range 115.82–130.08 ppm (Oğuzhan *et al*., 2017). The [13]CNMR spectral data of the carbon amide and CH_2 group are present at 160.58 (Shneine *et al*., 2017) and 40.00 ppm (Neelofar *et al*., 2017), respectively. The structural formula of the ligand (Fig. 7).

Table 4. [1]H and [13]C NMR positions (ppm) of the ligand.

NMR Spectroscopy of the ligand			
[1]HNMR		**[13]C NMR**	
Site	**Chemical Shift (ppm)**	**Site**	**Chemical Shift (ppm)**
CH=N-	8.55	CH=N-	160.35
NH	6.85	A.R.	115.82-130.08
NH_2	6.88	CH_2	40.00
A.R.	7.67-7.70	C=O	160.58
CH_2	2.50	-	-
H_2O	3.20	-	-

Eclética Química, vol. 48, n. 2, 2023, 66-82
ISSN: 1678-4618
DOI: 10.26850/1678-4618eqj.v48.2.2023.p66-82

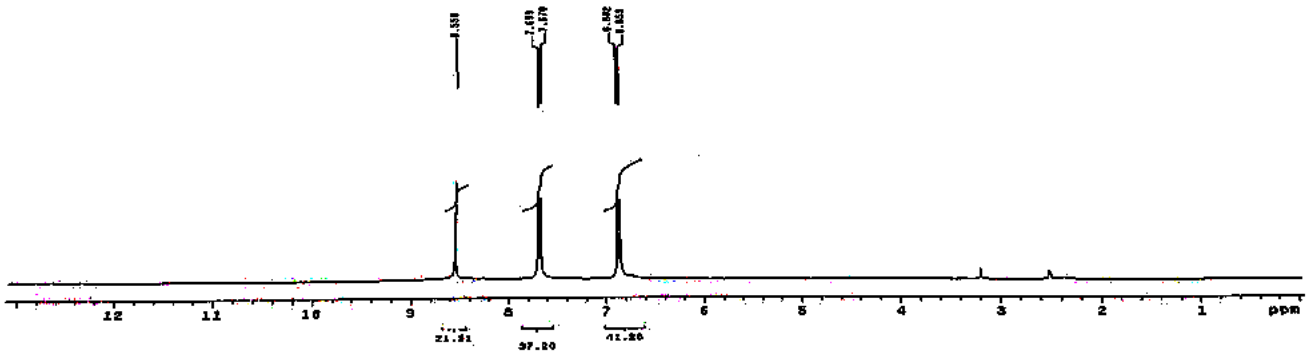

Figure 5. ^{1}HNMR spectrum of the ligand.

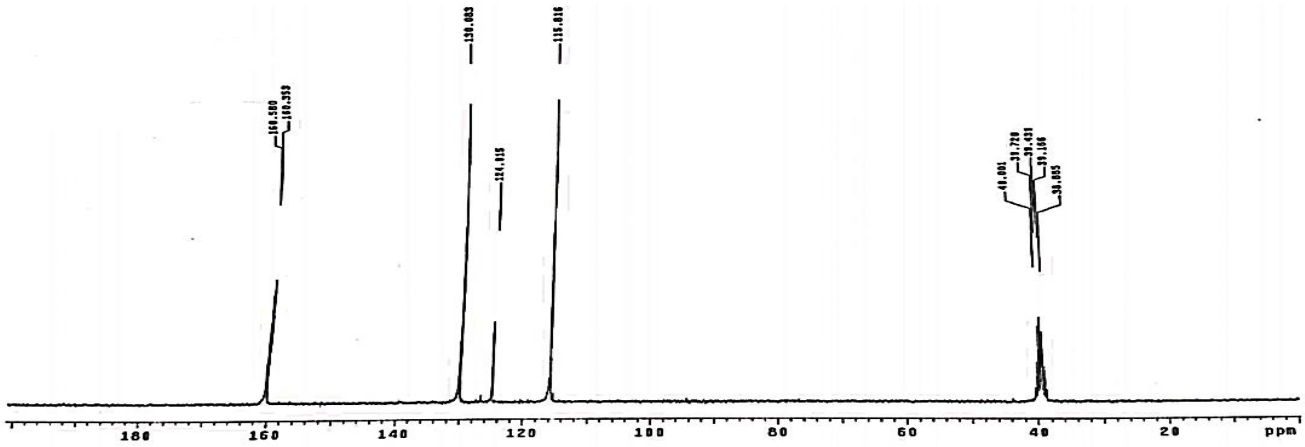

Figure 6. ^{13}CNMR spectrum of the ligand.

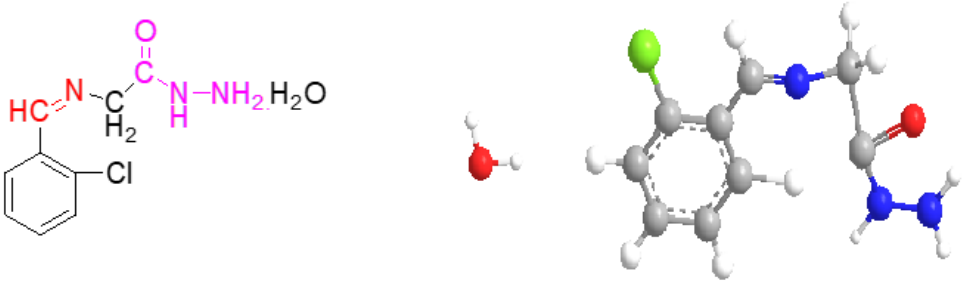

2-((2-chlorobenzylidene)amino)acetohydrazide hydrate = Ligand = L

Figure 7. The structural formula of the ligand.

3.4 Magnetic and electronic of the ligand and its complexes

The absorption spectrum of the ligand (Fig 11a) shows two absorption bands appearing at 45,454 and 33,333 cm^{-1}. The band appearing at low energy side at 33,333 cm^{-1} in the ligand is attributed to n-π* transitions of conjugation between the lone pair of electrons of p orbital of N-atom in C=N group and a conjugated π bond of aromatic rings (Hossain *et al.*, 2019). The band appearing at higher energy 45,454 cm^{-1} arise from π-π* transition within the phenyl and π-π* transitions of the C=N group (Sarwar *et al.*, 2018).

The electronic spectrum of the Co(II) complex as shown in Figs. 8 and 11b and Table 5, octahedral is suggested. This is based on the appearance of 13,513 cm^{-1} in the spectra recorded in DMSO solution, which is attributed to the $^{4}T_{1g} \rightarrow {}^{4}A_{2g}$ (ν_2) transitions (Patel *et al.*, 2012; Yousef *et al.*, 2016), also Co(II) complex has magnetic moment of 4.8 Bohr's magneton,

Eclética Química, vol. 48, n. 2, 2023, 66-82
ISSN: 1678-4618
DOI: 10.26850/1678-4618eqj.v48.2.2023.p66-82

BM, which lie in the range reported for octahedral geometry around the Co(II) ion (Sharma *et al*., 1994; Tulu and Yimer, 2018). Moreover, the purple color of the complex is in good agreement with this reported for octahedral Co(II) complex (Tulu and Yimer, 2018).

The magnetic measurements indicates that Ni(II) complex is a diamagnetic (Tulu and Yimer, 2018) and the electronic spectra of this complex in DMSO solution (Fig,11c and Table 5) showed two bands in 21,276 and 18,867 cm^{-1} attributed to $^1A_1g \rightarrow {}^1A_2$ g and $^1A_1g \rightarrow B_1g$ transitions, respectively, for square planar Ni(II) complex (Fig. 9) and the green color of this complex is additional evidence for square planar structure (Al-Jiboury and Al-Nama, 2019).

The electronic spectrum (Fig. 11d) of Cu(II) complex show one band at 21,730 cm^{-1}, assigned to the transitions $^2B_1g \rightarrow {}^2A_1g$, indicating square-planar geometry (Table 5 and Fig. 10) (Mahmood *et al*., 2013). This geometry is further supported as the values of the magnetic moment obtained 1.87 B.M, which is lying in the range reported for a square-planar structure (Mahmood *et al*., 2013; Mishra *et al*., 2012). The green color of this complex is additional evidence for square planar structure (Mahmood *et al*., 2013).

Also, the bands at 24,390, 22,222, and 24,691 cm^{-1} should be attributed to the charge transfer of Co(II) (Mahmood *et al*., 2013), Ni(II) (G. Mohamed *et al*., 2006) and Cu(II) complexes (Hossain *et al*., 2019), respectively.

Table 5. Magnetic moment, electronic spectral data in DMSO solution for the ligand and its complexes.

Compounds		L	$[Co(L)(H_2O)_3]Cl_2$	$[Ni(L)(H_2O)_2]Cl_2$	$[Cu(L)(H_2O)_2]Cl_2$
μ_{eff} (B.M.)		-	2.6	-	1.87
UV bands (cm^{-1})	π→π*	45,454	-	-	-
	n→π*	33,333	-	-	-
Charge transfer bands (cm^{-1})		-	24,390	22,222	24,691
d-d transition bands (cm^{-1})		-	13,513	18,867, 21,276, 13,698	21,739
Supposed structure		-	Octahedral	Square planar	Square planar

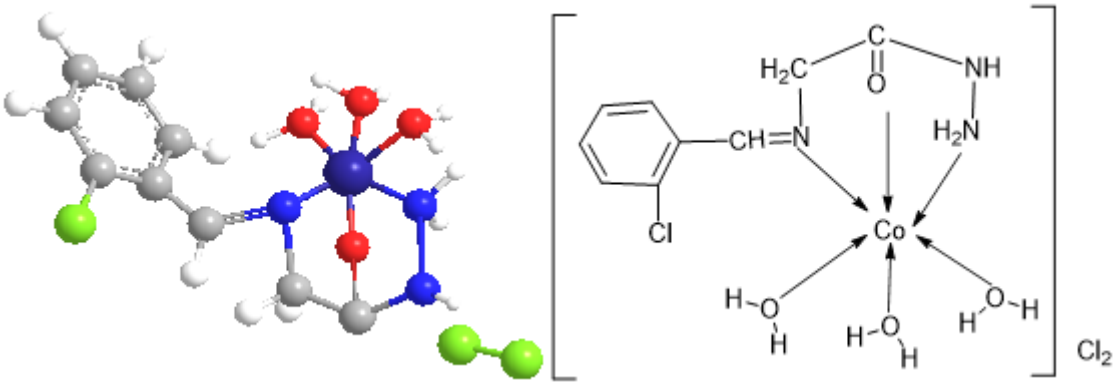

Figure 8. Complex containing the ligand with Co(II).

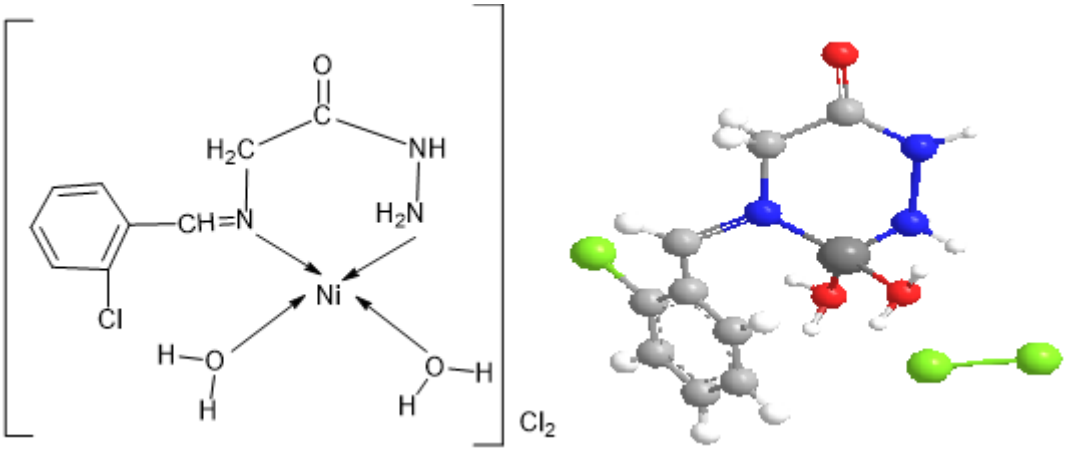

Figure 9. Complex of the ligand with Ni(II).

Eclética Química, vol. 48, n. 2, 2023, 66-82
ISSN: 1678-4618
DOI: 10.26850/1678-4618eqj.v48.2.2023.p66-82

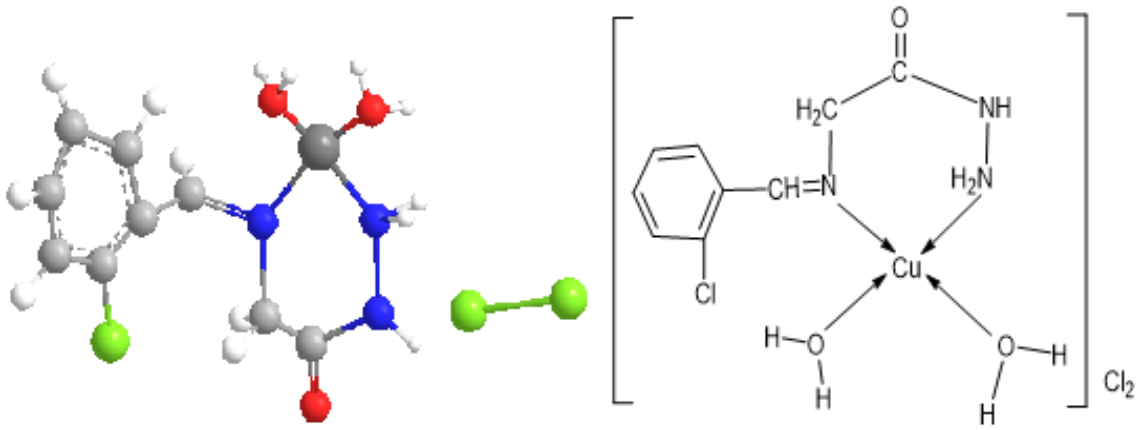

Figure 10. Complex of the ligand with Cu(II).

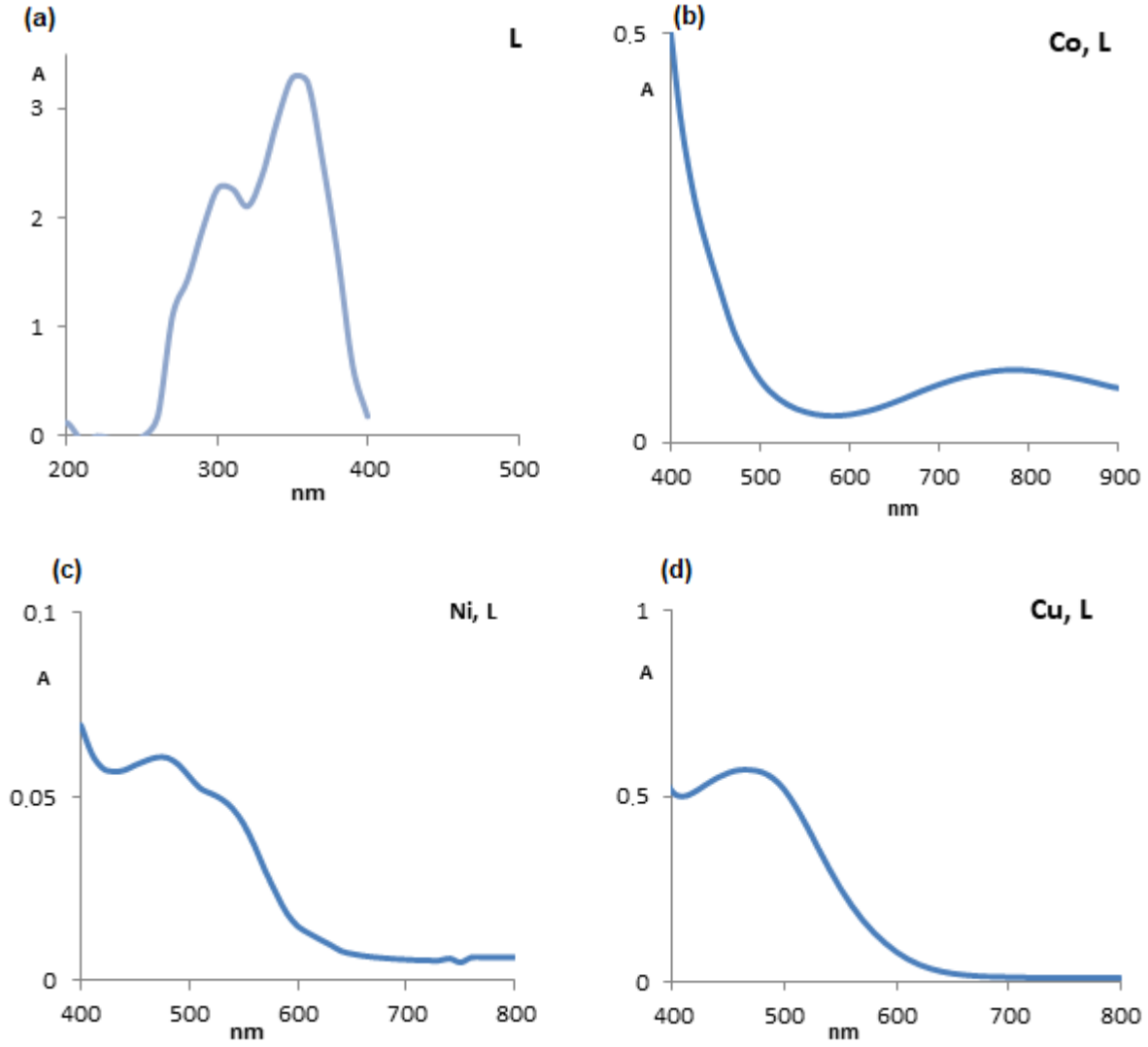

Figure 11. UV-visible electronic spectra of the ligand and its complexes in DMSO solution. **(a)** for the ligand; **(b)** for the Co complex; **(c)** for the Ni complex; **(d)** for the Cu complex.

Eclética Química, vol. 48, n. 2, 2023, 66-82
ISSN: 1678-4618
DOI: 10.26850/1678-4618eqj.v48.2.2023.p66-82

3.5 Powder X-ray diffraction of the ligand and its complexes

The powder X-ray powder diffraction patterns for the free ligand and its complexes were carried out in order to obtain an idea about the lattice dynamics of the resulted complexes. X-ray of these compounds are recorded and shown in Figs. 12 and 13.

The values of particle size, strain and relative intensity (%) of compounds are compiled in Table 6. The crystallite size could be estimated from X-ray diffraction (XRD) patterns by applying full width at half maximum (FWHM) of the characteristic peaks using Debye-Scherrer Eq. 1 (Al-Maydama *et al*., 2018; Refat *et al*., 2014a; b) and Williamson-Hall Eq. 2 (Abed *et al*., 2019).

$$D = K\lambda/\beta \cos\theta \quad (1)$$

$$D = K\lambda/intercept \quad (2)$$

where $\boldsymbol{K}$ is Scherrer constant and equals 0.94, $\boldsymbol{\lambda}$ is the X-ray wavelength of Cu-Kα radiation (0.15405 nm), $\boldsymbol{\beta}$ is FWHM, and $\boldsymbol{\theta}$ is Bragg diffraction angle in radian. The particle size of these compounds is located within the nano scale range (12.59–35.32 nm).

The strain calculated by applying Williamson-Hall Eq. 2 (Abed *et al*., 2019) which mean the slope as Eq. 3.

$$Strain\ (\varepsilon) = \beta \cos\theta\ /\ \sin\theta \quad (3)$$

It was shown through crystal strain from William's equation that the ligand, Co(II) and Cu(II) complexes have the property of crystal tensile, while the Ni(II) complex has the property of crystal compressive, which corresponds to the size of the crystals. It was found that the higher the compressive which negative values, the smaller the crystal size, while the higher the tensile with positive values, the higher the crystal size, and this is what was clarified in Table 6.

The percentage of crystallinity, $X_c(\%)$, was calculated on the basis of the integrated peak areas of the principal peaks (Al-Maydama *et al*., 2018). The crystallinity of the complex is calculated relative to the crystallinity of the ligand as a ratio (Eq. 4).

$$X_C(\%) = \frac{A_{complex}}{A_{ligand}} \times 100 \quad (4)$$

where $A_{complex}$ and A_{ligand} are the areas under the principal peaks of the complex and the ligand sample, respectively. The results of these calculations were that the crystalline percentage of the Ni(II) complex is high compared to the ligand, while it was low for the Co(II) and Cu(II) complexes when compared to the ligand.

Table 6. XRD spectral data of the highest value of intensity of the ligand and its complexes.

Compounds	Θ (Radian)	B(FWHM) (Radian)	βcosθ	4sinθ	D(nm)	Scherr Mean D(nm)	W-H D(nm)	Strain (ε) *10^{-4}	X%
L	0.1744	0.004660	0.004589	0.6939	31.55	26.66	31.48	11	100
	0.2047	0.006842	0.006699	0.8132	21.62				
	0.2381	0.005498	0.005343	0.9433	27.11				
	0.2656	0.005690	0.005490	10.501	26.38				
[Co(L)(H$_2$O)$_3$]Cl$_2$	0.1735	0.008116	0.007994	0.6905	18.12	21.87	20.40	0.2	80.66
	0.2000	0.004721	0.004636	0.7947	31.24				
	0.2311	0.009564	0.009310	0.9161	15.55				
	0.2663	0.006651	0.006415	10.528	22.57				
[Ni((L)(H$_2$O)$_2$]Cl$_2$	0.1737	0.008186	0.008062	0.6912	17.96	20.76	12.59	–49	130.79
	0.2068	0.006650	0.006508	0.8214	22.25				
	0.2323	0.008796	0.008560	0.9209	16.92				
	0.2665	0.005794	0.005590	10.535	25.91				
[Cu(L)(H$_2$O)$_2$]Cl$_2$	0.1744	0.00481	0.004727	0.6939	30.64	28	35.32	16	75.99
	0.2133	0.005515	0.005390	0.8467	26.87				
	0.2372	0.007871	0.007651	0.9399	18.93				
	0.2554	0.004206	0.004061	10.103	35.59				

Eclética Química, vol. 48, n. 1, 2023, 66-82
ISSN: 1678-4618
DOI: 10.26850/1678-4618eqj.v48.2.2023.p66-82

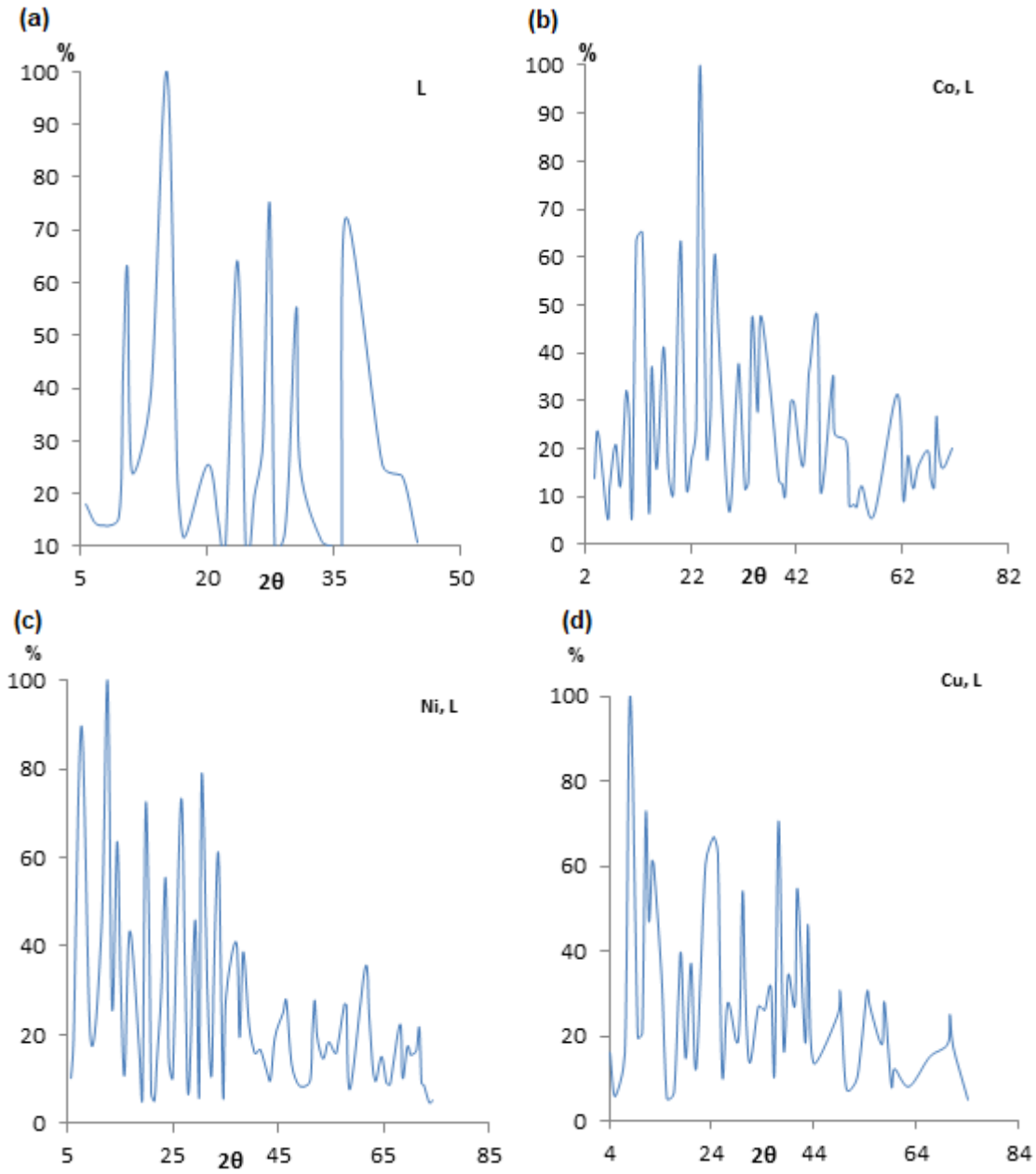

Figure 12. XRD patterns of the ligand and its complexes. **(a)** for the ligand; **(b)** for the Co complex; **(c)** for the Ni complex; **(d)** for the Cu complex.

Eclética Química, vol. 48, n. 2, 2023, 66-82
ISSN: 1678-4618
DOI: 10.26850/1678-4618eqj.v48.2.2023.p66-82

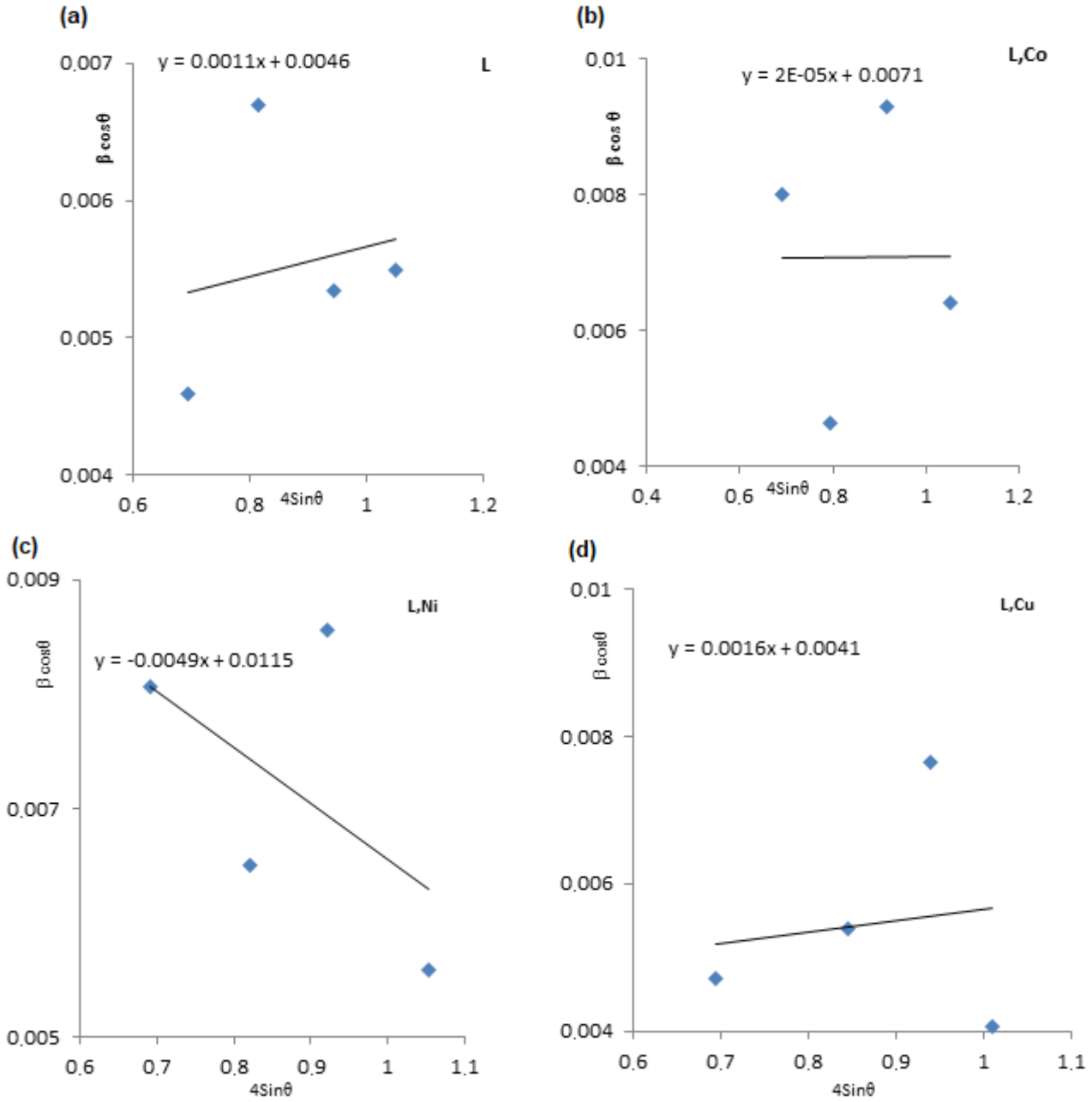

Figure 13. Particle size and strain by W-H of the ligand and its complexes. **(a)** for the ligand; **(b)** for the Co complex; **(c)** for the Ni complex; **(d)** for the Cu complex.

3.6 The ligand as antioxidant

The 2((2-chlorobenzylidene)amino)acetohydrazide hydrate=(L) has been synthesized, and the antioxidant properties were studied using ferric-bipyridine reducing capacity of total antioxidants method (Naji *et al*., 2020). As it was found that this ligand can be used as an antioxidant compared to ascorbic acid, which was used as a standard material in this analysis, but with less effectiveness than ascorbic acid, which gave 3.7453 mg compared with ascorbic acid, which was 1 mg, while the standard deviation of this ligand was ± 9.67 × 10^{-8}.

3.7 Antimicrobial of the ligand and its complexes

This analysis of the ligand and its mineral complexes clearly demonstrated that they have antibacterial and antifungal activity (Table 7, Figs. 14 and 15).

Comparison of the biological evaluation of the ligand and its complexes with standards of gentamicin (antibacterial agent), nystatin, miconazole, itraconazole

Eclética Química, vol. 48, n. 2, 2023, 66-82
ISSN: 1678-4618
DOI: 10.26850/1678-4618eqj.v48.2.2023.p66-82

and metronidazole (antifungal agents). The results of the highest-to-lowest-impact items can be summarized as follows:

a. *Staphylococcus aureus*
Ni > Co > Cu > ligand

b. *Bacillus subtilis*
Co > Cu > Ni > ligand

c. *Pseudomonas aeruginosa*
Co > Ni > ligand > Cu

d. *Escherichia coli*
Ni > ligand > Cu

e. *Aspergillus flavus*
Ni > Co > Cu > ligand

f. *Candida albicans*
ligand = Co > Ni > Cu

From these results, we can summarize that:

1. Generally, the active property of the free ligand and complexes against the used strains is enhanced;
2. The growth of *S. aureus* and *A. flavus* are inhibited by complex of Ni(II), Co(II), Cu(II), and the ligand, respectively;
3. *Bacillus subtilis* is inhibited by complex of Co(II) more than complexes of Cu(II), Ni(II) and the ligand. The growth of *E. coli* is just inhibited by complex of Ni(II), the ligand and complex of Cu(II) compared to the complex of Co(II) there is no inhibition;
4. The Inhibition zone of Co(II) complex toward *P. aeruginosa* was more than that of Ni(II), Cu(II) complexes and the ligand.
5. The ligand and complex of Co(II) have the same worthy effect against *C. albicans*, which are more than complexes of Ni(II) and Cu(II).

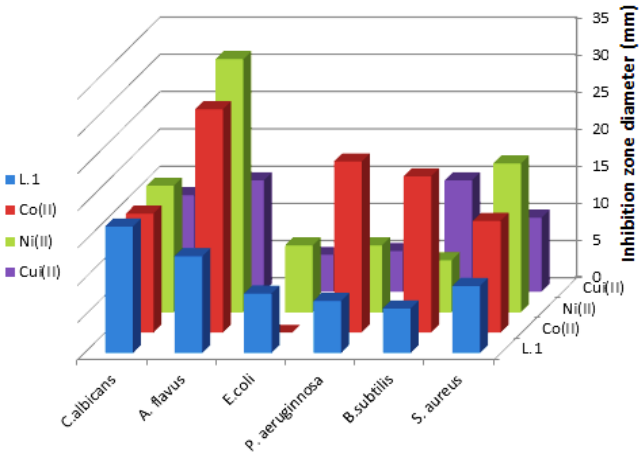

Figure 14. Diagram effect of the ligand and its complexes on the growth of bacteria and fungi (zone of inhibition in mm).

Table 7. Effect of the ligand and its complexes on the growth of bacteria and fungi (zone of inhibition in mm).

Compound (1000 µg mL^{-1})			Inhibition zone diameter (mm)					
			Bacteria				fungi	
			Gram positive		Gram negative			
			Staphylococcus aureus	*Bacillus subtilis*	*Pseudomonas aeruginosa*	*Escherichia coli*	*Aspergillus flavus*	*Candida albicans*
Control DMSO			0.0	0.0	0.0	0.0	0.0	0.0
Standard	Antibacterial agent Gentamicin 120 µg mL^{-1}		23	22	25	23	-	-
	Antifungal agent	Nystatin 100 µg mL^{-1}	-	-	-	-	25	**21**
		Miconazole 50 µg mL^{-1}	-	-	-	-	8	**22**
		Itraconazole 30 µg mL^{-1}	-	-	-	-	18	**20**
		Metronidazole 5 µg mL^{-1}	-	-	-	-	10	**17**
L			9	6	7	8	13	17
$[Co(L)(H_2O)_3]Cl_2$			15	21	23	0	30	16
$[Ni(L)(H_2O)_2]Cl_2$			20	7	9	9	34	17
$[Cu(L)(H_2O)_2]Cl_2$			10	15	5.5	5	15	13

Eclética Química, vol. 48, n. 2, 2023, 66-82
ISSN: 1678-4618
DOI: 10.26850/1678-4618eqj.v48.2.2023.p66-82

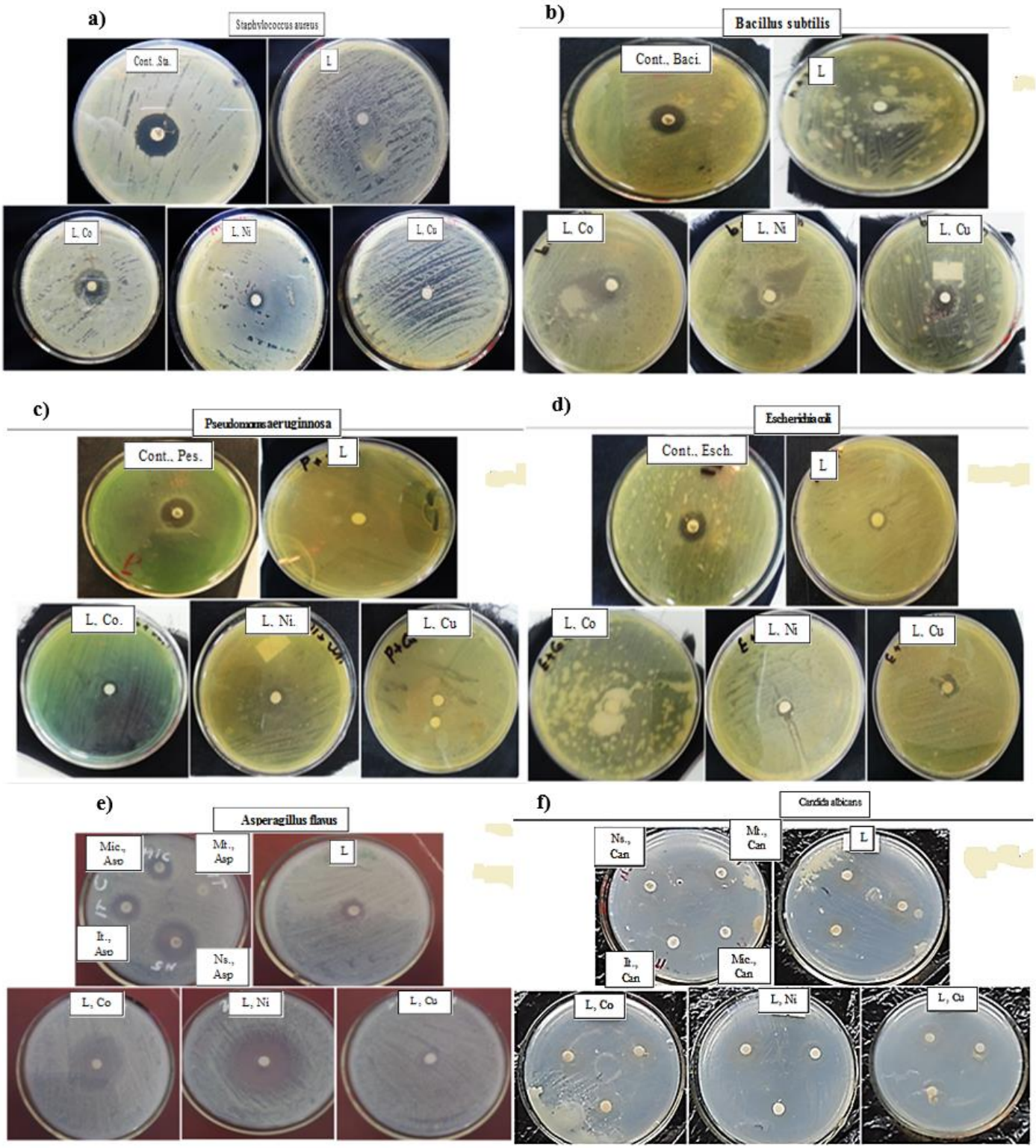

Figure 15. Biological activity of the ligand and its complexes . against **(a)** *Staphylococcus aureus*; **(b)** *Bacillus subtilis* **(c)** *Pseudomonas aeruginosa*; **(d)** *Escherichia coli*; **(e)** *Bacillus subtilis*; **(f)** *Pseudomonas aeruginosa*.

According to the concept of cell permeability, since the lipid membrane that surrounds the cell favors the passage of lipid-soluble substances since lipid solubility is an important factor, so the polarity of the metal ion is greatly reduced due to the overlap of the orbitals of the metal ion with the bound. It increases the delocalization of electrons on the chelated rings and enhances the lipophilicity of the complexes, which facilitates the

Eclética Química, vol. 48, n. 2, 2023, 66-82
ISSN: 1678-4618
DOI: 10.26850/1678-4618eqj.v48.2.2023.p66-82

penetration of the lipid membranes of microorganisms and facilitates the closure of the metal bonding sites with enzymes.

These compounds deactivate various cellular enzymes, which play a vital role in the various metabolic pathways of these organisms. It has also been suggested that the final action of the toxin is denaturation of one or more cell proteins, impairing normal cellular processes (Jamil *et al*., 2022; Omer and Al-Daher, 2019; Refat *et al*., 2015; Reiss *et al*., 2021).

4. Conclusions

The Schiff base hydrazide ligand derived from the condensation of 2-chlorobenzaldehyde, glycine and hydrazine hydrate have been successfully synthesized. These ligand were complexed with using Co(II), Ni(II) and Cu(II) ions. Coordination of amine nitrogen (-NH_2) and azomethine nitrogen (-C=N-) with Ni(II) and Cu(II) in additional to oxygen of carbonyl group with Co(II). These compounds have been indicated by various studies; hence, it has been liable for imparting the stability to the complexes. The structures of these compounds were characterized by elemental, ^{1}HNMR, ^{13}CNMR, FTIR spectra, molar ratio, XRD diffraction, UV-Vis spectra, and magnetic studies. The coordination of the ligand with Co(II), Ni(II) and Cu(II) ions showed molar ratio of 1:1. The complexes of Co(II) and Cu(II) presented square planar geometries, while Ni(II) presented octahedral geometry. Antioxidant study for the ligand provided its activity. The ligand with Schiff base and hydrazide groups and its complexes showed better biological activity. The results showed that the metal complexes have much higher antibacterial and antifungal activity compare to the parent ligand. It was found that the Co(II) complex was more effective than other metal complexes used against all types of bacteria and it was more effective against *P. aeruginosa* with diameter inhibition zone of 23 mm, while Ni(II) complex was more effective than other complexes used against two types of fungi and it was more effective against *A. flavus* than *C. albicans.*

Authors' contribution

Conceptualization: Al-Azab, F. M.; Jamil, Y. M.
Data curation: Al-Azab, F. M.; Jamil, Y. M.; Al-Gaadbi, A. A.
Formal Analysis: Al-Azab, F. M.; Jamil, Y. M.; Al-Gaadbi, A. A.
Funding acquisition: Not applicable.
Investigation: Al-Azab, F. M.; Jamil, Y. M.; Al-Gaadbi, A. A.
Methodology: Jamil, Y. M.; Al-Azab, F. M.
Project administration: Jamil, Y. M.; Al-Azab, F. M.
Resources: Al-Azab, F. M.; Jamil, Y. M.; Al-Gaadbi, A. A.
Software: Jamil Y. M.; Al-Gaadbi A. A.
Supervision: Al-Azab, F. M.; Jamil, Y. M.
Validation: Al-Azab, F. M.
Visualization: Al-Azab, F. M.; Jamil, Y. M.; Al-Gaadbi, A. A.
Writing – original draft: Al-Gaadbi, A. A.
Writing – review & editing: Jamil, Y. M.

Data availability statement

All data sets were generated or analyzed in the current study.

Funding

Not applicable.

Acknowledgments

Not applicable.

References

Abed, A. H.; Khodair Z. T.; Al-Saadi, T. M.; Al-Dhahir, T. A. Study the evaluation of Williamson–Hall (W-H) strain distribution in silver nanoparticles prepared by sol-gel method. *AIP Conf. Proc.* **2019**, *2123* (1), 020019. https://doi.org/10.1063/1.5116946

Al Zoubi, W. Biological Activities of Schiff Bases and Their Complexes: A Review of Recent Works. *Int. J. Org. Chem.* **2013**, *3* (3A), 73–95. https://doi.org/10.4236/ijoc.2013.33A008

Al-Garawi, Z. S. M.; Tomi, I. H. R.; Al-Daraji, A. H. R. Synthesis and characterization of new amino acid-Schiff bases and studies their effects on the activity of ACP, PAP and NPA enzymes (*In Vitro*). *J. Chem.* **2012**, *9* (2), 962–969. https://doi.org/10.1155/2012/218675

Ali, M. A.; Majumder, S. M. M.-u.-H.; Butcher, R. J.; Jasinski, J. P.; Jasinski, J. M. The preparation and characterization of bis-chelated nickel(II) complexes of the 6-methylpyridine-2-carboxaldehyde Schiff bases of S-alkyldithiocarbazates and the X-ray crystal structure of the bis {S-methyl-*β*-*N*-(6-methylpyrid-2-yl)- methylenedithiocarbazato}nickel(II) complex. *Polyhedron* **1997**, *16* (16), 2749–2754. https://doi.org/10.1016/S0277-5387(97)00036-3

Eclética Química, vol. 48, n. 2, 2023, 66-82
ISSN: 1678-4618
DOI: 10.26850/1678-4618eqj.v48.2.2023.p66-82

Al-Jiboury, M. M.; Al-Nama, K. S. Preparation, Characterization and Biological Activities of some Unsymmetrical Schiff bases derived from m-phenyelenediamine and their metal complexes. *Raf. J. Sci.* **2019**, *28* (2), 23–36. https://doi.org/10.33899/rjs.2019.159965

Al-Maydama, H. M.; Abduljabbar, A. A.; Al-Maqtari, M. A.; Naji, K. M. Study of temperature and irradiation influence on the physicochemical properties of aspirin. *J. Mol. Struct.* **2018**, *1157*, 364–373. https://doi.org/10.1016/j.molstruc.2017.12.062

Alomari, A. A. Synthesis, characterization and electrochemical studies of Cu(II), Fe(II), Fe(III) and Ni(II) complexes of Someo-phenylenediamine Schiff base. Master's Thesis, University of Malaya Kuala Lumpur, Kuala Lumpur, 2010.

Al-Salami, B. K.; Gata, R. A.; Asker, K. A. Synthesis Spectral, Thermal Stability and Bacterial Activity of Schiff Bases Derived from Selective Amino Acid and Their Complexes. *Adv. Appl. Sci. Res.* **2017**, *8* (3), 4–12.

Al-Salami, B. K.; Ul-Saheb, R. G. A.; Asker, K. A. Synthesis spectral, thermal stability and antibacterial activity of schiff bases derived from alanine and threonine and their complexes. *J. Chem. Pharm. Res.* **2015**, *7* (8), 792–803.

Ashraf, M. A.; Mahmood, K.; Wajid, A. Synthesis, Characterization and Biological Activity of Schiff Bases. *IPCBEE*. **2011**, *10*, 1–7.

Demirbaş, N. Demirbaş, A.; Sancak, K. Synthesis and characterization of some 3-alkyl-4-amino-5-cyanomethyl-4H-1,2,4-triazoles. *Turk J. Chem.* **2002**, *26*, 801–806.

Dzulkifli, N. N.; Farina, Y.; Baba, I.; Ibrahim, N. Synthesis, structural, antibacterial and spectral studies of Co(II) complexes with salicylaldehyde and *p*-chlorobenzaldehyde 4-phenylthiosemicarbazone. *Malaysian J. Anal. Sci.* **2012**, *16* (2), 103–109.

Ejelonu, B. C.; Oyeneyin, O. E.; Olagboye, S. A.; Akele, O. E. Synthesis, characterization and antimicrobial properties of transition metal complexes of aniline and sulphadiazine Schiff bases as mixed ligands. *J. Chem. Pharm. Res.* **2018**, *10* (5), 67–73.

Emriye, A. Y. Synthesis and characterization of Schiff base 1-Amino-4-methylpiperazine derivatives. *CBU J. of Sci*. **2016**, *12* (3), 375–392.

Gao, H. Synthesis, Characterisation and transition metal ion complexation studies of "pocket-like" imine and amide derivatives. Doctoral Dissertation, National University of Ireland Maynooth, Maynooth, 2013.

Ghara, A.; Si, A.; Majumder, M.; Bagchi, A.; Raha, A.; Mukherjee, P.; Pal, M.; Saha, R.; Bassu, S. A detailed study of Transition Metal Complexes of a Schiff base with its Physico-chemical properties by using an electrochemical method. *AJPP*. **2017**, *3* (3), 86–94.

Hossain, S.; Banu, L. A.; E-Zahan, K.; Haque, M. Synthesis, characterization and biological activity studies of mixed ligand complexes with Schiff base and 2,2-bipyridine. *Int. J. Appl. Sci. Res. Rev.* **2019**, *6* (1–2), 1–7.

Jamil, Y. M. S.; Al-Azab, F. M.; Al-Selwi, N. A.; Alorini, T.; Al-Hakimi, A. N. Preparation, physicochemical characterization, molecular docking and biological activity of a novel Schiff-base and organophosphorus Schiff base with some transition metal(II) ions. *Main Group Chemistry* **2022**, *Pre-press*, 1–26. https://doi.org/10.3233/MGC-220101

Kapadnis, K. H.; Jadhav, S. P.; Patil, A. P.; Hiray, A. P. Four synthesis methods of Schiff base ligands and preparation of their metal complex with Ir and antimicrobial investigation. *WJPPS.* **2016**, *5* (2), 1055–1063.

Mahmood, T. H.; Hassan, E. A.; Mubark, L. A. Preparation and characterization of Co(II), Ni(II) and Cu(II) ions binuclear complexes with macrocyclic Schiff base derived from acidhydrazide and α-hydroxy ketone. *JUAPS.* **2013**, *7* (2).

Majumdar, P.; Pati, A.; Patra, M.; Behera, R. K.; Behera, A. K. Acid hydrazides, potent reagents for synthesis of oxygen-, nitrogen-, and/or sulfur-containing heterocyclic rings. *Chem. Rev.* **2014**, *114* (5), 2942–2977. https://doi.org/10.1021/cr300122t

Malakyan, M.; Babayan, N.; Grigoryan, R.; Sarkisyan, N.; Tonoyan, V.; Tadevosya, D.; Matosyan, V.; Aroutiounian, R.; Arakelyan, A. Synthesis, characterization and toxicity studies of pyridinecarboxaldehydes and L-tryptophan derived Schiff bases and corresponding copper (II) complexes. *F1000 Research*. **2016**, *5*, 1921. https://doi.org/10.12688/f1000research.9226.1

Mathew, G.; Susselan, M. S.; Krishnan, R. Synthesis and characterisation of cobalt (II) complexes of chromen-2-one-3-carboxy hydrazide and 2-(chromen-2-onyl)-5-(aryl)1,3,4-oxadiazoe derivatives. *Indian J. Chem.* **2006**, *45A*, 2040–2044.

Mishra, A. P.; Sharma, N.; Jain, R. K. Microwave Synthesis, Spectral, Thermal and antimicrobial studies of some Ni(II) and Cu(II) Schiff base complexes. *Avances en Química* **2012**, *7* (1), 77–85.

Mohamed, E. A.; Mohamed, B.; Mustapha, H. Synthesis and characterization of N-salicylidèneglycinate (KHL) and caffeine complexes with Cd (II), Cu (II), Ni (II), Zn (II). *IJCPS*. **2014**, *3* (5), 22–34.

Mohamed, G. G.; Omar; M. M.; Hindy, A. M. Metal Complexes of Schiff Bases: Preparation, Characterization and Biological Activity. *Turk J. Chem*. **2006**, *30*, 361–382.

Naji, K. M.; Thamer, F. H.; Numan, A. A.; Dauqan, E. M.; Alshaibi, Y. M.; D'souza, M. R. Ferric-bipyridine assay: A novel spectrophotometric method for measurement of

Eclética Química, vol. 48, n. 2, 2023, 66-82
ISSN: 1678-4618
DOI: 10.26850/1678-4618eqj.v48.2.2023.p66-82

antioxidant capacity. *Heliyon.* **2020**, *6* (1), E03162. https://doi.org/10.1016/j.heliyon.2020.e03162

Neelofar, N. A.; Khan, A.; Amir, S.; Khan, N. A.; Bilal, M. Synthesis of Schiff bases derived from 2-hydroxy-1-naphthaldehyde and their tin(II) complexes for antimicrobial and antioxidant activities. *Bull. Chem. Soc. Ethiop.* **2017**, *31* (3), 445–456. https://doi.org/10.4314/bcse.v31i3.8

Oğuzhan, B.; Campolat, E.; Şahal, H.; Kaya, M. The synthesis, characterization of a novel Schiff base ligand and investigation of its transition metal complexes. *Adyu. J. Sci*. **2017**, *7* (1), 47–59.

Omer, D. A.; Al-Daher, A. G. M. New tridentate hydrazone metal complexes derived from 2-hydroxy-4-methoxyacetophenone and some acid hydrazides: synthesis, characterization and antibacterial activity evaluation. *Raf. J. Sci.* **2019**, *28* (2), 100–111. https://doi.org/10.33899/rjs.2019.159969

Patel, K. S.; Patel, J. C.; Dholariya, H. R.; Patel, V. K.; Patel, K. D. Synthesis of Cu(II), Ni(II), Co(II), and Mn(II) Complexes with Ciprofloxacin and Their Evaluation of Antimicrobial, Antioxidant and Anti-Tubercular Activity. *Open J. Met.* **2012**, *2* (3), 49–59. https://doi.org/10.4236/ojmetal.2012.23008

Refat, M. S.; Al-Maydama, H. M. A.; Al-Azab, F. M.; Amin, R. R.; Jamil, Y. M. S. Synthesis, thermal and spectroscopic behaviors of metal – drug complexes: La (III), Ce(III), Sm(III) and Y(III) amoxicillin trihydrate antibiotic drug complexes. *Spectrochim. Acta A Mol. Biomol. Spectrosc*. **2014a**, *128*, 427–446. https://doi.org/10.1016/j.saa.2014.02.160

Refat, M. S.; Al-Azab, F. M.; Al-Maydama, H. M. A.; Amin, R. R.; Jamil, Y. M. S. Synthesis and in vitro microbial evaluation of La(III), Ce(III), Sm(III) and Y(III) metal complexes of vitamin B6 drug. *Spectrochim. Acta A Mol. Biomol. Spectrosc*. **2014b**, *127*, 196–215. https://doi.org/10.1016/j.saa.2014.02.043

Refat, M. S.; Al-Azab, F. M.; Al-Maydama, H. M. A.; Amin, R. R.; Jamil, Y. M. S.; Kobeasy, M. I. Synthesis, spectroscopic and antimicrobial studies of La(III), Ce(III), Sm(III) and Y(III) metformin HCl chelates. *Spectrochim. Acta A Mol. Biomol. Spectrosc*. **2015**, *142*, 392–404. https://doi.org/10.1016/j.saa.2015.01.096

Reiss, A.; Cioteră, N.; Dobrițescu, A.; Rotaru, M.; Carabete, A. C.; Parisi, F.; Gănescu, A.; Dăbuleanu, I.; Spînu, C. I.; Rotaru, P. Bioactive Co(II), Ni(II), and Cu(II) complexes containing a tridentate sulfathiazole-based (ONN) Schiff base. *Molecules.* **2021**, *26* (10), 3062. https://doi.org/10.3390/molecules26103062

Safoura, F. Novel Synthesis of Schiff bases Bearing Glucosamine Moiety. *Res. J. Chem. Sci.* **2014**, *4* (2), 25–28.

Sakhare, D. T.; Chondhekar, T. K.; Shankarwar, S. G.; Shankarwar, A. G. Synthesis, characterization of some transition metal complexes of bidentate Schiff base and their antifungal and antimicrobial studies. *Adv. Appl. Sci. Res.* **2015**, *6* (6), 10–16.

Salawu, O. W.; Wuana, R. A.; Ashimom, J. T. Synthesis, characterization and corrosion inhibition of Co (II), Ni (II), Cu (II), and Zn (II) complexes derived from nicotinic acid hydrazide. In *39th CSN Annual International Conference*. Port Harcourt: Academic Journals; 2018, pp 2–6.

Sarwar, A.; Shamsuddin, M. B.; Lingtang, H. Synthesis, characterization and luminescence studies of metal-diimine complexes. *Mod. Chem. Appl.* **2018**, *6* (3), 1000262. https://doi.org/10.4172/2329-6798.1000262

Savalia, R. V.; Patel, A. P.; Trivedi, P. T.; Gohel, H. R.; Khetani, D. B. Rapid and economic synthesis of Schiff base of salicylaldehyde by microwave irradiation. *Res. J. Chem. Sci.* **2013**, *3* (10), 97–99.

Sharma, P. K.; Sen, A. K.; Dubey, S. N. Synthetic, spectral and thermal studies of cobalt(II), nickel(II), zinc(II) and cadmium(II) complexes with amino acid Schiff bases. *Indian J. Chem.* **1994**, *33* (A), 1031–1033.

Shneine, J. K.; Qassem, D. Z.; Mahmoud, S. S. Synthesis, characterization, and antibacterial activity of some amino acid derivatives. *Int. J. Chemtech Res.* **2017**, *10* (3), 604–612.

Tulu, M. M.; Yimer, A. M. Catalytic Studies on Schiff Base Complexes of Co (II) and Ni (II) using benzoylation of phenol. *Mod. Chem. Appl.* **2018**, *6* (3), 1000260. https://doi.org/10.4172/2329-6798.1000260

Yousef, E.; Radwan, L.; Othman, M. A. Synthesis of Co (II) and Cu (II) complexes with NO and N_2O_2 ligands derived from salicylaldehyde. *Chem. Mater. Res.* **2016**, *8* (7), 82–93.

Eclética Química, vol. 48, n. 2, 2023, 66-82
ISSN: 1678-4618
DOI: 10.26850/1678-4618eqj.v48.2.2023.p66-82